The Nature of the Bonding in Transition-Metal Compounds

Gernot Frenking* and Nikolaus Fröhlich

Fachbereich Chemie, Philipps-Universität Marburg, Hans-Meerwein-Strasse, D-35037 Marburg, Germany

Contents

I. Introduction

Although chemically binding interatomic interactions are the basis for chemistry as a whole, the understanding of the nature of the chemical bond is much less advanced than the experimental techniques which have been developed for the synthesis and analysis of new compounds. One reason for this is historical. Because classical physics could not give an explanation for the strong covalent interactions between neutral atoms, chemists developed simple ad hoc models which helped to establish ordering systems into the large number of compounds. The bonding models were remarkably successful in the synthesis of increasingly more complex compounds and substances, which also became the basis for a florishing industry that provided the income and wealth of many people. Pride in the experimental abilities and the direct impact on and interaction with chemical industry has shaped the way chemistry is taught and understood at universities . The successful synthesis of a new compound is generally valued much more highly than the results of a bonding analysis of a molecule. This is why chemistry has aquired during its history the character of being an engineering discipline.

Quantum chemically derived models have gained some acceptance in the past decades, but it still holds that the value of a bonding model is primarily judged by the simplicity of its application, rather than by its theoretical justification. Hückel[1] already showed in 1931 that quantum chemical methods could give an explanation for the stability and the chemical behavior of aromatic compounds, but his work was completely ignored in chemistry for several decades.[2,3] The reason for this was that the new quantum theory used complicated mathematical formulas in order to explain the chemical bond, while chemists were trained to employ simple models and empirically derived rules for rationalizing molecular structures and chemical reactivity.

It is one of the great achievements of Linus Pauling that he successfully introduced quantum chemistry as a valuable tool into chemistry.[3,4] Pauling realized that most chemists were not prepared nor willed to learn complicated mathematics in order to understand chemical bonding theory. He was able to build a bridge between quantum chemistry and the empirically derived models which were commonly used by chemists. Pauling favored valence-bond (VB) theory, because the familiar model of a two-electron bond could easily be retained. He introduced hybridization as a quantum chemical concept which became a very helpful device to rationalize the geometries, bond energies, and other physical properties of molecules. Although the model of hybridization already becomes less straightforward for heavier atoms than the first-row elements C—Ne,[5] it is still one of the most important quantum theoretically derived concepts that is used by many chemists.

Quantum chemical models became widely accepted first via VB theory, although the advantages of molecular orbital (MO) theory were already clearly seen in the early days of quantum chemistry.[1] It took more than three decades before MO theory also
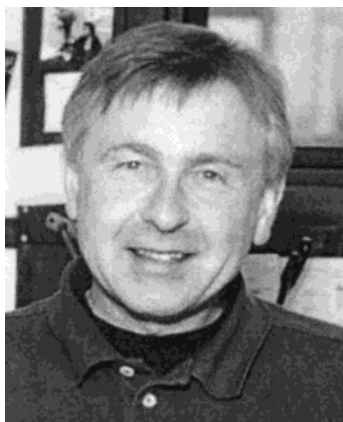
Gernot Frenking was born in Germany in 1946. He left school in 1960 and worked in chemical industry before he went to school again and finally entered university in 1969. He received his diploma in chemistry at the Rhenish-Westfalian Technical Highschool in Aachen in 1973. Following two years as a research student in the group of Professor Kenichi Fukui at Kyoto University (Japan), he returned to Germany and received his doctoral degree from the Technical University Berlin in 1979 under the guidance of Professor Horst Götz. After obtaining his Habilitation in Theoretical Organic Chemistry at the TU Berlin in 1984, he moved to the United States. Following one year as a visiting scientist in the group of Professor Henry F. Schaefer III at the University of California (Berkeley), he became a staff scientist at the Stanford Research Institute (SRI International) in Menlo Park, CA. In 1989 he returned to Germany and became an Associate Professor for Computational Chemistry at the Philipps Universität Marburg. In 1998 he was appointed Full Professor for Theoretical Chemistry. His current research interests lie in the field of theoretical inorganic chemistry. Major topics of interest are the nature of the chemical bond of heavy elements, particularly transition metals, reaction mechanisms of transition-metal-catalyzed reactions, and lately bioinorganic reactions.

Nikolaus Fröhlich was born in Bochum, Germany, in 1970. He started studying chemistry at the University of Konstanz. Following his Vordiplom in 1993, he went for a year abroad to the University of Sussex in Brighton where he joined the group of Professor M. F. Lappert. He returned to Germany to continue his studies at the University of Marburg. During his time in Marburg, his interests in computational chemistry grew. Consequently, he joined the group of Professor Frenking. He received his diploma in 1998. Since then, he has been working on his Ph.D. thesis, a theoretical study of the reaction mechanism of the rhodium-catalyzed oxidative amination of olefins. His fascination for computational chemistry lies in its ability to serve as an interface between theory and experiment.

became popular in mainstream chemistry. The striking success of frontier orbital theory[6] and MO symmetry rules[7] in explaining the stereoselectivity of pericyclic reactions[8-11] paved the way for MO theory to become a part of the standard curriculum for teaching chemical bonding theory in organic chemistry.[12-14] However, VB concepts such as hy-

bridization are still widely used in organic chemistry textbooks to explain the geometries and chemical bonds of organic molecules.[15-17] VB models are also commonly used in inorganic chemistry to explain chemical bonding of main-group elements.[18-21]

The importance of quantum chemistry in the field of transition-metal compounds was comparatively low until the end of the 1980s. In the foreword to the 1991 thematic issue of *Chemical Reviews* on Theoretical Chemistry, the guest editor wrote "The theory of transition-metal chemistry has lagged behind the quantum theory of organic chemistry because quantitative wave functions are more complicated".[22] The situation has dramatically changed in the past decade. This is largely due to the successful employment of gradient-corrected density functional theory (DFT) in calculating molecules, particularly of the heavier atoms,[23-26] and in the use of small-core relativistic effective core potentials (ECPs),[27] which set the stage for the calculation of geometries, bond energies, vibrational spectra, NMR chemical shifts, activation energies of chemical reactions, and other important properties of TM compounds with impressive accuracy.[25,28,29] These calculations also made it possible to analyze the chemical bonds of the molecules with the aim of gaining insight into the chemical bond and deriving bonding models which can be compared with the exisiting models of chemical bonding. Here, DFT again has proven to be very powerful because the Kohn–Sham orbitals turned out to be even more helpful for a bonding analysis in terms of orbital interactions than the Hartree–Fock orbitals, since the former include correlation effects.

We want to point out that a bonding model which is based on quantum chemical concepts is not necessarily more helpful for the synthetic design than an ad hoc model. A model is an abstract of the reality; it cannot be right or wrong; it can only be more or less useful. However, a model which is based on assumptions that are falsified by accurate calculations becomes questionable even if it offers the advantage of simplicity. The model of spd hybridization to "explain" the bonding in hypervalent compounds of heavier main-group elements is an example. Several quantum chemical studies have clearly shown that the d orbitals of the heavier main-group elements are not really engaged as valence orbitals in chemical bonding but rather serve as polarization functions.[30-35] This is acknowledged in the latest edition of a popular textbook of inorganic chemistry but then it continues "Nevertheless, the concept of hybrid orbitals retains advantages of simplicity and, in many instances, affords a very easy way to correlate and "explain" molecular structures".[36] The danger in using correlations as pseudoexplanations lies in the temptation to take good correlations as a proof for the existence of the underlying assumption. We will show more examples of this in the course of the review.

In this paper we want to discuss the progress which has been made mainly in the past decade toward an understanding of the binding interactions in TM compounds. The topics of the account are quantum chemical studies using DFT or ab initio methods which focus on the analysis of the chemical bond.

Work which is based on EHT calculations and earlier theoretical studies will only be discussed if it is relevant in the context of recent accurate studies. Theoretical investigations which primarily aim at calculating geometries, bond energies, and other observable properties will also not be considered, unless they give information about the nature of the chemical bond.

A final remark shall be made about the results of theoretical bonding analyses. Most quantum chemical studies do not really strive at gaining insight into the physical mechanism of the chemical bond. The aim of most theoretical investigations of the chemical bond is to find a correlation between the chemical behavior of the molecules or its physical observables and calculated data such as charge distribution or orbital structure. However, an important difference between quantum theoretical concepts and ad hoc interpretations of chemical bonding is that the former models are in agreement with the calculated data while the latter may or may not. On the other hand, a strict analysis of the physical origin of interatomic interactions is much more complicated[37−41] and may lead to results which are counterintuitive.[42]

II. Present Bonding Models for Transition-Metal Compounds

The most widely used bonding model for transition-metal compounds which is presently found in modern textbooks of inorganic chemistry,[18−21] transition-metal chemistry,[43−45] and chemical bonding theory[46,47] is ligand field theory (LFT).[48−50] LFT can be considered as a simplified MO theory that considers mainly the valence d orbitals of the TM and the frontier orbitals of the ligands. Alternatively, it can also be considered as a more sophisticated version of crystal field theory (CFT), which considers only electrostatic interactions between the metal and the ligands. A related method to LFT which has been parametrized for estimating the strength of the metal−ligand interactions in terms of overlap integrals between metal and ligand orbitals is the angular overlap model (AOM).[51,52] AOM and LFT are very powerful models to explain trends in geometries, magnetic properties, bond energies, excitation energies, and other physical properties of TM compounds.[18−21,43−50] In particular, the splitting of the d-orbital energy levels in a highly symmetric field of 4−6 ligands is a very helpful model to rationalize molecular properties of TM complexes. This model is described in many chemistry textbooks and shall not be presented here.

Another MO−theoretical model frequently used in conjunction with LFT considers the TM−ligand interactions in terms of L → TM donation and L ← TM back-donation. This model was originally introduced by Dewar[53] and by Chatt and Duncanson[54] to describe TM−olefin interactions in ethene complexes. The synergistic bonding model was later extended to other metal−ligand bonds where the energetically high-lying occupied orbitals of the ligand, which have in most cases σ symmetry with regard to the whole complex, are considered as donor orbitals. The back-donation then occurs between occupied orbitals of the metal, which have usually π symmetry, with low-lying empty π* orbitals of the ligand. The Dewar−
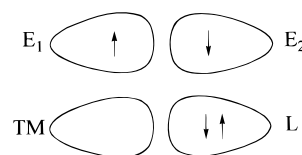

Figure 1. Schematic representation of the common bonding model for a covalent bond between main-group elements E (top) and between a transition metal and a ligand (bottom).

Chatt−Duncanson (DCD) model is frequently used to explain properties of TM complexes. For example, spectroscopic data like vibrational frequencies are often correlated with the π acceptor strength of the ligands, and it has become common in the inorganic community to take spectroscopic data as a "proof" for the π acceptor strength of a ligand, neglecting the possibility that other factors such as charge polarization effects might have a significant influence on the vibrational spectrum. It is important to recognize that a good correlation is merely a helpful ordering scheme which does not prove anything concerning the true binding interactions. Several quantum chemical studies of TM bonding that focused on the validity of the DCD model have been published recently. They will be discussed in the sections below.

There is an interesting difference between the most important bonding models for main-group elements and those for transition metals that are used in most textbooks. The chemical bonds of main-group elements are usually described as ionic or covalent, and the latter are then discussed in terms of orbital interactions between two sp^x-hybridized orbitals (Figure 1). The important point here is that each binding partner contributes one electron to the electron pair bond. The bonding model of LFT considers the covalent bond of a TM compound to arise from the interactions between doubly occupied orbitals of the ligand and empty orbitals of the TM and vice versa, i.e., LFT considers *all* TM compounds as if they are coordination complexes. The bonds are analyzed in terms of donor−acceptor interactions even when the TM−X bond dissociates homolytically. Thus, WCl_6 is discussed as the product of W^{6+} and $6Cl^-$ and not as W and 6Cl. The reason for the popularity of the donor−acceptor bonding model in TM chemistry is partly due to the fact that coordination chemistry plays a much bigger role for the transition metals than for main-group elements. Another reason is the success of LFT in explaining chemical bonding even in TM compounds which are not coordination compounds. A popular textbook in inorganic chemistry expresses this with the words "It is, however, traditional and convenient, in discussions of coordination compounds, to view the central metal as a cation, and to view the ligands as Lewis bases".[55] But it *is* possible to analyze and discuss covalent bonds of TM compounds in the same way as it is done for molecules of main-group elements. The difference is that the valence orbitals of main-group elements are s and p orbitals while the lowest lying valence orbitals of the TMs are s and d and possibly p functions. In short, *main-group chemistry means sp hybridization and TM chemistry means sd (and possibly sdp) hybridization.*

It is suprising to see that comparatively little has been done in the past to investigate TM bonding in terms of sd hybridization. Recent work, particularly by Landis and co-workers,[56–59] has shown that VB theory which uses sd-hybridized orbitals is a very powerful model that explains the surprising structures of simple TM alkyls and hydrides. This will be discussed below.

To avoid confusion about the names for different types of chemical bonds, we will use the term "covalent bond" for a two-electron bond where each binding partner provides one electron (top of Figure 1). The chemical bond in a coordination compound is named a "donor–acceptor bond" (bottom of Figure 1).[60] We want to point out that donor–acceptor bonds may also have large covalent contributions to the binding interactions.

III. Valence Orbitals of Transition Metals and spd Hybridization

The most important valence orbitals of the transition metals are the d orbitals. The ground-state configuration of all TMs is $(n)s^a(n-1)d^b$, where a can be 0, 1, or 2. One puzzling aspect concerns the ground-state configurations of the atoms of the first TM row Sc–Zn, which is $Ar(4)s^2(3)d^b$, with the exception of Cr and Cu adopting $Ar(4)s^1(3)d^{b+1}$.[61] The corresponding dications TM^{2+}, however, all have the configuration $Ar(3)d^b$, which suggests that the 3d electrons are more tightly bound than the 4s electrons. Also, Hartree–Fock calculations using very large atomic basis sets show that the energy of the 3d orbital is always below 4s. Two recent papers dealt with the question of why the 4s orbital becomes occupied before 3d for first-row TMs.[62,63] Both studies came to the same conclusion, which were said to correct previous misleading statements and unsound explanations.[64–66] The most important finding concerns the repulsive interactions between electrons that occupy s and d orbitals. The s orbitals are much more diffuse than the d orbitals, and two electrons occupying the 4s orbital repel each other much less than two electrons distributed over the five 3d orbitals. The order for the electron–electron repulsion thus becomes (4s,4s) < (4s,3d) < (3d,3d).[62] The influence of the different repulsive forces on the orbital energies is shown in Figure 2 using scandium as an example. Although the 3d orbital is energetically lower lying than 4s, the configuration $(4)s^2(3)d^1$ is more stable than $(4)s^1(3)d^2$, because the strong (3d,3d) repulsion raises the total energy of the $(4)s^1(3)d^2$ configuration above that of $(4)s^2(3)d^1$. Thus, the configuration $(4)s^1(3)d^2$ does *not* lead to the situation which is shown on the left side of Figure 2 but rather to the energetically less favorable situation which is shown on the right side.

A similar reasoning holds for the electron configuration of the TM ions, where the $(4)s^1(3)d^n$ form is now energetically below $(4)s^2(3)d^{n-1}$.[61] The effective higher nuclear charge stabilizes 3d more than 4s, which leads to an increase in the 4s–3d energy difference. Figure 3 schematically shows the changes of the orbital levels and electron configurations of Mn and isoelectronic Co^{2+}.[62] It holds for both Mn and
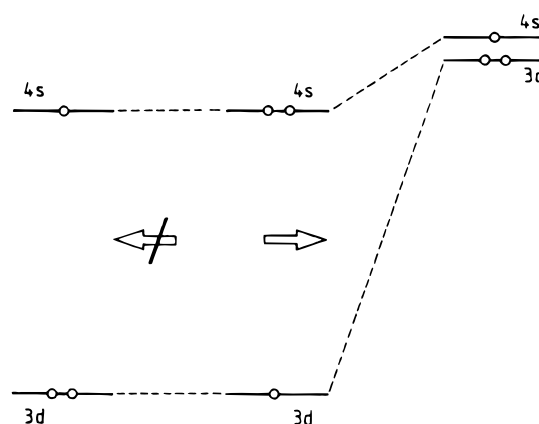

Figure 2. Schematic representation of the transition $(4)s^2(3)d^1 \rightarrow (4)s^1(3)d^2$ in scandium. The left-hand side shows a hypothetical process where the orbital energy is not a function of the occupation number. The right-hand side shows the result of an actual Hartree–Fock calculation. (Reproduced with permission from ref 62. Copyright 1994 American Chemical Society.)
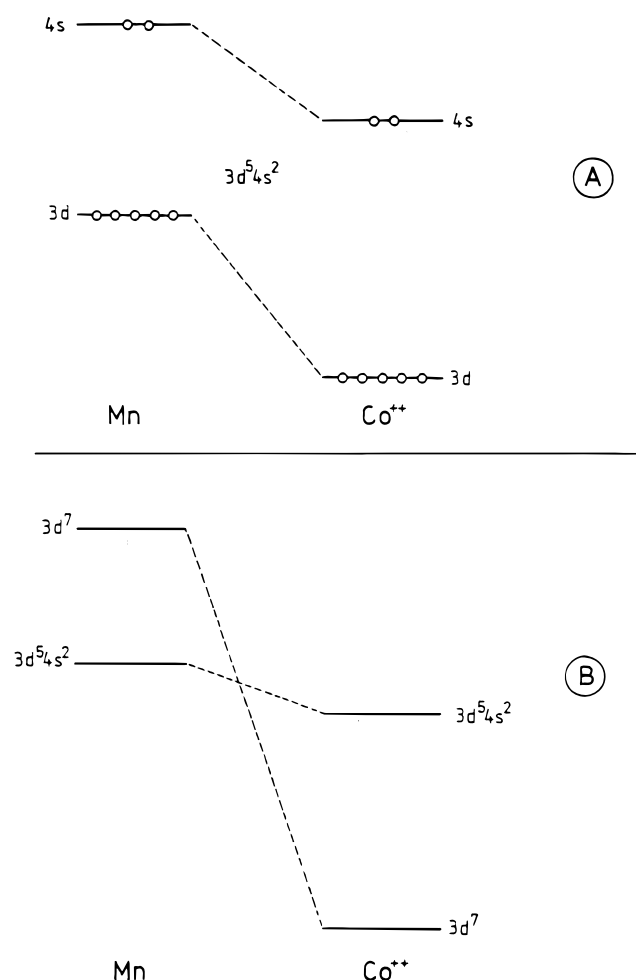
Figure 3. (A) Comparison of the 3d and 4s orbitals in the $(4)s^2(3)d^5$ configuration of Mn and Co^{2+}. (B) Inversion of the configuration energies of $(4)s^2(3)d^5$ and $(3)d^7$ between Mn and Co^{2+}. (Reproduced with permission from ref 62. Copyright 1994 American Chemical Society.)

Co^{2+} that 4s is higher in energy than 3d but the (3d, 3d) electron repulsion in Co^{2+} is not strong enough to compensate for the energy difference between the 3d- and 4s-orbital energies, as it is in Mn.
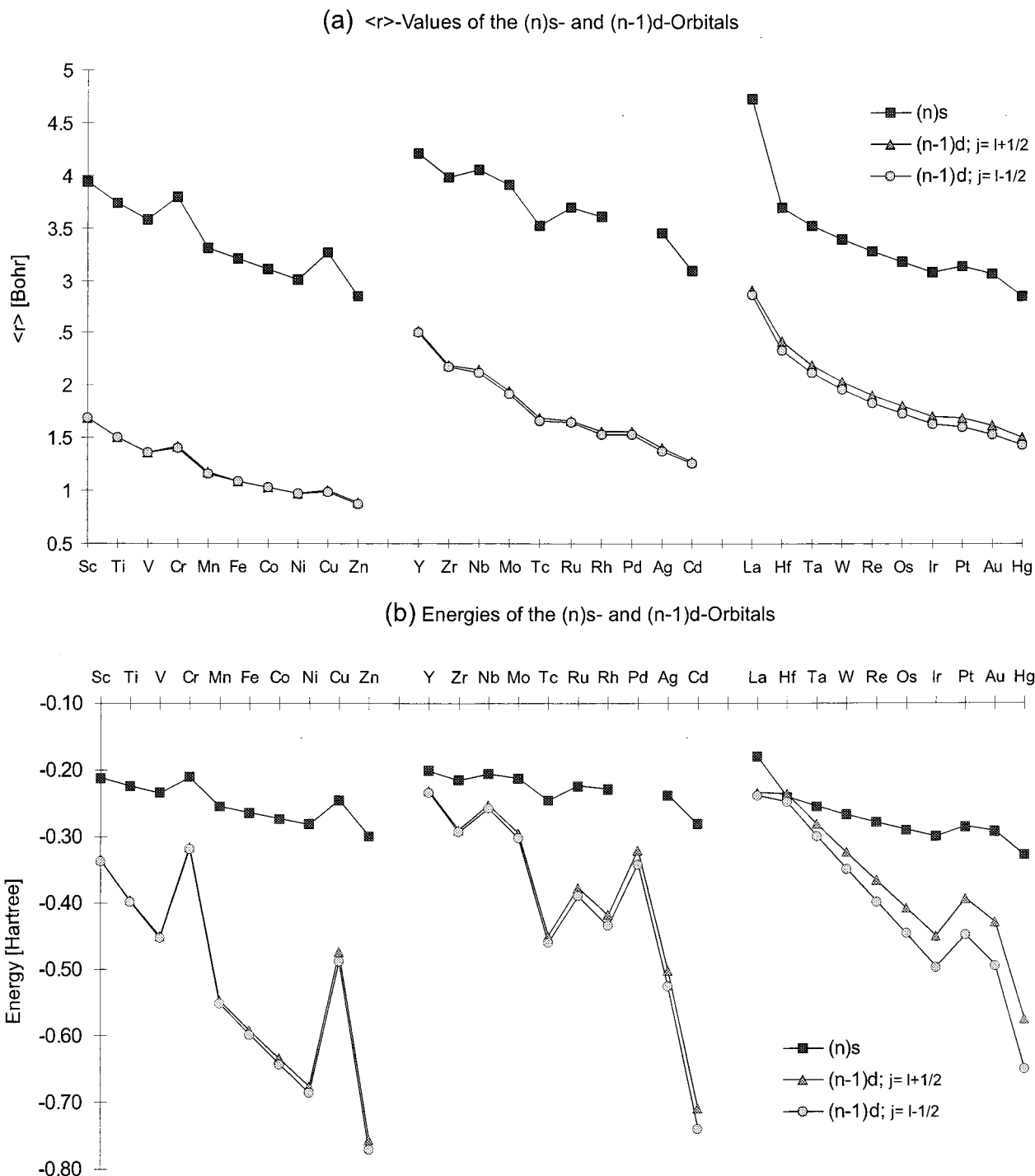
(a) <r>-Values of the (n)s- and (n-1)d-Orbitals

(b) Energies of the (n)s- and (n-1)d-Orbitals

Figure 4. (a) Dirac−Fock energies of the (n)s and $(n-1)$d orbitals of the transition metals. (b) Calculated radii $\langle r \rangle$ of the (n)s and $(n-1)$d orbitals of the transition metals. The values have been taken from ref 67.

From the above discussion it can be concluded that the s and d orbitals must be considered as valence orbitals of the TMs. Figure 4 shows the radii and energy eigenvalues of the valence s and d orbitals of the TMs in the ground-state configuration taken from numerical Dirac−Fock calculations.[67] As expected, the radii become smaller and the orbital energies become lower from the left to the right because of the increasing nuclear charge. The kinks in the curves arise from the changes in the ground-state configuration. For example, Cr and Cu have a (4)s$^1(3)$d^n valence configuration while the other 3d elements have (4)s$^2(3)$d^{n-1}. The curves clearly show

the different behavior of the first TM row compared to the second and third TM row. The energy differences between the 4s and 3d orbitals are generally larger than between 5s and 4d or 6s and 5d, respectively. This is related to the spacial extension of the orbitals. The most important point is the comparatively small radius of the 3d orbitals. Interelectronic repulsion between electrons having the same spin which occupy orbitals with the same spacial symmetry ($ns-ms$, $np-mp$, $nd-md$) is rather high because of the Pauli repulsion. The 3d orbitals are the first orbitals of d symmetry and, thus, can therefore penetrate rather deeply into the core region. The first

TM row atoms have a significantly different ratio of the s/d radii compared to the second and third TM row, which is one reason the chemical behavior of the 3d elements differs from that of the heavier analogues. This is similar to the changes between the main-group elements of the first full row Li−Ne and the heavier elements which are caused by the different ratio of the s and p valence orbital radii.[5] Here, the radius of the 2p orbitals is rather small and becomes comparable to the radius of the 2s orbitals, which leads to effective 2s/2p hybridization.

The much smaller radius of the 3d than the 4s orbital has led to the suggestion that in compounds of the first TM row, the metal 4s orbital should be the dominant metal contribution in the bonding, particularly when the TM is in a high oxidation state.[43,68] Because of the radial waveform of the TM 3d and 4s functions, there should be poor overlap of 3d with ligand orbitals. This hypothesis is the central thesis for a recent textbook on transition-metal chemistry by Gerloch and Constable.[43] Quantum chemical calculations do not support this idea. For example, the Ti−C and Ti−Cl localized orbitals in Me_nTiCl_{4-n} are ~sd^3-hybridized at titanium, which demonstrates that the 3d orbitals contribute even more to the titanium bonds than the 4s orbital.[69,70]

While the importance of the valence (n)s and $(n-1)$d functions for the description of TM bonds is undisputed, the status of the empty (n)p orbitals is controversially discussed. Landis has introduced a VB model which rationalizes the unusual molecular shapes of simple TM alkyls and hydrides in terms of sd-hybridized orbitals.[56−59] Many TM alkyls and hydrides such as WH_6, a distorted trigonal prism (C_{3v}),[71−73] or the experimentally known[74−76] $W(CH_3)_6$, which has C_3 symmetry,[77] deviate strongly from maximum symmetry.[78] This finding cannot be explained by the original valence shell electron pair repulsion (VSEPR) method.[79−81] Landis could show that the bond angles between adjacent sd^n hybrids agree nicely with the observed or calculated bond angles of alkyls and hydrides with the formula TMH_{n+1} and TMR_{n+1}. Figure 5 shows the orientations of sd^n hybrid orbitals and their corresponding polyhedral coordination geometries as given by Landis.[59] Figure 6 shows the energy functions for sd^n hybrids which have been derived[82] using Pauling's formulas[83] for hybrid orbital strength functions.[56] Table 1 gives molecular shapes which are associated with the different sp^n and sd^n bond hybridizations.

Table 1 shows that the model of ideal sd-hybridized bond orbitals is in agreement with many experimentally observed or theoretically predicted geometries but does not lead to a definite correlation between molecular shape and sd^n hybridization for $n = 3-5$. This is because the energy curves as a function of the bond angle have two minima, one <90° and one >90° (Figure 6). There are three structures which accommodate the two angular preferences of sd^3 hybridization (T_d, C_{4v}, C_{3v}), four structures are possible for sd^5 hybridization ($2 \times C_{3v}$, $2 \times C_{5v}$), and even six structures were found for sd^4 hybridization ($3 \times C_s$, $2 \times C_{4v}$, C_{5v}). Note that there is no O_h form among the sd^5-hybridized structures and no D_{3h} form among the sd^4 species which are predicted as local minima.
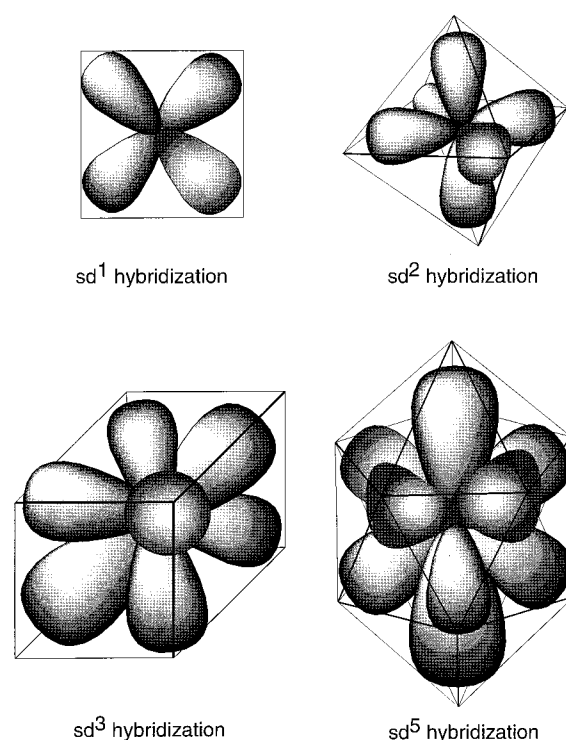
Figure 5. Orientation of sd^n hybrid orbitals and their corresponding polyhedral coordination geometries. (Reproduced with permission from ref 59. Copyright 1998 American Chemical Society.)
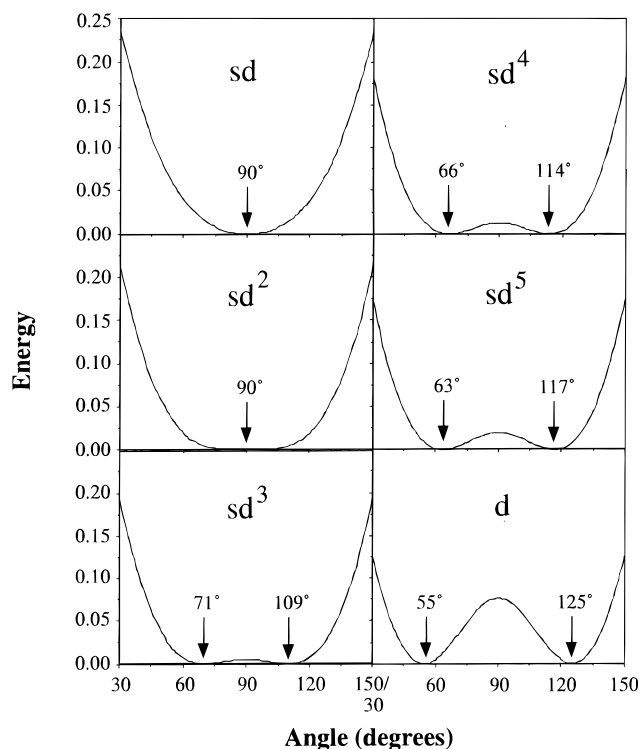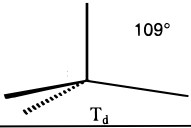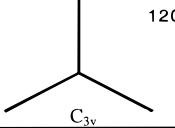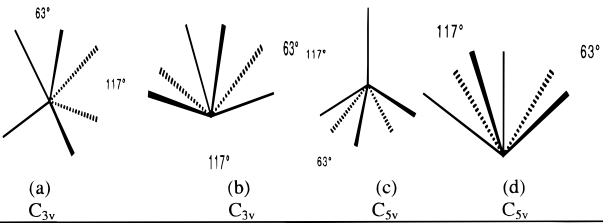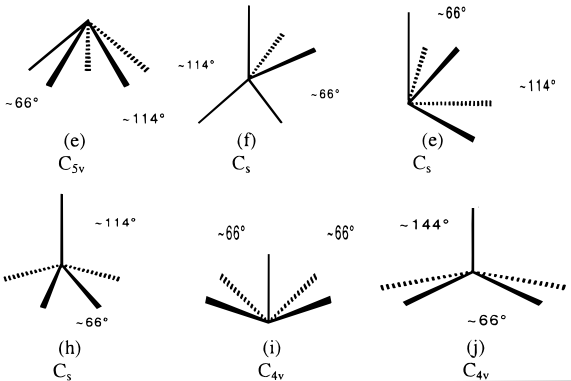
Figure 6. Energies of pairs of sd^n hybrid orbitals and pure d orbitals as a function of bond angle. (Reproduced with permission from ref 56. Copyright 1995 American Chemical Society.)

This is in agreement with ab initio calculations of CrH_6 and WH_6 which show that the O_h forms are energetically very high lying (>100 kcal/mol above the global minima) saddle points on the potential energy surface.[71−73,84,85]

Table 1. Molecular Shapes Associated with Different Bond Hybridizations[a]

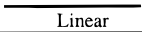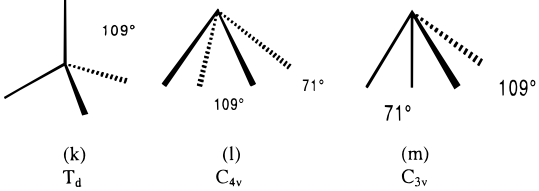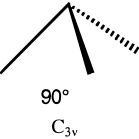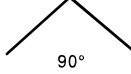| Idealized Hybridization and Angles	Idealized Molecular Shape	Examples of Indicated Formal Hybridization
sp^3 109.5°	109° T_d	CH_4
sp^2 120°	120° C_{3v}	BCl_3
sp 180°	180° Linear	C_2H_2
sd^5 117° and 63°	63° 117° (a) C_{3v} — 63° 117° 117° (b) C_{3v} — 117° (c) C_{5v} 63° — 117° 63° (d) C_{5v}	Computational: WH_6, $[TcH_6]^+$ Experimental: $W(Me)_6$, $[Zr(Me)_6]^{2-}$ $W(o\text{-Xylidene})_3$
sd^4 114° and 66°	~66° ~114° (e) C_{5v} — ~114° ~66° (f) C_s — ~66° ~114° (e) C_s ~114° ~66° (h) C_s — ~66° ~66° (i) C_{4v} — ~144° ~66° (j) C_{4v}	Computational: $[WH_5]^+$, ReH_5 Experimental: $Ta(Me)_5$ $Ta(CH_2\text{-}p\text{-Tol})_5$
sd^3 119° and 71°	109° (k) T_d — 109° 71° (l) C_{4v} — 71° 109° (m) C_{3v}	Computational: RuH_4, $[TaH_4]^+$ Experimental: $Os(Ph)_4$, $Mo(Nor)_4$ $Cr(2,2\text{-dimethyl, 1-phenylethenyl})_4$ $[Os(o\text{-Tol})_4]^+$, $Os(o\text{-Tol})_4$ $Re(o\text{-Tol})_4$, $Ru(o\text{-Tol})_4$ $Mo(o\text{-Tol})_4$, $Ru(C_6H_{11})_4$ $Os(C_6H_{11})_4$, $Cr(C_6H_{11})_4$ $Ru(Mes)_4$, $[Ir(Mes)_4]^+$
sd^2 90°	90° C_{3v}	Computational: RhH_3, $[ZrH_3]^+$ Experimental: $La(CH(SiMe_3)_2)_3$ $Rh(Mes)_3$, $Ir(Mes)_3$
sd 90°	90°	Computational: $Pt(Me)_2$, PtH_2

[a] Taken from ref 57.

The observation that several energy minima for TMR_4, TMR_5, and TMR_6 are possible leaves some ambiguity about the prediction of the sd-restricted VB model concerning the most stable structure.

Table 2. NBO Analysis of Me$_2$MCl$_2$ (M = C, Si, Ge, Sn, Pb, Ti, Zr, Hf) at MP2/VDZ+P[a]

	calcd (exp) bond angle		M−C[b]				M−Cl[b]			
	C−M−C	Cl−M−Cl	%M	%s(M)	%p(M)	%d(M)	%M	%s(M)	%p(M)	%d(M)
Me$_2$CCl$_2$	113.1 (113.0)	108.7 (108.3)	52.5	31.4	68.5	0.1	46.1	18.6	81.1	0.2
Me$_2$SiCl$_2$	114.2 (114.7)	108.2 (107.2)	26.4	29.3	69.2	1.5	22.8	20.7	76.8	2.6
Me$_2$GeCl$_2$	118.3 (121.7)	106.6 (106.1)	29.1	30.7	68.8	0.5	22.3	19.3	79.4	1.3
Me$_2$SnCl$_2$	122.0 (110.1)	105.9 (107.5)	26.9	30.6	69.3	0.2	18.4	19.4	79.8	0.8
Me$_2$PbCl$_2$	128.9	105.1	31.2	31.8	68.2	0.0	18.6	18.2	81.6	0.2
Me$_2$TiCl$_2$	102.7 (106.2)	120.1 (116.7)	29.5	22.7	0.1	77.2	16.6	27.1	0.3	72.6
Me$_2$ZrCl$_2$	105.0	117.6	21.4	24.2	0.2	75.7	12.5	25.7	0.5	73.8
Me$_2$HfCl$_2$	104.9	116.5	15.6	25.5	5.4	69.1	9.8	24.4	11.0	64.6

[a] Taken from ref 70. [b] % M gives the polarization of the M−C and M−Cl bonds; % s(M), % p(M), and % d(M) give the hybridization of the M−C and M−Cl bonds at the central atom M.

Landis noticed that, in particular, the TMR$_5$ potential energy surface for shape distortions will be complex and soft and that it is difficult to predict the final equilibrium geometry as it depends on a subtle balance of forces.[57] He has given three rules which should help to find the lowest lying structure. Besides the restriction to s and d valence orbitals (rule 1), rule 2 says that for TM molecules with mixed ligands the distribution of d character among the hybrid orbitals depends on the relative electronegativities of the ligands. Bent's rule is employed, which was originally derived for sp-hybridized main-group elements.[86] It says that "Atomic s character concentrates in orbitals directed towards electropositive substituents". Landis suggests that Bent's rule should also apply to sd-hybridized orbitals of TM compounds. However, this postulate is in conflict with experimental data and quantum chemical calculations published by Frenking et al.[70]

Table 2 shows that the Cl−M−Cl bond angle in (CH$_3$)$_2$MCl$_2$ (M = C, Si, Ge, Sn, Pb) is always smaller than the angle C−M−C and that the %s character at M in the M−Cl bond orbitals is always lower than %s(M−C). This is exactly what is predicted by Bent's rule. The opposite trends are found when M = Ti, Zr, Hf. Here, the Cl−M−Cl bond angle is always larger than C−M−C and the %s character of the Ti−Cl and Zr−Cl bonds is higher than %s(Ti−C) and %s-(Zr−C), respectively. The %s character of the Hf−C and Hf−Cl bonds shows a different ratio, because there is an unusually high participation of the p(Hf) orbital (Table 2). In all cases it holds for the TM compounds that %d(M−C) > %d(M−Cl), while the main-group elements show the order %p(M−C) < %p-(M−Cl). The opposite trend of sp and sd hybridization in main-group and TM compounds led Frenking et al. to suggest a modified form of Bent's rule: "The energetically lower lying valence orbital concentrates in bonds directed toward electropositive elements".[70] The lower lying valence orbital of main-group elements is the s orbital, while for transition metals it is a d orbital (Figure 4). Landis explained the large Cl−Ti−Cl angle in (CH$_3$)$_2$TiCl$_2$ with the importance of ionic resonance contributions to the Ti−Cl bond.[57]

The VB model of Landis rests on the assumption that the bond angles of covalently bound TM compounds are mainly determined by the angle between the sd-hybridized bond orbitals, i.e., that there is a correlation between bond angles and hybridization. It has been shown by Kutzelnigg in his epochal paper

about the chemical bond of the higher main-group elements that this correlation is already no longer valid for sp-hybridized bonds of the heavier atoms.[5] Table 1 shows the well-known result that CH$_4$ has T_d symmetry and sp^3-hybridized C−H bonds. It is much less known that the higher homologue SiH$_4$, which also has T_d geometry, has Si−H bond orbitals that are ∼sp^2-hybridized rather than sp^3-hybridized.[5] The reason for the lower %p character of the Si−H bond is that the 3s AO of Si has a significantly smaller radius than the 3p AO. It makes the hybridization less efficient than that for the 2s and 2p orbitals of carbon, which have a similar radius. There is a competition between energy gain due to better overlapping of hybridized orbitals and the price which has to be paid for the promotion. The bond angle of 109.5° in SiH$_4$ does *not* correlate with the angle between the ∼sp^2-hybridized bond orbitals at Si. One reason SiH$_4$ has T_d symmetry is the polarity of the bond Si$^{\delta+}$−H$^{\delta-}$, which means that the hybridization at Si is less important for the overlap than that for the C$^{\delta-}$−H$^{\delta+}$ bonds of CH$_4$. Another reason is the Pauli repulsion between the Si−H bonds, which favors larger bond angles. Kutzelnigg has shown that the Pauli repulsion between bond orbitals or between bond orbitals and lone-pair electrons may be more important for the bond angles than the optimal overlap between the bound atoms.[5] Table 2 shows that the TM−C and TM−Cl bonds are strongly polarized toward carbon and chlorine, respectively. This means that the hybridization at the TMs should have comparatively little influence on the molecular geometries.

The relation between bond angles and electronic structure in high-valent TM compounds has recently been examined by Kaupp.[87] The author calculated the geometries of several d^0 compounds and analyzed the bonding situation with the NBO partitioning scheme. He came to the conclusion that the influence of π bonding on the bond angles is much more important than the hybridization of the σ bonds. However, analyses of the model systems ScF$_2$+ and ZrO$_2$ indicated a rather complicated dependence of π bonding on bond angles. The in-plane π bonding exhibits a nonmonotonic behavior, while the out-of-plane π bonding (Figure 7) shows a more regular dependence, which can be understood from the nodal properties of the relevant TM d orbitals.[87] The net π-bonding behavior then depends sensitively on the donor properties of the ligands. Kaupp distinguishes
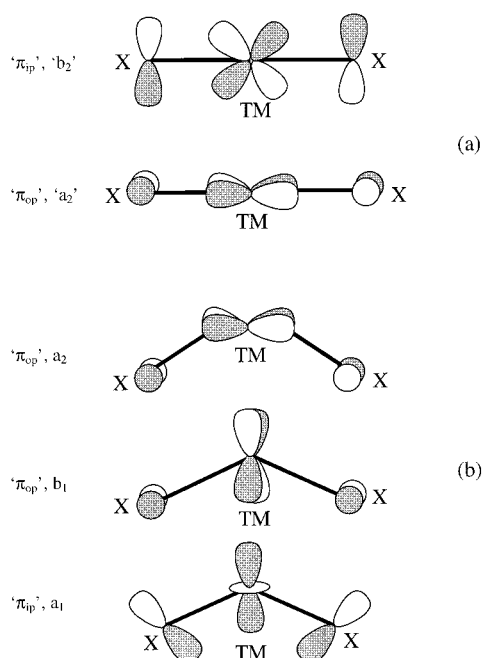
Figure 7. Schematic representation of the TM d orbitals available as π-bonding acceptors for (a) linear and (b) bent TMX$_2$ complexes. (Reproduced with permission from ref 87. Copyright 1999 Wiley-VCH.)

between "strong π-donor cases" like ZrO$_2$, where π-bonding favors a bent equilibrium geometry, and "weak π-donor cases" like ScF$_2$+, where π-bonding favors a linear structure. The bent equilibrium geometry of ScF$_2^+$ is said to be caused by the σ bonds. The author suggests that the "inverse Bent's rule structure" of (CH$_3$)$_2$TiCl$_2$ is related to the improved in-plane π(Ti–Cl) bonding rather than to hybridization. It seems that Bent's rule is less helpful for TM compounds than for main-group molecules. Unfortunately, the dominant influence of π bonding does not lead to simple rules for predicting the bond angles in TM compounds. We want to point out that π bonding has been suggested also by other authors as an important factor for determining bond angles in TM compounds.[88–91]

The restriction to valence s and d functions for TMs suggested by Landis[57–59] means that 12 electrons will fill the TM valence shell rather than the 18 electrons that can be accommodated if the (n)p orbitals were also part of the valence shell. This is astonishing in light of the well-established 18e rule for TM compounds. The reader should be reminded, however, that a related situation once existed in main-group chemistry, when the stability of hypervalent compounds of the heavier atoms was explained with spd-hybridized bond orbitals. Quantum chemical calculations have clearly shown that the (n)d orbitals of main-group elements are not accessible for chemical bonding.[30–35] The more appropriate VB model for hypervalent main-group elements invokes the use of ionic–covalent resonance forms, i.e., three-center–four-electron (3c–4e) bonds. Consequently, the same VB description is suggested by Landis for TM compounds with more than 12 electrons.[56–59] The author explicitly points out that his VB model "leads to the conclusion that most transition-metal complexes are hypervalent!."[56]

As support for the hypothesis of the 12-electron valence space, Landis presented the results of DFT calculations of TM hydrides which gave geometries that are in agreement with the prediction of the VB model.[57–59] He also gave the results of an NBO analysis of the TM–hydrogen bonds, which show dominantly sd^n-hybridized bond orbitals and negligible p participation at the metals.[57] Thus, quantum chemical analysis of the TM–hydrogen bonding apparently supports the restriction of the TM valence orbitals to s and d function. However, there is a serious technical flaw in the analysis. The NBO method requires a preselection of those orbitals which are considered as valence orbitals and may become occupied in the population analysis and those orbitals which belong to the Rydberg space.[92,93] The standard version of NBO makes the arbitrary decision *not* to include the (n)p functions into the valence space of the TMs. In an important paper by Maseras and Morokuma[94] (MM), it was shown that the (n)p population of the TMs changes significantly when a modified version of NBO with the valence space (n)s-(n − 1)d(n)p is employed. The population of the 4p$_z$ AO of Ni in NiH$_2$ is only 0.05 e when a 3d4s valence space is used, but it increases to 0.27 e when a 3d4s3p valence space is chosen.[94] It becomes clear that NBO results cannot be used to determine the importance of the TM (n)p orbitals for chemical bonding. Another important result concerns the results of the still widely used Mulliken population analysis.[95] The population of the 4p$_z$ AO of Ni in NiH$_2$ is 0.74 e, which is much higher than the population of the 3d$_z$ AO (0.32 e). It follows that the Mulliken analysis grossly overestimates the importance of the TM (n)p orbitals.

Because of the problems with the NBO analysis, Bayse and Hall (BH)[96] presented analyses of Foster–Boyd[97] and Pipek–Mezey[98] localized molecular orbitals (LMOs) of [PdH$_3$]$^-$, which was discussed by Landis as a hypervalent 14-electron complex with one 3c–4e H–Pd–H bond.[56–59] Both LMO methods gave three localized 2c–2e Pd–H bonds. The Pd–H$_{ax}$ bond was found to be a mixture of mainly s and d contributions of the metal, while the Pd–H$_{eq}$ bonds have almost a 1:1:1 ratio for s, p, and d character.[96] The LMO calculations suggest that the (n)p functions of the TMs may significantly contribute to the bond orbitals.

Although the VB model of Landis excludes the (n)p orbitals from the TM valence space, BH point out that the optimal exponent for a d function is roughly the same for any main-group element while an accurate representation of TM (n)p orbitals is necessary to describe correctly the energetics of TM complexes.[96,99] They refer to previous work by Couty and Hall (CH),[99] who found that the lowest lying excitation energies for the (n)s,p → (n)d transitions of the main-group elements are 2–9 times larger than the (n)s(n − 1)d → (n)p transitions of the TMs. Thus, the TM (n)p orbitals should more easily be accessible for chemical bonding than the (n)d orbitals of the main-group elements. BH introduced a method for predicting the structure of TM polyhydride complexes through the use of symmetry analysis coupled with the preferential but not exclusive bonding of the

Table 3. Orbital Counts ($d^m sp^n$) for Each Stoichiometry and d Electron Count[a]

	D^0	d^2	d^4	d^6	d^8
MH$_3$	D^{2}s	d^{2}s	d^{2}s	d^{2}s	dsp
MH$_4$	D^{3}s	d^{3}s	d^{3}s	d^{2}sp	dsp^2
MH$_5$	D^{4}s	d^{4}s	d^{3}sp	d^{2}sp^2	dsp^3
MH$_6$	d^{5}s	d^{4}sp	d^{3}sp^2	d^{2}sp^3	
MH$_7$	d^{5}sp	d^{4}sp^2	d^{3}sp^3		
MH$_8$	d^{5}sp^2	d^{4}sp^3			
MH$_9$	d^{5}sp^3				

[a] Taken from ref 96.

hydrides to the TM (n)s and ($n - 1$)d orbitals. They call it the orbitally ranked symmetry analysis method (ORSAM).[96] The difference from the scheme of Landis is that the TM (n)p orbitals are incorporated into the bonding scheme if the systems have more than 12 valence electrons, which can therefore be described without invoking hypervalency. This leads to the principle hybridization scheme for TMH$_n$ compounds shown in Table 3. Note that p orbitals are only considered if the number of valence electrons is >12. BH point out, however, that early TMs in high oxidation states may already use their (n)p valence orbitals for chemical bonding because their energy level is rather low.

The ORSAM method of BH is closely related to the application of symmetry to molecular geometry recently discussed by King.[100] The latter work is very important because it shows that certain molecular shapes of TM compounds require p orbitals in their hybridization. Table 4 is taken from the paper of King.[100] It shows the possible molecular shapes and corresponding irreducible representations of the hybrid orbitals for coordination numbers 3−6 based on the sd^5 manifold. The entries in boldface are those which have p orbitals in the hybridization. The required p orbitals in the irreducible representations are underlined. Note that the O_h and D_{3h} forms of TMH$_5$ belong to molecular shapes which require p orbitals. This is in agreement with the molecular shapes which are predicted by the sd-hybridization model of Landis.[56−59]

Table 5 shows the sets of possible geometries for TMH$_n$ compounds which are predicted by ORSAM.[96] The actual minimum energy forms have been opti-

mized at the HF and (for neutral third-row TM hydrides) MP2 levels using valence basis sets having double-ζ or triple-ζ quality. Table 6 gives the symmetries of the energy minimum structures which were found for TMH$_6$ species. The results of the geometry optimizations are in agreement with the predictions of ORSAM (Table 5), except for [TaH$_6$]$^-$. Tantalum is an early transition metal, and BH explain the D_{3h} form of [TaH$_6$]$^-$ with the incorporation of the 6p orbitals into the hybridization. The authors point out that the d^2 and d^4 complexes are hypervalent according to Landis' model[56−59] and would thus be expected to have linear H−M−H interactions. The calculations show, however, that none of the TMH$_5$ species with d^2 and d^4 configuration have linear H−M−H units.

Neither the work of BH[96] nor the work of Landis et al.[56−59] give a definite answer concerning the importance of the valence (n)p functions of the TMs for chemical bonding. Both authors present qualitative bonding models which appear to be helpful for predicting molecular shapes of covalently bound TM compounds. Landis uses the VB model as a working hypothesis for deriving functions and parameters for his molecular mechanics algorithms VALBOND.[56−59,82] Even if the VALBOND calculations would yield accurate geometries, it would not be proof of the underlying assumption that only s and d orbitals are valence functions of the TMs is correct. The answer to this can only be given through an analysis of accurate quantum chemical calculations that is not biased in the evaluation algorithm like the NBO method. The calculations of BH using the Foster−Boyd[97] and Pipek−Mezey[98] LMO methods are important in this regard, but they are restricted to only one molecule. In this context, another theoretical analysis which addresses the question of the TM valence orbitals shall be mentioned. This work is discussed in detail in the section about TM carbonyl complexes. The paper by Diefenbach, Bickelhaupt, and Frenking (DBF) gives the results of isoelectronic hexacarbonyls TM^q(CO)$_6$ (TM^q = Hf^{2-}, Ta$^-$, W, Re$^+$, Os^{2+}, Ir^{3+}), which shows that the TM 6p orbitals are energetically less important for the metal−CO interactions than the 6s and particularly the 5d orbitals but that they are not negligible.[101] It seems possible

Table 4. Irreducible Representations for the Hybrid Orbitals Corresponding to Configurations for Coordination Numbers n = 3−6 Based on an sd^5 Six-Orbital Manifold[a]

configuration	group	n	Γ_σ[b]
trigonal planar	D_{3h}	3	A$_1$(s,z^2) + E$'$(x^2-y^2,xy)
trigonal pyramidal	C_{3v}	3	A$_1$(s,z^2) + E(x^2-y^2,xy',xz,yz)
tetrahedral	T_d	4	A$_1$(s) + T$_2$(xy,xz,yz)
pyramidal	C_{3v}	4	2A$_1$(s,z^2) + E(x^2-y^2,xy',xz,yz)
square pyramid base	C_{4v}	4	A$_1$(s,z^2) + B$_1$(x^2-y^2) + E(xz,yz)
square planar	**D_{4h}**	**4**	**A$_{1g}$(s,z^2) + B$_{1g}$(x^2-y^2) + $\underline{E_u(x,y)}$**
square pyramid	C_{4v}	5	2A$_1$(s,z^2) + B$_1$(x^2-y^2) + E(xz,yz)
pentagonal pyramid base	C_{5v}	5	A$_1$(s,z^2) + E$_1$(xz,yz) + E$_2$(x^2-y^2,xy)
trigonal bipyramid	**D_{3h}**	**5**	**2A$_1'$(s,z^2) + E$'$(x^2-y^2,xy) + $\underline{A_2''(z)}$**
pentagonal pyramid	C_{5v}	6	2A$_1$(s,z^2) + E$_1$(xz,yz) + E$_2$(x^2-y^2,xy)
distorted trigonal prism	C_{3v}	6	2A$_1$(s,z^2) + 2E(x^2-y^2,xy',xz,yz)
trigonal prism	**D_{3h}**	**6**	**A$_1$(s,z^2) + E$'$(x^2-y^2,xy) + $\underline{A_2''(z)}$ + E$''$(xz, yz)**
octahedron	**O_h**	**6**	**A$_1$(s) + E$_g$(z^2,x^2-y^2) + $\underline{T_{1u}(x,y,z)}$**
bicapped tetrahedron	**C_{2v}**	**6**	**3A$_1$(s,x^2-y^2,z^2) + B$_1$(xz) + $\underline{2B_2(yz,y)}$**

[a] Taken from ref 100. [b] Polyhedra listed in boldface require p orbitals in their hybridization. The required p orbitals are underlined.

Table 5. Sets of Possible Geometries for TMH$_n$^{a}

		$\{TMH_n\}+O(<C_{2v})$
TMH$_3$	d^0	$D_{3h}, C_{3v}, C_{2v}, C_{2v}'$
	d^2	$D_{3h}, C_{3v}, C_{2v}, C_{2v}'$
	d^4	$D_{3h}, C_{3v}, C_{2v}, C_{2v}'$
	d^6	$D_{3h}, C_{3v}, C_{2v}, C_{2v}'$
	d^8	C_{2v}, C_{2v}'
TMH$_4$	d^0	$T_d, D_{2d}, C_{4v}, C_{3v}, C_{2v}, C_{2v}', C_{2v}''$
	d^2	$D_{2d}, C_{4v}, C_{2v}, C_{2v}', C_{2v}''$
	d^4	$T_d, D_{2d}, C_{4v}, C_{3v}, C_{2v}, C_{2v}', C_{2v}''$
	d^6	$D_{2d}, C_{3v}, C_{2v}, C_{2v}', C_{2v}''$
	d^8	$D_{4h}, D_{2h}, D_{2d}, C_{4v}, C_{3v}, C_{2v}, C_{2v}', C_{2v}''$
TMH$_5$	d^0	$C_{5v}, C_{4v}, C_{2v}, C_{2v}'$
	d^2	$C_{5v}, C_{4v}, C_{2v}, C_{2v}'$
	d^4	$D_{3h}, C_{4v}, C_{3v}, C_{2v}, C_{2v}', C_{2v}''$
	d^6	$D_{5h}, C_{5v}, C_{4v}, C_{2v}, C_{2v}', C_{2v}''$
	d^8	$D_{3h}, C_{4v}, C_{3v}, C_{2v}, C_{2v}'$
TMH$_6$	d^0	C_{5v}, C_{3v}, C_{3v}'
	d^2	$D_{3h}, D_{2d}, C_{5v}, C_{4v}, C_{3v}, C_{3v}', C_{2v}, C_{2v}', C_{2v}'',C_{2v}'''$
	d^4	$C_{5v}, C_{3v}, C_{3v}', C_{2v}, C_{2v}', C_{2v}'', C_{2v}'''$
	d^6	$O_h, D_{4h}, D_{3h}, D_{2h}, D_{3d}, D_{2d}, C_{5v}, C_{4v}, C_{3v}, C_{3v}',$
		$\quad C_{2v}, C_{2v}', C_{2v}'', C_{2v}'''$
TMH$_7$	d^0	$C_{5v}, C_{3v}, C_{3v}', C_{2v}, C_{2v}'''$
	d^2	$C_{2v}, C_{2v}', C_{2v}'', C_{2v}'''$
	d^4	$D_{5h}, C_{5v}, C_{3v}, C_{3v}', C_{2v}, C_{2v}', C_{2v}'', C_{2v}'''$
TMH$_8$	d^0	$D_{2d}', C_{4v}', C_{2v}', C_{2v}'', C_{2v}''''$
	d^2	$D_{4d}, D_{2d}, D_{2d}', C_{4v}', C_{2v}, C_{2v}', C_{2v}'', C_{2v}''''$
TMH$_9$	d^0	$D_{3h}, D_{3h}', C_{4v}', C_{3v}, C_{3v}', C_{2v}'$

^{a} Taken from ref 96.

Table 6. Minimum Energy Structure for TMH$_6$^{a}

	species		species		species	
d^0	[NbH$_6$]$^-$	C_{3v}	MoH$_6$	C_{3v}	[TeH$_6$]$^+$	C_{3v}
	[TaH$_6$]$^-$	D_{3h}	WH$_6$	C_{3v}	[ReH$_6$]$^+$	C_{3v}'
d^2	[TeH$_6$]$^-$	C_{2v}''	RuH$_6$	$C_{2v}''^d$	[RhH$_6$]$^+$	$<C_{2v}^c (C_S)$
	[ReH$_6$]$^-$	$<C_{2v}(C_S)$	OsH$_6$	C_{2v}''	[IrH$_6$]$^+$	$<C_{2v}^c (C_S)$
d^4	[RhH$_6$]$^-$	C_{5v}	PdH$_6$	$<C_{2v}^b$		
	[IrH$_6$]$^-$	C_{5v}	PtH$_6$	$C_{2v}''^c$		

^{a} Taken from ref 96. ^{b} Complex dissociates to H$_2$ + Pd(η^2-H$_2$)$_2$ (D_{2d}). ^{c} Dihydrogen complex: [RhH$_6$]$^+$, C_{2v} d^6 ML$_4$; [IrH$_6$]$^+$, C_S d^4 ML$_5$; PtH$_6$, D_{4h} d^8 ML$_4$. ^{d} MP2-optimized geometry.

that the participation of the TM (n)p orbitals may depend on the nature of the interactions (covalent or donor−acceptor bond) and on the nature and oxidation state of the bound atoms. There clearly is a need for quantum chemical investigations which address this question. The results presented so far suggest that the (n)p functions may be more important for the TM bonds than the (n)d functions for the main-group elements.

The work of Landis et al.[56−59] and Bayse and Hall[96] clearly shows that the analysis of TM bonding in terms of covalent sd- or (sd + p)-hybridized bonds is a valuable alternative to the traditional way of describing TM bonds in terms of donor−acceptor interactions. Other authors attribute the distortion of TMR$_6$ and TMR$_5$ molecules, where R has little or no π-bonding capacity, to a second-order Jahn−Teller effect, which leads to symmetry distorted structures that have an improved overlap between ligand and metal d orbitals.[72,84,102] The starting point of this explanation is a MO diagram which uses the (n)p orbitals of the TMs as a valence function.

A polarization of the outermost core electrons by the substituents has also been proposed as an important factor which may distort the otherwise highly symmetric forms of TM compounds.[103] The latter effect was suggested in order to rationalize why the VSEPR model fails to explain the distortion of the maximum molecular symmetry of some metal compounds including TM complexes.[104] Calculations of Landis et al. have shown, however, that the C_{3v} and C_{5v} forms of WH$_6$ are predicted even when a nonpolarizable effective core potential for W is employed.[57] The preference for these molecular shapes over the highly symmetric O_h form can easily be explained with the sd^5-hybridization model, which for symmetry reasons does not give an octahedral configuration but only C_{3v} and C_{5v} geometries (Table 4).

While many TM alkyls and hydrides have geometries which do not have maximum symmetry, TMX$_n$ compounds, where X is a very electronegative element like halogen or chalcogen, usually exhibit highly symmetric structures. For example, OsO$_4$ has T_d symmetry, VF$_5$, NbCl$_5$, and TaCl$_5$ have D_{3h} symmetry, and WX$_6$ (X = F, Cl, Br) has O_h symmetry. The geometry of CrF$_6$ has been controversially discussed. An octahedral equilibrium structure was theoretically predicted using MP2 calculations by Kang et al.[84] Marsden and Wolynec found that the D_{3h} form of CrF$_6$ was lower in energy than the O_h structure.[105] All recent calculations agree that CrF$_6$ has O_h symmetry.[364]

IV. Quantum Chemical Methods for Analyzing the Chemical Bond

The past decades have not only witnessed unprecedented progress in sophisticated quantum chemical methods for calculating measurable properties of molecules such as energies, geometries, vibrational frequencies, etc., but theoretical methods have also been developed in order to analyze the calculated electronic structure aiming to give insight into the bonding situation of the molecule, thus following the famous appeal of Charles Coulson "Give us insight, not numbers". The impressive state-of-the-art of computational chemistry has recently been summarized in the five-volume set *Encyclopedia of Computational Chemistry*.[106]

The goal of the interpretative theoretical research is to present models which help to qualitatively understand and predict the structures and reactivities of molecules. The numbers and pictures given by these models must be useful to order the manifold of chemical phenomena in a way which helps the chemist to understand the physical world on a molecular scale. At the same time the model should form a bridge between the chemical behavior of a molecule and the underlying physical laws. This is a difficult task, because heuristic models and historically grown ad hoc concepts as well as chemical intuition, which play an fundamental role in chemical research, are usually not based on physical laws. It is not easy to find a quantum chemical approach for chemical intuition. For example, the charge distribution in a molecule is often used to explain its structure and reactivity. However, atomic partial charges are not an observable quantity. A large variety of partitioning schemes of the molecular charge distribution in atomic subdomains has been suggested in the literature.[320] The acceptance of a particular partitioning scheme is often determined

by the answer to the question of whether the calculated partial charges agree or disagree with chemical intuition. This may be misleading, because the actual charge interactions between atoms and molecules are significantly influenced by the three-dimensional charge distribution of the interacting species which can be very anisotropic.

In the following we will give a short outline of the essential features of six quantum chemical methods which are now widely used for analyzing the chemical bond in TM compounds. These are the natural bond orbital (NBO) method developed by Weinhold,[92,93] the charge distribution analysis (CDA) proposed by Dapprich and Frenking,[107] the atoms-in-molecules (AIM) method suggested by Bader,[108] and the energy decomposition analysis (EDA) of Morokuma[109] which is very similar to the extended transition state (ETS) method of Ziegler and Rauk.[110] We will also discuss the constrained space orbital variation (CSOV) method by Bagus, Hermann, and Bauschlicher.[111] We will focus on the strength and weakness of the methods rather than on the mathematical details which can be found in the original literature. We want to point out that an overview of methods for electronic wave function analyses has recently been presented by Cioslowski.[112]

IV.1. Natural Bond Orbital Methods

The pivotal point in any quantum chemical partitioning scheme for assigning the electronic charge distribution to different regions in space is the definition of the atomic subspaces in a molecule. The partitioning can either be defined in the $3N$-dimensional Hilbert space which is spanned by the basis functions in terms of the atomic and molecular orbitals or by dividing the 3-dimensional space of the electronic charge distribution into atomic basins. Most definitions of atomic partial charges are based on orbital concepts. The still very popular and widespread Mulliken population analysis[95] has the disadvantage that the results are unduly sensitive to the basis set and that the calculated population can have unphysical negative numbers. It seems that the Mulliken analysis has been replaced by the superior NBO method, which is quite robust toward changing the basis set and which can be used for HF and correlated wave functions as well as for DFT methods. The NBO method[92,93] uses the one-electron density matrix as the starting point for the partitioning procedure. The first step is the diagonalization of the one-center (atomic) blocks, which yields the pre-natural atomic orbitals (pre-NAOs). This is a straightforward procedure.

The second step is crucial in the NBO method particularly for TM compounds. The pre-NAOs at the different atoms which are not orthogonal to each other become orthogonalized yielding the natural atomic orbitals (NAOs). The pre-NAOs are first divided into two sets. One set consists of the strongly occupied minimal basis set which describes the atomic electron density in the ground state. The other set consist of the remaining weakly occupied orbitals which are called Rydberg functions. The subsequent sequence of orthogonalization steps treats the mini-

mal functions and the Rydberg functions in different ways. The "occupancy-weighted symmetric orthogonalization" (OWSO transformation), which was developed with the goal of preserving maximum resemblance of the NAOs with the pre-NAOs, strongly favors the minimal basis set in the description of the NAOs. Another reason for introducing the weighting factor was to ensure the stability of the orthogonalization procedure toward basis set enlargement.[113] The results of the NBO analysis are indeed quite robust against changing the basis set. However, it is important to recognize that the weighting factor automatically disfavors atomic basis functions which are empty in the atomic ground state in the description of the chemical bond. Thus, the NBO method excludes a priori the outermost d orbitals of the heavier main-group elements and the outermost p orbitals of the TMs from the valence space! It has been shown by Maseras and Morokuma (MM)[94] that the outermost p orbitals of the transition metals become significantly occupied if they are part of the valence functions during the orthogonalization procedure. Thus, the results of the NBO method cannot be used to investigate the question of whether the d functions of main-group elements and the p functions of the TMs are true valence orbitals or polarization functions, because the answer is already enforced by the preselection of the orbitals belonging to the valence space in the occupancy-weighted orthogonalization.

The third step of the NBO algorithm is the calculation of the natural hybrid orbitals (NHOs) which form the two-center (sometimes three-center) natural bond orbitals (NBOs). The density matrix in the NAO basis is first partitioned into one-center and two-center subblocks. Each one-center block is searched for NAOs which have an occupancy ≥ 1.90 e. These one-center orbitals are labeled as core or valence lone-pair orbitals. The latter are depleted from the two-center subblocks which are then orthogonalized (again via OWSO transformation) yielding the final orthogonal set of NHOs. This leads to a set of $N/2$ (N being the number of electrons) NBOs. The search for NBOs is then repeated with lower occupancy thresholds than 1.90 e in steps of 0.1 e up to 1.50 e. The set of NBOs which accommodates most electrons is then given as the optimal Lewis structure of the molecule.

A nice feature of the NBO method is that the strength of the intramolecular orbital interactions can be estimated either by a perturbation calculation or by deleting the pair of interacting orbitals from the Fock matrix. The NBO method has lately been extended to quantitatively investigate the phenomenon of resonance ("natural resonance theory").[114] This and other features of the NBO approach are described in the literature.[92,93,114]

IV.2. Charge Decomposition Analysis

Another orbital-based population analysis is the CDA[107] method, which has been developed in order to analyze chemical bonding in donor–acceptor complexes. The CDA can be seen as a quantitative expression of the Dewar–Chatt–Duncanson (DCD) model[54] of synergistic metal–ligand bonding, which

considers the ligand → metal σ-donation and ligand ← metal π-back-donation as the dominant factors for the metal−ligand bond. Because donor−acceptor bonds are much more common in TM chemistry than in main-group chemistry, the CDA has mainly been used to investigate the chemical bonds of TM compounds. In the CDA, the wave function of a complex $L_nTM−X$ is expressed as a linear combination of the fragment molecular orbitals of the ligand X and the remaining metal fragment L_nTM both in closed-shell configurations. The orbital contributions of the fragments to the wave function of the complex are divided into four parts: (i) mixing of the occupied MOs of X and the unoccupied MOs of L_nTM (donation X → TML_n); (ii) mixing of the unoccupied MOs of X and the occupied of L_nTM (back-donation X ← TML_n); (iii) mixing of the occupied MOs of X and the occupied MOs of L_nTM (repulsive polarization X ↔ TML_n); (iv) mixing of the unoccupied MOs of X and the unoccupied MOs of L_nTM (rest term Δ). The latter term should not contribute to the electronic structure of the complex. It has been found that the rest term is a sensitive probe if the compound can be classified as a donor−acceptor complex.[115,116] A significant deviation from $\Delta = 0$ indicates that the bond L_n-TM−X has the character of a normal covalent bond between two open-shell fragments, rather than a donor−acceptor bond between a Lewis acid and Lewis base. Since the donation and the back-donation are calculated for each MO separately, it is possible to estimate the contributions of the ligand → metal σ-donation and ligand ← metal π-back-donation to the total charge exchange. The CDA may be used in conjunction with HF and natural orbitals from correlated calculations and with Kohn−Sham orbitals given by DFT calculations. Early test calculations showed that the CDA results do not change significantly when the basis set becomes larger.[107] However, more recent work has shown that the CDA may deteriorate with larger basis sets.[303]

IV.3. Atoms-In-Molecules

A theoretical tool for analyzing the electronic structure of a molecule which is not based on orbitals but rather on the electron density distribution is the AIM method.[108] An attractive feature of the AIM model is that the electron density is an observable quantity. Therefore, the AIM procedure may also be used in conjunction with experimental results. The central idea of AIM is that the topology of the electron density distribution $\rho(\mathbf{r})$ contains information about the bonding situation which can be elucidated when $\rho(\mathbf{r})$ becomes the subject of a mathematical analysis. It has been shown that the topological analysis of $\rho(\mathbf{r})$, its first derivative (gradient field) $\nabla\rho(\mathbf{r})$, and second derivative (Laplacian) $\nabla^2\rho(\mathbf{r})$ reveals helpful information about the electronic structure of a molecule. Another very attractive feature of the AIM method is that the results of the topological analysis directly give the atomic subspaces (basins) of a molecule and the bonding connectivity between the atoms. Atomic basins are defined as the regions in Cartesian space that are bordered by zero-flux surfaces in the gradient of the electron density. Bader

could show[108] that the virial theorem holds for the thus defined atomic basins, which can be considered as a rigorous quantum theoretical proof that the model of discussing the chemical behavior of a molecule in terms of atomic properties is justified.

The position of the atomic nucleus is defined in the AIM model as a critical point in the three-dimensional space where the first derivatives $\nabla\rho(\mathbf{r})$ are zero and the principle curvatures (eigenvalues) of the associated second derivatives of $\rho(\mathbf{r})$ are all negative. Other critical points at which the gradient of the electron density $\nabla\rho(\mathbf{r})$ vanishes define bonds, rings, and cages. The zero-flux surfaces which separate the atomic basins are defined as the gradient vector field whose trajectories of $\nabla\rho(\mathbf{r})$ do not vanish at the atomic nuclei but at the bond critical point $\mathbf{r}_b$. A bond critical point $\mathbf{r}_b$ has two negative and one positive eigenvalues of the second derivatives of $\rho(\mathbf{r}_b)$. The trajectory which belongs to the positive eigenvalue connects the bond critical point $\mathbf{r}_b$ and the bonded atomic nuclei. It is called the bond path and thus gives a physically sound description of the skeletal structure of the molecule in terms of atomic nuclei and chemical bonds.

The results of the topological analysis are often visualized in graphical plots. Figure 26a, which will be discussed later in the section about carbene complexes, shows an example of a two-dimensional pictorial representation of the topological analysis of $(CO)_5WCH_2$ in the plane which contains the carbene carbon atom (right), tungsten, and the CO ligand which is trans to the CH_2 group. The solid lines which separate the atoms indicate the zero-flux surfaces crossing the plane. The solid lines which connect the atoms are the bond paths. The bond paths at tungsten do not end at the nucleus because the core electrons of W have been replaced by an ECP. The remaining thin lines give the Laplacian distribution in the plane, i.e., they show the values of the second derivative $\nabla^2\rho(\mathbf{r})$. Solid lines show areas where $\nabla^2\rho(\mathbf{r}) < 0$, which indicates relative charge concentration. Dashed lines show areas of relative charge depletion ($\nabla^2\rho(\mathbf{r}) > 0$). Figure 26a shows that the areas of charge concentration nicely correlate with conventional bonding models. For example, the CO ligand and the carbene carbon atom have an area of charge concentration toward the tungsten atom which can be identified as the carbon σ lone pairs. The arrows at the carbene carbon atom show the area of charge depletion which comes from the empty $p(\pi)$ AO at C. This can be correlated with the direction where a nucleophilic attack may occur.

Although the AIM method is the most straightforward partitioning scheme of the electronic structure of a molecule, it has not yet been fully accepted by the chemical community as a model for describing the bonding situation in chemical compounds. One reason is that it is sometimes difficult to connect traditional bonding concepts with the results of the AIM analysis. The bonding connectivity given by the bond paths does not always agree with the notion of a chemical bond. Also, the atomic partial charges which are obtained by integrating $\rho(\mathbf{r})$ over the atomic basins suggest that molecules are usually

much more ionic than generally assumed and predicted by orbital based methods such as the NBO model. The partial charge at the carbon atom of CO given by the AIM method is +1.40,[122] which indicates a much higher ionic character than traditionally assumed. Another example is BF_3. AIM calculations give a partial charge of +2.58 at the boron atom.[123] It has therefore been suggested that the rather short B–F bonds in BF_3 should not be discussed in terms of B ← F π-donation yielding partial double bonds, but rather as strong ionic bonds between B^{3+} and F^-.[123] This unorthodox view of the nature of the chemical bond challenges traditional concepts. The correspondence between orbital concepts and electron distributions was analyzed,[124] and attempts have been made to establish links between the AIM method and classical bonding models such as bond order. Cioslowski and Mixon (CM)[125] proposed covalent bond orders which are based on partitioning of the number of electrons within the topological theory of AIM. The covalent bond order according to CM for CO calculated at HF/6-31G(d) is 1.509.[125] The orbital-based Wiberg bond order[126] gives a value of 2.14 at the same level of theory,[127] which is closer to the traditional notion that CO has a weak triple bond. However, the trend of the bond orders defined by CM agrees with orbital-based models.[125] Another criterion for the degree of covalency which is based on the AIM model is the energy density at the bond critical point H_b. Cremer and Kraka (CK)[128] have shown that covalent bonds (shared-electron interactions) have negative values for H_b while ionic bonds and van der Waals bonds (closed-shell interactions) have $H_b \geq 0$.

IV.4. Energy Decomposition Methods: ETS, EDA, and CSOV

The three methods NBO, CDA, and AIM are partitioning schemes for the electronic *charge* distribution in a molecule. There are also important methods which define the partitioning of the *energy* of a chemical bond in different contributions. One method is the EDA of Morokuma,[109] which is very similar to the ETS method that was introduced by Ziegler and Rauk.[110] The basic ideas of the EDA and ETS methods are the following.

The total bond energy ΔE of a bond A–B is partitioned into four components which are calculated separately in four consecutive steps:

$$\Delta E = \Delta E_{\text{prep}} + \Delta E_{\text{els}} + \Delta E_{\text{Pauli}} + \Delta E_{\text{orb}}$$

ΔE_{prep} is the energy which is necessary to promote fragments A and B from their equilibrium geometry and electronic ground state to the geometry and electronic state which they acquire in the compound AB. ΔE_{els} is the electrostatic interaction energy between the fragments which are calculated with a frozen electron density distribution in the geometry of the complex. This term is usually attractive. ΔE_{Pauli} gives the repulsive energy caused by exchange (Pauli) repulsion, which is calculated when the wave function after step two is orthogonalized and antisymmetrized. The energy terms ΔE_{els} and ΔE_{Pauli} are frequently summed up to give the so-called steric

term ΔE°:

$$\Delta E^\circ = \Delta E_{\text{els}} + \Delta E_{\text{Pauli}}$$

ΔE° should not be confused with the loosely defined steric interaction between substituents in a molecule. The final term ΔE_{orb} gives the stabilization which arises from the orbital interactions when the wave function in step four is relaxed. The latter term can be broken down into orbital contributions with different symmetry. This makes it possible to calculate energy contributions by σ and π interactions separately.

Other methods which have been developed for partitioning the bond energy are not as widely used as those above. Another energy partitioning scheme which has been applied to TM–carbonyl bonds[132] is the constrained space orbital variation (CSOV) method by Bagus, Hermann, and Bauschlicher (BHB).[111] Like the EDA and ETS methods, the CSOV partitioning scheme uses the frozen orbitals of the fragments as the starting point for the energy decomposition by superimposing them fixed at their separated unit character. Starting from the superposition of the fragments, the wave function of the complex is optimized in a series of steps. The energy changes which are associated with changing the size of the variational space indicate the importance of the different orbital interactions for the bond energy.

V. Classes of Transition-Metal Compounds

In the following sections we will review recent theoretical work about chemical bonding in different classes of TM compounds. We will focus on selected classes of TM compounds as representative examples for different kinds of TM–ligand bonding interactions. It is not possible to cover chemical bonding of all classes of TM compounds, but the theoretical work which will be reviewed and discussed is comprehensive enough to show the progress that has been made in the past decade in gaining insight into the chemical bond of transition metals.

V.1. Carbonyl Complexes and Related Compounds

Carbonyl complexes are the theoretically best investigated class of TM compounds, and many studies have been devoted to the analysis of the TM–CO interactions. The dominant bonding model considers the TM–CO bond in terms of donor–acceptor interactions between (a) the 5σ HOMO of CO and an empty TM AO of σ symmetry (usually the d_{z^2} orbital) and (b) occupied π-type d orbitals of the TM and the degenerate $2\pi^*$ MO of CO. This is schematically shown in Figure 8.

The model of synergistic OC → TM σ-donation and OC ← TM π-back-donation is an example of the DCD model of TM–ligand orbital interactions which was already mentioned above.[53,54] Many theoretical studies using ab initio methods appeared in the 1980s and early 1990s evaluating the relative contribution of σ-donation and π-back-donation to the TM–CO interactions. Using different partitioning techniques,
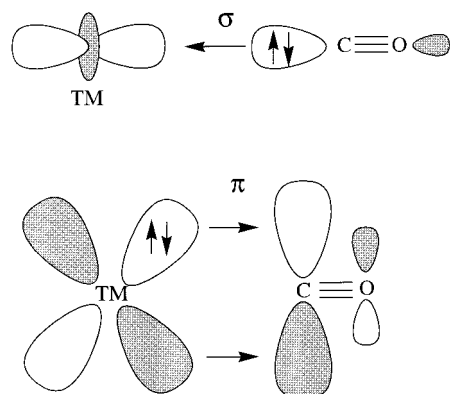
Figure 8. Schematic representation of the synergistic OC → TM σ-donation and OC ← TM π-back-donation.

all studies agree that for the TM–CO bond energy π-back-bonding is more important than σ-donation.[132-156] There was one early X_α DFT calculation which predicted that σ-donation should be more important than π-back-donation.[157] More recent calculations using different methods showed that the prediction is not justified.[132-156] It is important to realize that the change in the charge distribution caused by the σ and π interactions does not automatically indicate the size of the associated energy changes.

The most thorough theoretical analysis of the TM–carbonyl bond was presented in three benchmark papers in 1992–1993 by Davidson and co-workers.[129-131] They calculated $Cr(CO)_6$ at the Hartree–Fock[130] and correlated[131] levels of theory and analyzed the Cr–CO bonding interactions using the EDA energy partitioning scheme developed by Morokuma.[109] The EDA method and the very similar ETS procedure of Ziegler[110] have been described in the methods section. The results for $Cr(CO)_6$ were as follows.[129-131]

The energy ΔE_{prep} which is calculated in the first step involves the excitation of a Cr atom from the (s^1d^5) ^7S ground state to the (t_{2g}^6) $^1A_{1g}$ excited state. For CO, it means a slight stretching of the C–O distance. Table 7 shows the calculated energies ΔE_{prep} at the HF level using large atomic basis sets.[129] The $^7S \rightarrow t_{2g}$ excitation energy of Cr is very high (232 kcal/mol), while the stretching of the 6 CO molecules requires only 6 kcal/mol.

The second step assembles the promoted bonding partners Cr and 6 CO into the position of $Cr(CO)_6$ and then calculates the molecule using the frozen electron densities of the fragments. This gives the electrostatic contribution ΔE_{els} which is due to purely electrostatic interactions between the binding partners. Table 7 shows that the cage formation of $(CO)_6$ without the metal yields a small stabilization of −26 kcal/mol. The Cr insertion into the ligand cage leads to an energy lowering by −272 kcal/mol caused by Coulomb attraction. The electronic structure of $Cr(CO)_6$ after step two violates the Pauli principle, which is considered in step three. The wave function of $Cr(CO)_6$ is now antisymmetrized and orthogonalized but not fully optimized. The calculated energy in step 3 gives the Pauli repulsion (exchange repulsion) ΔE_{Pauli} between electrons that have the same

Table 7. Breakdown of the Energy Contributions to the Formation of $Cr(CO)_6$ at the HF, DFT, and MR–CI Levels of Theory Given by the EDA Method[a]

step	system	HF	DFT	MR–CI	exp
ΔE_{prep}	Cr $^7S \rightarrow t_{2g}^6$	232	155	159	
	6CO stretch	6	0	0	
	Σ	238	155	159	
ΔE_{els}	$(CO)_6$	−26			
	$Cr(CO)_6$	−272			
	Σ	−298			
ΔE_{Pauli}	$(CO)_6$	110			
	$Cr(CO)_6$	357			
	Σ	467			
$\Delta E° = \Delta E_{els} + \Delta E_{Pauli}$		169	104		
ΔE_{orb}	t_{2g}	−204			
	e_g	−68			
	other	−54			
	Σ	−321[b]	−417		
$\Delta E_{els} + \Delta E_{Pauli} + \Delta E_{orb}$		−152	−313	−306	
$\Sigma\Delta E$		86	−158	−147	−162

[a] Taken from ref 129. Values are given in kcal/mol. [b] The sum of the orbital relaxation was corrected for BSSE effects, which are not included in the individual orbital contributions (Davidson, E. R. Personal communication).

spin. Table 7 shows that the Pauli repulsion makes the largest contribution to the overall Cr–CO interactions! The cage assembly of $(CO)_6$ contributes with 110 kcal/mol, and the insertion of Cr adds another 357 kcal/mol.

The final step, four, considers the relaxation of the orbitals among the fragments. This gives the orbital interaction energy ΔE_{orb} that is usually considered as the dominant term for the bond formation. Therefore, the Pauli repulsion ΔE_{Pauli} and the Coulomb interaction ΔE_{els}, which have opposite signs and roughly cancel, are frequently added to give the energy term $\Delta E°$ called steric interaction.[109,110] It is an arbitrary decision to add ΔE_{Pauli} and ΔE_{els} into a single term $\Delta E°$ and to correlate only ΔE_{orb} with the bond energy. It seems that the EDA and ETS partitioning schemes overestimate the size of the Coulombic interactions. Table 7 shows that the calculated value for $\Delta E_{els} = -298$ kcal/mol is much higher than the total bond energy, which would suggest that $Cr(CO)_6$ is only bound by electrostatic forces. The overestimation of the electrostatic forces appears to be partly corrected by the ΔE_{Pauli} term, which justifies the addition of the two terms into a single term $\Delta E°$.

The results in Table 7 show that the metal–CO orbital interactions are *not* the largest term of the TM–CO bond energies! The breakdown of the orbital relaxation term ΔE_{orb} into orbitals of different symmetry clearly shows that the t_{2g} orbitals, which give the OC ← TM π-back-donation, contribute much more to the bond energy (−204 kcal/mol) than the e_g orbitals (−68 kcal/mol), which give the largest part of the OC → TM σ-donation. The remaining −54 kcal/mol comes from σ-donation of orbitals with other symmetry (−37 kcal/mol), while −17 kcal/mol stems from orbital relaxation of the cage orbitals of $(CO)_6$ without metal–CO interactions.[129] It is important to recognize that the contributions to the stabilizing energy term ΔE_{orb} arise not only from interactions
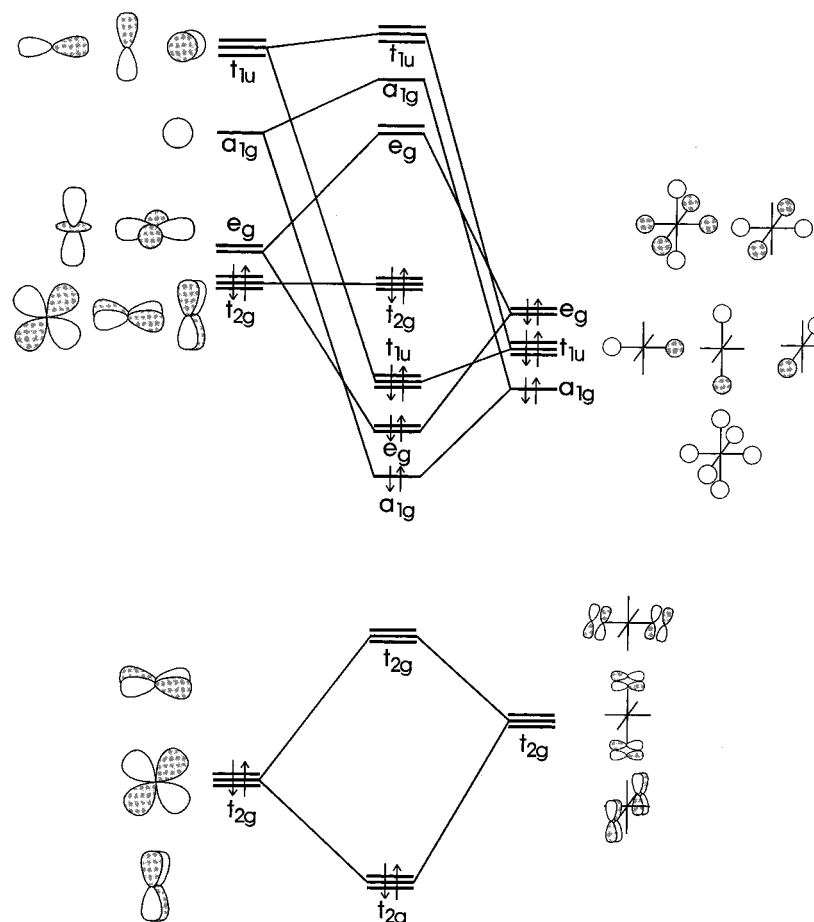
Figure 9. Splitting of the orbital energy levels of an octahedral d^6 transition-metal complex TML_6 where the ligand L has occupied donor orbitals with σ symmetry (top) and empty acceptor orbitals with π symmetry.

between the two fragments, but also from relaxation of orbitals at one fragment without mixing with orbitals at the other fragment. Thus, part of the stabilization energy given by ΔE_{orb} is actually due to electrostatic effects which stabilize the orbitals in the relaxation step. Energy effects due to BSSE have been prevented by including the Cr basis functions during the relaxation step of the $(CO)_6$ orbitals.[129] It should be noted that the partitioning of the energy terms into unique orbital contributions can only be made with a predefined choice of a partitioning scheme. Davidson et al. have tested several such procedures.[130] All methods agree that the (3d) t_{2g} relaxation is the dominant term.

It is illuminating to compare the standard orbital interaction diagram for $M(CO)_6$ that is found in many textbooks (Figure 9) with the change in the orbital energy levels after the various steps of the EDA given by Davidson et al.[129] Figure 10 shows on the left-hand side the effect of the $(CO)_6$ ligand cage formation, the steric interactions when a promoted Cr atom is inserted into the ligand cage which leads to the wave function Ψ^o, and finally the relaxation of the wave function. The right-hand side shows the effect of the electron excitation of the Cr atom.

The orbital interaction diagram shown in Figure 9 indicates that the OC → TM σ-donation involves the t_{1u}, e_g, and a_{1g} orbitals, while OC ← TM π-back-donation takes place through the t_{2g} orbital. From the calculated energy values associated with the
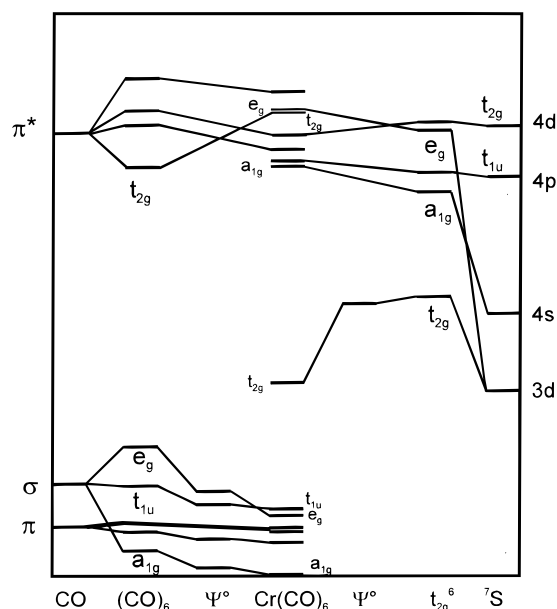
Figure 10. Calculated orbital energies (eV) after various steps of the EDA in forming $Cr(CO)_6$. (Reproduced with permission from ref 129. Copyright 1993 American Chemical Society.)

orbital interactions (Table 7), it might be concluded that the (t_{2g}) OC ← TM π-back-donation is much more important for the bond formation than the σ-donation and that only the e_g orbitals are significant for the (less important) σ-donation. This picture about the
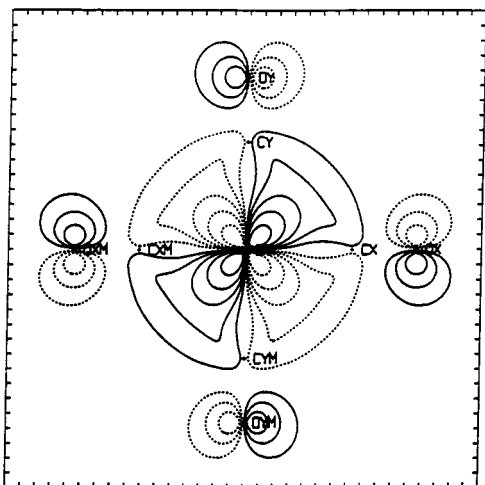
Figure 11. Contour plot of the 3d t_{2g} xy orbital of $Cr(CO)_6$. (Reproduced with permission from ref 129. Copyright 1993 American Chemical Society.)

Cr—CO bonding interaction must be modified when the change in the orbital energies shown in Figure 10 are considered. The most relevant information concerns the change in the energy level of the 5σ (e_g) orbital of the cage $(CO)_6$ when the $Cr(t_{2g}^6)$ atom is inserted (Ψ^o). There is a large energy lowering of the orbital which already takes place prior to the orbital relaxation step, i.e., it is a purely electrostatic effect *without* covalent bond formation. The breakdown of the energy contributions (Table 7) shows that the electrostatic attraction between chromium and the hexacarbonyl cage is very large (−272 kcal/mol), which comes mainly from the penetration of the occupied 5σ orbitals of $(CO)_6$ into the metal 3spd shell leading to less shielding and thus stronger attraction by the highly charged metal nucleus. The metal 3d-(t_{2g}) orbital energy by contrast is nearly unchanged in the metal insertion step (Figure 10). Note that the steric energy of the Cr insertion step is repulsive, despite the lowering of the orbital energy levels. This comes from the large Pauli repulsion (357 kcal/mol) which compensates for the electrostatic attraction.

The energy level of the $3d(t_{2g})$ orbital lowers considerably in the orbital relaxation step, while the $\pi^*(t_{2g})$ orbital increases in energy (Figure 10). This could be taken as evidence for the Cr—CO bond energy contribution caused by OC ← Cr π-back-donation (Figure 9). Davidson et al. give a different interpretation.[129] Inspection of the contour map of the $3d(t_{2g})$ metal orbital after relaxation (Figure 11) shows that the orbital has become more diffuse but has acquired very little metal—CO bonding character. There is an increased shielding of the 3d electrons from the metal nucleus by the penetrating CO 5σ electrons, which makes the 3d orbital more diffuse and leads to some mixing with the empty $2\pi^*(t_{2g})$ orbital of the ligand cage. However, the mixing is described as primarily not a covalency effect but a relaxation of the 3d electrons.[130] This is the reason the authors did not draw a line between the $3d(t_{2g})$ metal orbital and the $\pi^*(t_{2g})$ orbital of $(CO)_6$.

The sum of the energy contributions to the Cr—CO interactions in $Cr(CO)_6$ at the HF level is +86 kcal/mol, i.e., $Cr(CO)_6$ is thermodynamically unstable at this level of theory. Davidson et al.[129,131] investigated the influence of the correlation energy on the Cr—CO bond energy. They found two major contributions to the total bond energy which lead to a reasonable agreement with the experimental value. The first contribution is not directly related to the metal—CO interaction. This is the Cr $^7S \rightarrow t_{2g}$ excitation energy which is poorly described at the SCF level. The second major contribution to the correlation energy comes somewhat unexpectedly from the charge-transfer double replacement ($3d(t_{2g})$ $\rightarrow 2\pi^*(t_{2g})$) ($5\sigma$ (e_g) $\rightarrow 3d(e_g)$).[129,131] This describes the correlation between the electrons in the 5σ CO orbitals moving toward chromium and the electrons in the Cr $3d(t_{2g})$ orbital moving toward the $2\pi^*$ orbital of CO. This can be regarded as dynamic shielding of the $3d(t_{2g})$ orbital of the metal by the 5σ electrons of the ligand cage, while the expansion of the $3d(t_{2g})$ orbital in the relaxation step may be considered as static shielding. Davidson et al. conclude that "the driving force for the bond is the electrostatic energy from the penetration of the 5σ electrons into the chromium valence shell".[129] The work of Davidson et al.[129–131] shows that *the physical origin of the metal–CO bonds in $Cr(CO)_6$ is different from the common bonding model* given in Figure 9, although the EDA calculation gives numerical values that can be associated with the orbital interactions which are considered in the model.

Davidson et al. also presented an energy partitioning analysis for $Cr(CO)_6$ using DFT calculations, and they compared the results with the ab initio calculations.[129] The numerical values are shown in Table 7. The advantage of using DFT calculations is that the Kohn—Sham orbital energies include correlation effects, and thus, orbital contributions can be directly correlated with total energies. The disadvantage is that the exchange and correlation energy in DFT calculations depend in an unphysical way on the parametrization of the functionals. It was found that the energy partitioning of the total bonding energy and the energy change for each physical step of the bonding analysis (cage assembly 6 CO → $(CO)_6$ and Cr insertion) are similar at the DFT and ab initio approaches, but the correlation effects in the ab initio calculations are mostly accounted for by a different estimate of the exchange energy in the DFT method.[129] Table 7 shows that the energy values for ΔE_{prep} and for the sum of the interactions $\Delta E_{els} + \Delta E_{Pauli} + \Delta E_{orb}$ at the DFT and MR—CI levels are very similar. It follows that DFT calculations may also be used for gaining insight into the metal—ligand interactions, but the partitioning of the energy contributions into exchange repulsion and correlation terms can be very different from ab initio calculations.

A similar energy partitioning for the metal—CO bond as given by Davidson et al.[129–131] for $Cr(CO)_6$ has recently been presented for the series of isoelectronic hexacarbonyls $TM^q(CO)_6$ ($TM^q = Hf^{2-}$, Ta^-, W, Re^+, Os^{2+}, Ir^{3+}) at the nonlocal DFT level by Diefenbach, Bickelhaupt, and Frenking (DBF).[101] The work was a sequel of a previous study by Szilagyi and Frenking[158] (SF) which focused on analysis of the charge distribution. SF calculated the relative OC →
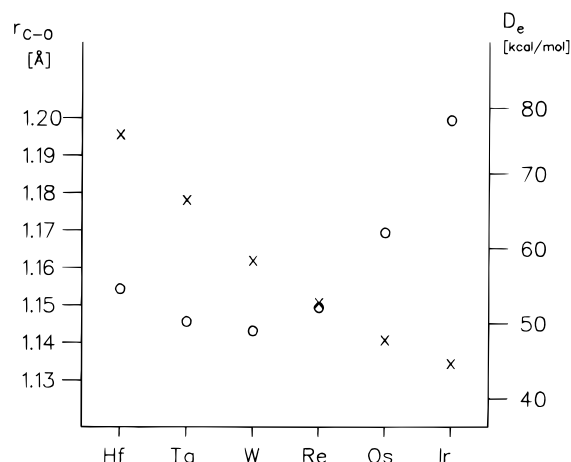
Figure 12. Trends of the calculated FBDE D_e and the C−O bond lengths at BP86/II of the TM hexacarbonyls $TM^q(CO)_6$. (Reproduced with permission from ref 158. Copyright 1997 American Chemical Society.)

TM^q electron donation and OC ← TM^q back-donation with the CDA method and compared the results with the trend of the calculated and experimental C−O bond distances and stretching frequencies. The authors found a regular decrease of the C−O bond length, increase of the C−O stretching mode, and decrease of OC ← TM^q π-back-donation from $Hf(CO)_6^{2-}$ to $Ir(CO)_6^{3+}$.[158] The correlation, which is in agreement with the DCD model of TM−CO bonding, was not surprising. Unexpected were the results for the calculated first bond dissociation energies (FBDE), which showed that the neutral complex $W(CO)_6$ has the lowest FBDE, while the negatively charged hexacarbonyls and particularly the positively charged species have much higher FBDEs. Since it was firmly established that the OC ← TM π-back-donation gives the largest contribution to the orbital interactions, a regular decrease of the FBDE from $Hf(CO)_6^{2-}$ to $Ir(CO)_6^{3+}$ might have been expected. Figure 12 shows the surprising trend of the FBDE, which does not correlate with the C−O distance.

DBF[101] analyzed the FBDEs $(CO)_5TM^q$−CO and the total bond energies TM^q-$(CO)_6$ using the ETS method of Ziegler and Rauk.[110] Since the partitioning scheme of the ETS method is basically the same as that in the Morokuma analysis,[109] the results of DBF
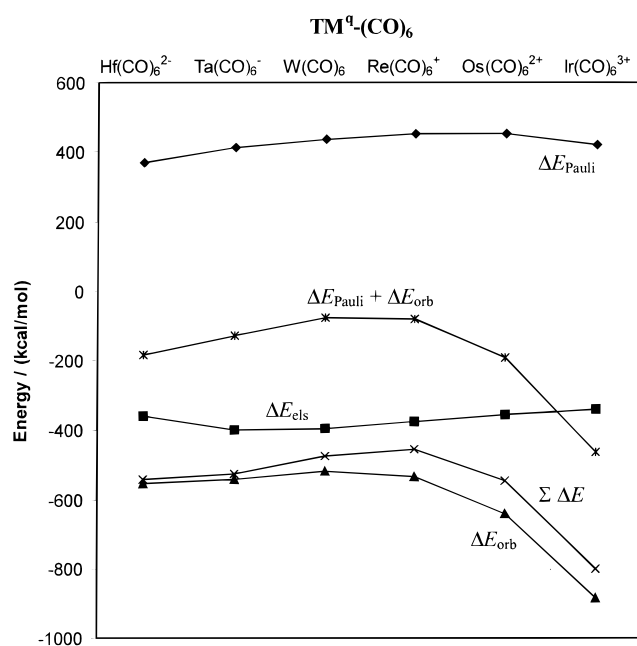
Figure 13. Trend of the various terms of the ETS decomposition of TM^q−$(CO)_6$. (Reproduced with permission from ref 101. Copyright American Chemical Society.)

may be compared with the study of Davidson et al.[129] about $Cr(CO)_6$. We will first discuss the results of the energy partitioning of the total bond energies TM^q-$(CO)_6$. The most important results are summarized in Table 8. Because the bonding analysis focused on the metal−CO interactions, the energies for promotion of the fragments and for the cage assembly 6CO → $(CO)_6$ are not given. Thus, the ΔE values refer to the binding interactions between TM^q in the t_{2g}^6 state and $(CO)_6$.

Table 8 shows that the calculated binding energies ΔE reported by DBF[101] exhibit a comparable U-shaped trend from $Hf(CO)_6^-$ to $Ir(CO)_6^{3+}$ as found for the FBDEs (Figure 12), except that the lowest total bond energy is now found for $Re(CO)_6^+$. The largest total bond energy ΔE (Table 8) and FBDE (Figure 12) is predicted for $Ir(CO)_6^{3+}$. Figure 13 shows the trend of the various terms of the binding energies of the metal carbonyls. It becomes obvious that the orbital interaction energies ΔE_{orb} correlate nicely with the trend of ΔE. The same holds true for the

Table 8. ETS Analysis of the Binding Interactions between TM^q and $(CO)_6$ in TM Hexacarbonyls[a]

|	$Hf(CO)_6^{2-}$	$Ta(CO)_6^-$	$W(CO)_6$	$Re(CO)_6^+$	$Os(CO)_6^{2+}$	$Ir(CO)_6^{3+}$
ΔE_{Pauli}	367.4	413.4	438.8	454.5	451.3	420.9
ΔE_{els}	−358.6	−397.6	−396.2	−375.1	−353.4	−337.8
$\Delta E^0 = \Delta E_{els} + \Delta E_{Pauli}$	8.8	15.8	42.6	79.4	97.9	83.1
a_{1g}	−9.5	−10.5	−15.4	−27.4	−47.6	−78.8
a_{2g}	0.0	0.0	0.0	0.0	0.0	0.0
e_g	−83.4	−113.1	−159.1	−233.7	−348.8	−520.7
t_{1g}	−1.3	−1.0	−2.9	−8.9	−19.4	−33.9
t_{2g}	−437.4	−397.6	−308.2	−200.3	−101.1	−43.8
a_{1u}	0.0	0.0	0.0	0.0	0.0	0.0
e_u	0.0	0.0	0.0	0.0	0.0	0.0
t_{2u}	−2.7	−2.0	−4.4	−11.6	−23.9	−40.2
t_{1u}	−18.4	−17.2	−26.5	−54.0	−101.4	−167.3
ΔE_{orb}	−552.7	−541.3	−516.4	−536.0	−642.3	−884.7
$\Sigma\Delta E$	−543.9	−525.6	−473.9	−456.6	−544.4	−801.6

[a] Taken from ref 101. Values are given in kcal/mol.
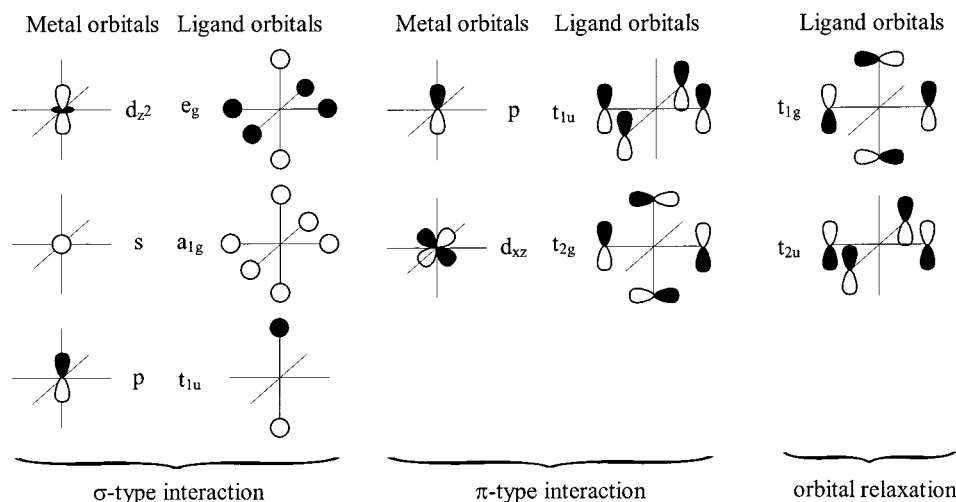
Figure 14. Graphical representation of the orbital interaction terms of the ETS decomposition of $TM^q-(CO)_6$ given in Table 8. (Reproduced with permission from ref 101. Copyright American Chemical Society.)

energy values $\Delta E_{orb} + \Delta E_{pauli}$, which gives the sum of the attractive orbital interactions and the repulsive interactions between occupied orbitals. It is interesting to see that the electrostatic term ΔE_{els} hardly changes from the dianion to the trication. The very large ΔE value for $Ir(CO)_6^{3+}$ is mainly caused by the increase in the ΔE_{orb} contribution to the bond energy and not by Coulombic attraction, which is smallest in the trication.

Examination of the ΔE_{orb} values shows (Table 8) that the e_g orbital interactions, which give the $(OC)_6 \rightarrow Ir^{3+}$ σ-donation into the $d(\sigma)$ orbitals of the metal (Figure 9), clearly make the largest contribution to ΔE_{orb} and, thus, to the total binding energy. Unlike in neutral $W(CO)_6$ (and $Cr(CO)_6$, see above), where the $OC \leftarrow W$ π-back-donation via the t_{2g} orbital contributions is more important for the bond energy than the $OC \rightarrow W$ σ-donation, the σ-donation is the dominant term for the bond energy of $Ir(CO)_6^{3+}$. Even the $OC \rightarrow Ir^{3+}$ σ-donations via the t_{1u} and a_{1g} orbitals (donation into the p and s valence orbitals of the metal, see Figure 9) become more important than the t_{2g} π-back-donation (Table 8). The opposite situation is found in $Hf(CO)_6^{2-}$. Here, the t_{2g} π-back-donation is clearly the largest contribution to the bond energy.

Table 8 shows that there are other orbital contributions to the ΔE_{orb} term which are not negligible in $Ir(CO)_6^{3+}$, i.e., t_{1g} and t_{2u}. Figure 14 shows that these energy contributions arise solely from the relaxation of ligand orbitals. There are no metal orbitals which have t_{1g} and t_{2u} symmetry. Figure 14 shows also that the orbital interactions having t_{1u} symmetry actually have two components. One component is the σ-donation into the $p(\sigma)$ orbitals of the metal as shown in the orbital interaction diagram in Figure 9. The second component is the π-donation from the filled π orbital of CO into the $p(\pi)$ orbitals of the metal. The latter orbital interaction is frequently neglected, but it has been suggested that it may play a role in TM carbonyls.[321] Since $OC \rightarrow TM,p(\sigma)$ and $OC \rightarrow TM,p(\pi)$ donation both have t_{1u} symmetry, it is not possible to separate them unambigiously. DBF[101] estimated the σ and π contributions in the t_{1u} term using the respective metal–CO overlap. This leads

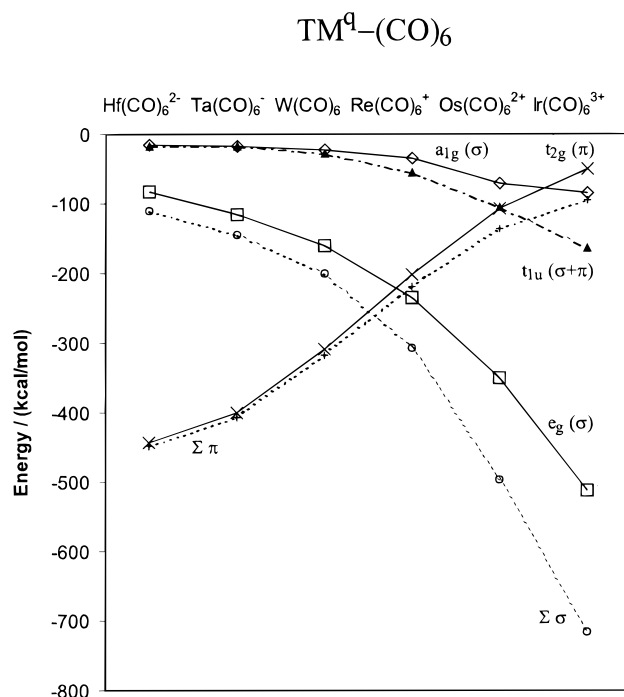**Figure 15.** Trend of the orbital interaction terms of the ETS decomposition of $TM^q-(CO)_6$. (Reproduced with permission from ref 101. Copyright American Chemical Society.)

to a total $\sim$70% π contribution and $\sim$30% σ contribution. Figure 15 shows the trend of the ΔE_{orb} contributions having different symmetry for the TM hexacarbonyls. It becomes obvious that the $t_{2g}(\pi)$ term is the most important contributor to ΔE_{orb} in the neutral and negatively charged complexes, while the $e_g(\sigma)$ contribution becomes the most important term in the cations.

The calculated values for the ΔE_{orb} term given in Table 8 have been used by DBF[101] to estimate the relative importance of the s, p, and d valence orbitals of the metals for the TM^q-CO interactions. There is no ambiguity in assigning the TM valence orbitals to the symmetry of the metal–CO interactions. Figure 14 shows that e_g and t_{2g} give the d contribution, a_{1g} gives the s contribution, and t_{1u} gives the p

Table 9. Energy Contribution of the TM Valence Orbitals to the OC → TM^q Donation Given by the ETS Analysis^a

	Hf(CO)$_6$$^{2-}$	Ta(CO)$_6$$^-$	W(CO)$_6$	Re(CO)$_6$$^+$	Os(CO)$_6$$^{2+}$	Ir(CO)$_6$$^{3+}$
d	−41.7	−56.5	−79.5	−116.9	−174.4	−260.3
s	−9.5	−10.5	−15.4	−27.4	−47.6	−78.8
p	−6.1	−5.7	−8.8	−18.0	−33.8	−55.8

^{a} Taken from ref 101. Values are given in kcal/mol for one orbital.

contribution. The data in Table 8 show that the total contribution of the TM valence orbitals to ΔE_{orb} have the trend d ≫ p ≥ s. However, this does not correctly reflect the relative importance of the metal orbitals, because the d functions are involved in donation and back-donation while the p and s functions are only acceptor orbitals. Also, there are five d functions, three p functions, and one s function. A more balanced comparison considers only the orbitals which are involved in OC → TM^q donation, i.e., e$_g$, a$_{1g}$, and t$_{1u}$. Two d, one s, and three p TM orbitals must be considered. This leads to the energy values shown in Table 9. The data suggest that the relative importance of the TM valence orbitals is d ≫ s > p. The energy values associated with the p functions are clearly smaller than those for the s functions but are not negligible.

Although the trend of the total binding energies ΔE of the hexacarbonyls is similar to the trend of the orbital interaction energies ΔE_{orb}, there is a significant influence of the steric term $\Delta E° = \Delta E_{Pauli} + \Delta E_{els}$ on the bond energies. Table 8 shows that $\Delta E°$ is stabilizing in Hf(CO)$_6$$^{2-}$ and, thus, leads to a higher bond energy while it lowers the bond energy of Os(CO)$_6$$^{2+}$ by more than 100 kcal/mol. The net result is a nearly identical total binding energy for Hf(CO)$_6$$^{2-}$ and Os(CO)$_6$$^{2+}$, although the latter has a significantly higher orbital interaction energy than the former. Thus, the electrostatic interactions and Pauli repulsions may have a significant influence on the trend of the bond energies, and it may be misleading to explain the difference between the two bond strengths solely by orbital interactions. Examples for this have been given in the paper by DBF,[101] who also investigated the factors which influence the trend of the

FBDEs of the hexacarbonyls. Table 10 shows the breakdown of the energy components for the (CO)$_5$TM^q−CO bond given by DBF.[101] An ETS analysis of the FBDE in these and other hexacarbonyls TM(CO)$_6$^{q} has also been carried out by Ehlers et al.[160] using the ETS method, but the authors gave only the σ- and π-orbital contributions and not the energy components which are associated with the charge interactions and exchange repulsion. The calculated values for $\Delta E_{orb}(\sigma)$ and $\Delta E_{orb}(\pi)$ are very similar to the results shown in Table 10.

Since the metal fragment TM(CO)$_5$^{q} has C_{4v} symmetry, the energy decomposition gives contributions from orbital interactions with a$_1$, a$_2$, b$_1$, b$_2$, and e symmetry. Only the a$_1$ (OC → TM(CO)$_5$^{q} σ-donation) and e interactions (OC ← TM(CO)$_5$^{q} π-back-donation) give significant contributions (Table 10). The calculated total binding energies ΔE, which arise from the interactions between CO and TM(CO)$_5$^{q} in the frozen geometries of the complexes, exhibit the same U-shaped trend from Hf(CO)$_6$$^{2-}$ to Ir(CO)$_6$$^{3+}$ with W(CO)$_6$ as the lowest energy point as the bond energies which are calculated with relaxed geometries (see Figure 12). The ETS results given in Table 10 show that the U-shaped trend is *not* found for the sum of the orbital interaction terms ΔE_{orb}, which continuously increase from Hf(CO)$_6$$^{2-}$ to Ir(CO)$_6$$^{3+}$. The decrease in the bond energy from Hf(CO)$_6$$^{2-}$ to W(CO)$_6$ is related to the increase in the repulsive steric term $\Delta E°$, which comes from the large increase in the Pauli repulsion. Thus, the trend in the FBDE from Hf(CO)$_6$$^{2-}$ to W(CO)$_6$ is *not* caused by orbital interactions but rather by the change in the Pauli repulsion. The ΔE_{els} and ΔE_{Pauli} values for the interactions between TM(CO)$_5$^{q} and CO directly correlate with the TM−CO distance, which becomes shorter from Hf^{2-} to Os^{2+} and then lengthens to Ir^{3+} (Table 10).

An interesting aspect of the metal^q−(CO)$_6$ bonds found by DBF concerns the relative importance of electrostatic attraction and orbital interactions for the bond strength.[101] A plausible explanation for the very large bond energy ΔE of Ir(CO)$_6$$^{3+}$, which is the largest among the TM(CO)^q hexacarbonyls (Table 8) could be that the Coulombic attraction between the

Table 10. Bond Lengths and ETS Analysis of the Binding Interactions between TM(CO)$_5$^{q} and CO in TM Hexacarbonyls^a

	Hf(CO)$_6$$^{2-}$	Ta(CO)$_6$$^-$	W(CO)$_6$	Re(CO)$_6$$^+$	Os(CO)$_6$$^{2+}$	Ir(CO)$_6$$^{3+}$
			Energy Decomposition/kcal/mol			
ΔE_{Pauli}	76.6	100.7	118.3	126.9	125.4	115.9
ΔE_{els}	−59.4	−76.6	−90.1	−97.7	−98.5	−93.1
$\Delta E^0 = \Delta E_{els} + \Delta E_{Pauli}$	17.3	24.2	28.2	29.2	27.0	22.9
a$_1$	−17.2	−25.8	−35.9	−47.3	−60.1	−75.4
a$_2$	0.0	0.0	0.0	0.0	0.0	0.0
b$_1$	0.1	0.0	0.0	−0.1	−0.1	−0.1
b$_2$	−0.1	−0.1	−0.1	−0.1	−0.1	−0.1
e	−56.6	−49.6	−41.9	−34.4	−28.6	−26.2
ΔE_{orb}	−73.8	−75.5	−77.9	−81.9	−88.9	−101.8
$\Sigma\Delta E$	−56.6	−51.3	−49.6	−52.7	−61.9	−78.9
			Bond Lengths/Å			
TM−C	2.195	2.112	2.061	2.036	2.034	2.055
C−O	1.185	1.169	1.153	1.139	1.129	1.129

^{a} Taken from ref 101.

highly charged Ir^{3+} and $(CO)_6$ is the reason for the large ΔE. The results of the energy partitioning shows that the intuitive explanation is not correct. On the contrary, the value for ΔE_{els} of $Ir(CO)_6^{3+}$ is the *lowest* among the hexacarbonyls while the neutral $W(CO)_6$ has the second highest Coulombic stabilization (Figure 13)! It was pointed out by Davidson et al.[129] that the large electrostatic attraction in Cr-$(CO)_6$ is due to the penetration of the 5σ electrons of CO into the metal 3spd shell so that these 5σ electrons are not fully shielded from the highly charged metal nucleus. The higher nucleus charge of Ir should lead to stronger electrostatic attraction of the 5σ electrons of $(CO)_6$ in $Ir(CO)_6^{3+}$ compared with $W(CO)_6$, because the TM–CO distance in the latter complex is slightly longer than in the former compound (Table 10). However, the outermost core and occupied valence orbitals $Ir(CO)_6^{3+}$ are more compact, yielding stonger electron–electron repulsion, which apparently compensates the stronger attraction by the nucleus. It seems difficult to predict the trend for the electrostatic interactions between TM^q and $(CO)_6$, because the net forces are the sum over a large number of attractive and repulsive Coulombic interactions. The strength of the Pauli repulsion ΔE_{Pauli} between the metal and the ligand cage $(CO)_6$ (Table 8) correlates with the TM^q–CO interatomic distance (Table 10).

The ETS method has been also used to analyze the TM–CO bonds in $TM(CO)_6$ (M = Cr, Mo, W), TM-$(CO)_5$ (TM = Fe, Ru, Os), and $TM(CO)_4$ (TM = Ni, Pd, Pt) at the DFT level of theory by Ziegler, Tschinke, and Ursenbach (ZTU).[161] This paper gives the contributions of the steric interaction ΔE° (the further breakdown into ΔE_{els} and ΔE_{Pauli} is not given) and the orbital interactions ΔE_{orb} to the FBDEs and the total $TM-(CO)_n$ bond energies. The relativistic energy contributions are also given. The OC ← TM π-back-donation was always found to be more important for the bond energy than the OC → TM σ-donation. ZTU also found that the repulsive interactions ΔE° are particularly strong in the pentacarbonyls and the tetracarbonyls and that the OC ← TM π-back-donation is stronger in the 3d TMs than in the 4d and 5d elements. Relativistic effects only become significant for the 5d elements. The very large repulsive interactions ΔE° were suggested to be the main reason for the finding that $Pd(CO)_4$ and $Pt(CO)_4$ are only stable under low-temperature matrix conditions.[161] The results of the bonding analysis by ZTU must be taken with caution, however, because the calculations were carried out with a simple DFT scheme in which nonlocal corrections were treated as a perturbation to the energy expression based on the LDA.[161] The more recent calculations of DBF[101] using nonlocal DFT have shown that the ΔE° term in the calculations of ZTU[161] is probably too large.[101] For example, ΔE° in $W-(CO)_6$ is 40.9 kcal/mol at the NL-DFT level (Table 8),[101] while the much larger value 222.3 kcal/mol was reported by ZTU.[161] It is not clear which factors will be predicted by NL-DFT calculations as being the main reason for the trends in the bond energies of neutral TM carbonyls across the periodic system.

Table 11. ETS Decomposition of FBDE (kcal/mol) for $Pt(CO)_4$, $Os(CO)_5$, and $W(CO)_6$ at the Nonrelativistic NL-SCF (NR) and Relativistic NL-SCF+QR (R) Levels[a]

		ΔE^0	$\Delta E(a_1)$	$\Delta E(e)^b$	ΔE_{orb}^c	ΔE_{prep}	FBDE
$Pt(CO)_4$	NR	51.6	−25.5	−31.0	−56.5	2.8	2.1
	R	47.7	−30.7	−35.6	−66.3	2.9	15.7
$Os(CO)_5$	NR	69.5	−54.5	−42.5	−97.0	4.0	23.5
	R	65.3	−37.3	−67.2	−104.5	4.5	34.7
$W(CO)_6$	NR	39.5	−29.2	−44.2	−73.4	0.3	34.2
	R	35.0	−19.6	−60.1	−79.7	1.0	43.7

^{a} Taken from ref 162. ^{b} For $Os(CO)_5$, $\Delta E(b_1 + b_2)$. ^{c} $\Delta E_{orb} = \Delta E(a_1) + \Delta E(e)$.

A reinvestigation of the FBDEs in $TM(CO)_6$ (M = Cr, Mo, W), $TM(CO)_5$ (TM = Fe, Ru, Os), and TM-$(CO)_4$ (TM = Ni, Pd, Pt) at the quasirelativistic NL-DFT level was later given by Li, Schreckenbach, and Ziegler (LSZ).[162] The ETS analysis of the bonding situation was restricted, however, to the FBDE in the 5d metal carbonyls $Pt(CO)_4$, $Os(CO)_5$, and $W(CO)_6$. LSZ[162] give the energy contribution of the steric term to the $(CO)_5W-CO$ bond as $\Delta E^\circ = 35.0$ kcal/mol, which is in much better agreement with the value $\Delta E^\circ = 40.9$ kcal/mol reported by DBF.[101] Table 11 shows the decomposition of the FBDE of $Pt(CO)_4$, Os-$(CO)_5$, and $W(CO)_6$ at the nonrelativistic and relativistic levels given by LSZ.[162] The results suggest that the much lower FBDE of $Pt(CO)_4$ is not due to the large steric repulsion but rather to the significantly smaller contribution of the π-bonding term $\Delta E(e)$ to the metal−CO interactions. Relativistic effects increase the contribution of the $\Delta E(e)$ term, but the increase of $Pt(CO)_4$ is the smallest among the TM carbonyls, because the energy levels of the d orbitals of Pt are clearly lower than those of W and Os. Note that the values for ΔE_{orb} are given as −19.6 (a_1) and −60.1 kcal/mol (e_g). The more recent calculations of DBF[101] (Table 10) give much more balanced values for the (a_1) σ donation (−38.82 kcal/mol) and (e_1) π-back-donation (−42.04 kcal/mol). The latter values are in agreement with the data reported by Ehlers et al.,[160] who reported $\Delta E_{orb}(\sigma) = 35.8$ kcal/mol and $\Delta E_{orb}(\pi) = 41.3$ kcal/mol.

The nature of the $TM^+-(CO)_n$ interactions in positively charged carbonyl complexes has been investigated by several authors in the past decade using accurate quantum chemical methods.[163−170] There is general agreement that the bonding between TM^+ and one CO in $TM(CO)^+$ is dominantly electrostatic, but covalent contributions may become increasingly important in $TM(CO)_n^+$ when $n > 1$. Mavridis, Harrison, and Allison (MHA)[163] calculated the potential energy curves of the early TM monocarbonyls $TM(CO)^+$ for TM = Sc^+, Ti^+, V^+, and Cr^+ as a function of the TM^+-CO distance using GVB and CI wave functions and compared them with the curves obtained from electrostatic potentials which were calculated using the multipole moment tensor elements of CO up to octapole. The curves are very similar. The authors concluded that the TM^+-CO bonding is mainly electrostatic with less than 10% OC → TM^+ σ-donation and practically no OC ← TM^+ π-back-donation. The latter conclusion was reached using the Mulliken population analysis.
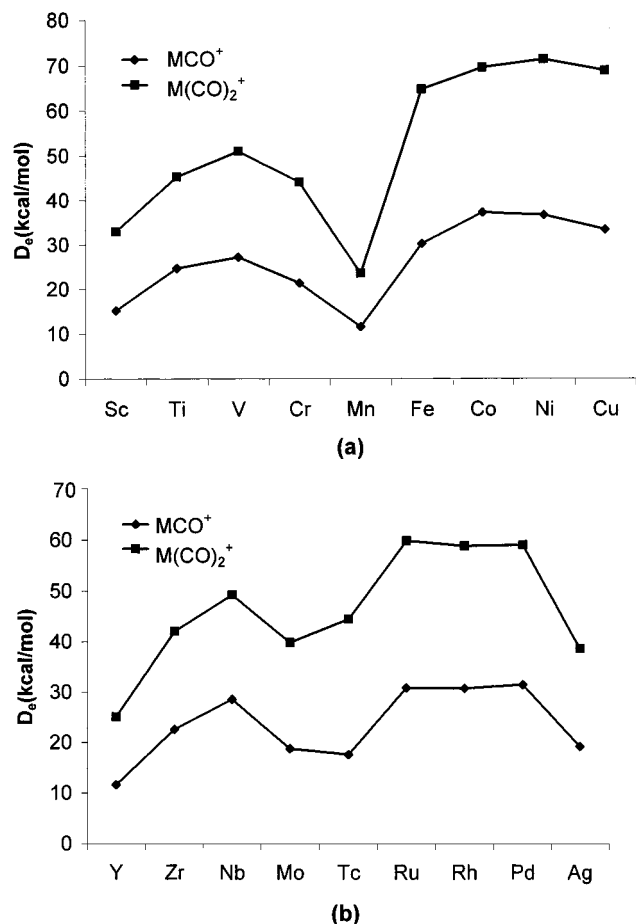
(a)

(b)

Figure 16. Trends of the calculated dissociation energies at the MCPF level for (a) the first TM-row mono- and dicarbonyls and (b) the second TM-row mono- and dicarbonyls. (Reproduced with permission from ref 165. Copyright 1990 American Institute of Physics.)

A complete first and second TM row sweep for the mono- and dicarbonyls $TM^+ = Sc^+-Cu^+$ and Y^+-Ag^+ was presented by Barnes, Rosi, and Bauschlicher (BRB90),[165] who calculated the bond dissociation energies of the ground and lowest-lying excited states at the modified coupled-pair functional (MCPF) method. The authors explain the trends in the $TM^+-(CO)_n$ bond energies (Figure 16) in terms of dominantly electrostatic bonding interactions. The curves have a double-maximum shape along the first and second TM rows with a minimum for the bond energies of $Mn(CO)_n^+$ (first row) and $Tc(CO)^+/Mo(CO)_2+$ (second row). Mn^+ has a s^1d^5 (^7S) ground state and rather high-lying excited quintet states. The interactions of Mn^+ (^7S) with CO encounters Coulombic repulsion in the septet ground states of the carbonyls, which leads to weak and long Mn^+-CO distances.[165] Tc^+ also has a s^1d^5 (^7S) ground state, but the s^0d^6 (^5D) excited state lies much lower than the corresponding state of Mn^+. This leads to quintet ground states for $Tc(CO)_n^+$ which have similar bond energies to $Mo(CO)_n^+$ (Figure 16). The less important covalent part of the bond energy is determined by the energy levels of low-lying electronic states, the ionization potentials, and the s and d orbital sizes of TM^+. Compared to the neutral atoms, both the d and s valence orbitals contract on ionization but the s orbital much more so than the d orbital. The ratio of
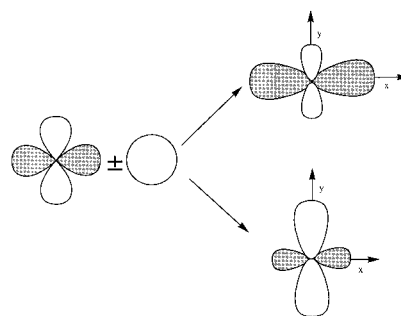
Figure 17. Schematic representation of the $sd_{x^2-y^2}$ hybridization at the transition metal which facilitates the approach of a second ligand trans to the first ligand.

the orbital radii $\langle r \rangle_s / \langle d \rangle_d$ of Sc^+-Cu^+ and Y^+-Ag^+ varies from 2.11 for Sc^+ to 2.82 for Cu^+ in the first TM row and from 1.57 for Y^+ to 2.15 for Ag^+ in the second TM row. This is clearly less than what is found for the neutral atoms (Figure 4). The ionization potentials for the first- and second-row TM ions were given, which are important for understanding the trend of the $OC \leftarrow TM^+$ back-donation. BRB90[165] conclude that the effect of $OC \leftarrow TM^+$ π-back-donation in $TM(CO)^+$ and $TM(CO)_2^+$ is small but should be larger in the dicarbonyl ions than in the monocarbonyls, because $(n)s(n-1)d_\sigma$ hybridization leads to less repulsion and stronger π-back-donation. This was given as the reason numerous dicarbonyls $TM(CO)_2^+$ have a larger FBDE than the monocarbonyls, which cannot be explained by purely electrostatic binding. The same reasoning was later used by other authors.[168,171] Figure 17 schematically shows the effect of sd_σ hybridization, which enhances the $OC \leftarrow TM^+$ π-back-donation and reduces the electron repulsion, on the metal–CO interactions.

Barnes and Bauschlicher (BB89) also studied the bonding in several neutral TM mono- and dicarbonyl complexes at the MCPF level.[172] The bonding mechanism was found to be similar to the TM^+–carbonyl cations, but the covalent contributions dominate in the neutral species. The electronic state of the transition metals plays a pivotal role for the TM–CO interactions in the neutral compounds. Transition metals with a $(n)s^2(n-1)d^x$ ground state encounter repulsive interactions between the filled s orbital and the carbon σ-lone-pair electrons. The $TM(n)s \leftrightarrow C(\sigma)$ repulsion is reduced and the $OC \leftarrow TM$ π-back-donation enhanced when the transition metal has the electron configuration $(n)s^1(n-1)d^{x+1}$ or even $(n)s^0(n-1)d^{x+2}$. For example, the potential energy curve between Ti in the $(4)s^2(3)d^2$ (^3F) ground state and CO ($^1\Sigma^+$) yielding the $^3\Phi$ state of TiCO is unbound.[172] The lowest lying state of TiCO is the $^5\Delta$ state, which correlates with the $(4)s^1(3)d^3$ (^5F) first excited state of Ti being 0.78 eV above the ground state.[173] The Ti–CO binding interactions in the $^5\Delta$ ground state are strong enough to compensate for the $^5F \leftarrow {}^5\Delta$ excitation energy. TiCO ($^5\Delta$) is theoretically predicted to be bound by 14.3 kcal/mol with respect to the electronic ground state of Ti.[172]

The interplay between the electron configuration of the metal and the bonding situation in the carbonyls $Fe(CO)_n$ when going from $n = 1$ to 5 has been investigated at the MCPF level of theory using
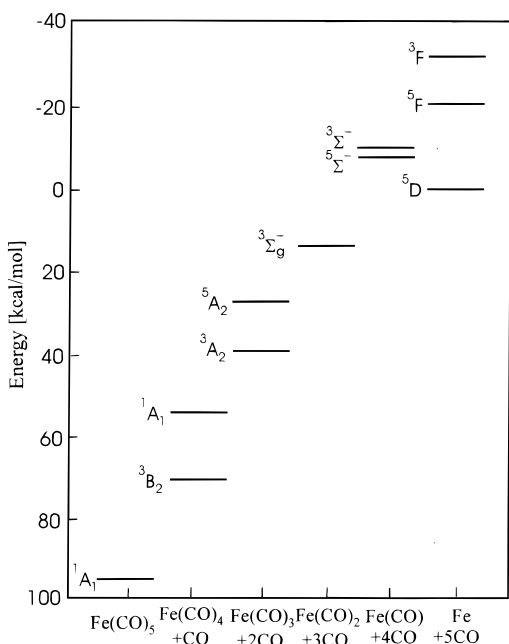
Figure 18. Calculated relative energies at the MCPF level for the $Fe(CO)_n$ systems. The zero of energy is the ground-state Fe atom and five ground-state CO molecules. (Reproduced with permission from ref 174. Copyright 1991 American Institute of Physics.)
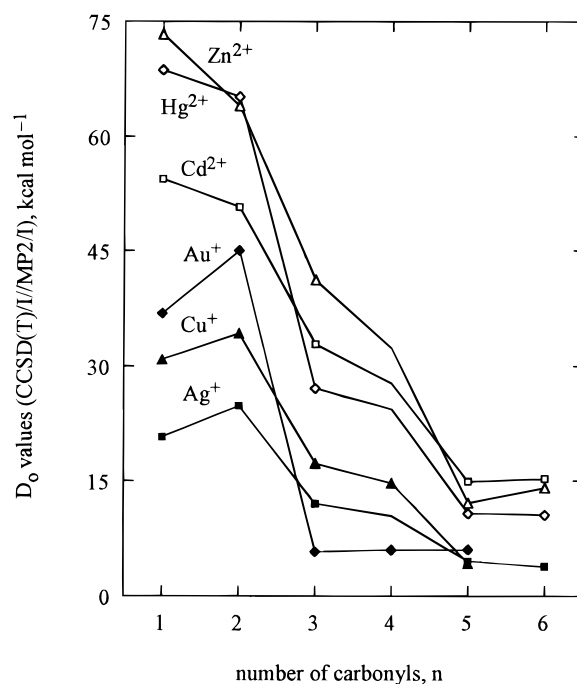

Figure 19. Trend of the calculated FBDEs for the TM^q-$(CO)_n$ ($n = 1-6$) systems. (Reproduced with permission from ref 168. Copyright 1999 Wiley-VCH.)

large basis sets by Barnes, Rosi, and Bauschlicher (BRB91).[174] Figure 18 shows the results which are important for an understanding of the metal–CO bonding. Fe has a $(4)s^2(3)d^6$ (^5D) ground state, which does not give a bound state with CO. Important for the binding interactions with CO are the first excited quintet state $(4)s^1(3)d^7$ (^5F) and the lowest lying triplet state $(4)s^1(3)d^7$ (^3F), which are 20 and 34 kcal/mol above the ground state, respectively.[173] Fe(CO) has nearly degenerate low-lying bound states with $^3\Sigma^-$ and $^5\Sigma^-$ symmetry which arise from the ^3F and ^5F state of Fe, respectively. The binding interactions in $^3\Sigma^-$ and $^5\Sigma^-$ Fe(CO) are not strong enough to stabilize the monocarbonyls thermodynamically with respect to Fe and CO in the electronic ground states (Figure 18). A second CO drastically increases the $^5\Sigma_g^-$ state arising from ($^5\Sigma^-$) Fe(CO) + CO due to Fe–CO repulsion, while the interactions of ($^3\Sigma^-$) Fe(CO) with CO yield linear $Fe(CO)_2$ in the $^3\Sigma_g^-$ ground state. Further addition of CO leads to C_{3v}-symmetric Fe-$(CO)_3$ with a $^3A_2$ ground state and a $^5A_2$ excited state. An energetically low-lying singlet state for the iron carbonyls, which arises from the highly excited $3d^8$ configuration of the metal, is eventually found with the $^1A_1$ state of $Fe(CO)_4$. This is not the ground state, however, which has $^3B_2$ symmetry (Figure 18). Only in $Fe(CO)_5$ is the metal–CO binding energy strong enough to overcome the $(4)s^2(3)d^6 \rightarrow (4)s^0(3)d^8$ excitation energy such that the $^1A_1$ state becomes the ground state.

The driving force for the spin changes in $W(CO)_n^+$ as the number of ligands increases from $n = 1$ to 6 has recently been studied at the B3LYP and ab initio levels by Büker, Maitre, and Ohanessian (BMO).[167] The authors discussed the $W^+–(CO)_n$ interactions in terms of OC $\rightarrow$ W^+ σ-donation and OC $\leftarrow$ W^+ π-back-donation using the NBO partitioning scheme.[92,93] It was found that σ-donation is more favorable when

involving the 5d rather than 6p orbital of tungsten, which leads to a preference for bent rather than linear structures of $W(CO)_n^+$ with $n = 2-4$.[167] Spin lowering enhances the OC $\leftarrow$ W^+ π-back-donation and reduces the repulsive interactions between occupied σ orbitals and, thus, is crucial for the energies of the low-lying electronic states. The chemical bonding in $Ni(CO)_n$ ($n = 1-4$), $Fe(CO)_5$, and $Cr(CO)_6$ has been investigated at the CASSCF and CASPT2 levels of theory by Persson, Roos, and Pierlot (PRP).[175] The authors found that the correlation energy increases the OC $\rightarrow$ M σ-donation and OC $\leftarrow$ M π-back-donation. The focus of this work, however, was on the accurate calculation of bond lengths and bond energies.

The trend in the strength and nature of the chemical bonds in TM carbonyls where the spin of the TM does not change has been investigated in a theoretical study of $TM^q(CO)_n$ ($TM^q = Cu^+$, Ag^+, Au^+, Zn^{2+}, Cd^{2+}, Hg^{2+}; $n = 1-6$) at the DFT (BP86) and CCSD(T) levels of theory by Lupinetti, Jonas, Thiel, Strauss, and Frenking (LJTSF).[168] The $TM^q–CO$ interactions are largely ionic, but the covalent contributions may become important for the *trend* of the bond energies, particularly for the heaviest elements gold and mercury. Figure 19 shows the trend of the calculated FBDEs of the carbonyls, which exhibits some unexpected features. From the group 11 ions, Au^+ clearly has the strongest bond among the mono- and dicarbonyls but the weakest bound tricarbonyl and tetracarbonyl. A similarly sharp drop in the bonding energy from di- to tricarbonyl is found for Hg^{2+} (Figure 19). This was explained by LJTSF with the loss of the covalent contributions to the $M^q–CO$ bonds.[168] The favorable sd(σ) hybridization at the metal which is found in the dicarbonyls (Figure 17) leading to less σ-repulsion and stronger OC $\leftarrow$ TM^q π-back-donation is lost in the tricarbonyls. This effect

is particularly large for Au^+ and Hg^{2+}, because relativistic effects, which are very strong in 6d elements, lead to contraction of the s orbital and expansion of the d orbitals.[176−179]

The picture of $OC \rightarrow TM$ σ-donation and $OC \leftarrow TM$ π-back-donation has become a standard model for the chemical bond in TM carbonyl complexes. It is common to correlate physical properties, in particular the C−O stretching frequencies, with the size of the donor−acceptor interactions. The custom of correlating stretching frequencies with donation and back-donation has led to the situation that the measured frequencies are frequently taken as evidence for the $OC \rightarrow TM$ σ-donation and $OC \leftarrow TM$ π-back-donation, without the nature of the actual TM−CO bond being analyzed. This is dangerous because the conclusion from the theoretical work suggests that electrostatic interactions are as important as orbital interactions for the binding energies. The question arises of whether electrostatic interactions may also play a role for the C−O stretching frequencies in TM carbonyls. Two papers by Goldman and Krogh-Jespersen (GK)[180] and by Lupinetti, Fau, Frenking, and Strauss (LFFS)[170] addressed this question.

Both papers focused on the interactions between CO and positively charged atoms X^+. It is well-known that many species $X(CO)^+$ have a higher C−O stretching frequency than free CO. If X^+ is a transition-metal ion TM^+, the term *nonclassical carbonyl* has been suggested for species $TM(CO)_n^q$ with vibrational frequencies $\nu(C-O) > 2143$ cm^{-1}, which is the value for free CO.[181−183] Most TM carbonyls have $\nu(C-O) < 2143$ cm^{-1}, and the lower frequency is explained by the $OC \leftarrow TM$ π-back-donation which leads to a partial population of the CO π^* orbital. The CDA study of Szilagyi and Frenking[158] about the trend in the C−O stretching mode in $TM(CO)_6^q$ ($TM^q = Hf^{2-}$, Ta^-, W, Re^+, Os^{2+}, Ir^{3+}) found that the $OC \leftarrow TM^q$ π-back-donation becomes higher and $\nu(C-O)$ becomes lower from Ir^{3+} to Hf^{2-}.[158] While this result can be taken as evidence that the lowering of the CO stretching frequency below 2143 cm^{-1} is indeed caused by increasing $OC \leftarrow TM^q$ π-back-donation, it is not clear why $Os(CO)_6^{2+}$ and $Ir(CO)_6^{3+}$ have $\nu(C-O) > 2143$ cm^{-1}. One possible explanation is that the 5σ orbital (HOMO) of CO is antibonding. This has been claimed in several theoretical studies.[184−188] If the TM^q−CO interactions are mainly caused by $OC \rightarrow TM^q$ σ-donation, which is indeed the case in positively charged species,[158] the depopulation of the antibonding σ orbital should yield a shorter and stronger C−O bond with $\nu(C-O) > 2143$ cm^{-1}. A striking example where only σ-donation is possible is HCO^+, which has a C−O stretching frequency of 2184 cm^{-1}, much higher than in free CO.[189] Indeed, the Mulliken overlap population of the 5σ MO of CO is negative.[187,188] However, the 5σ HOMO of isoelectronic N_2 also has a negative overlap population,[187,188] but the N−N stretching frequency of HNN^+ is lower than in free N_2.[190]

The papers by GF and LFFS clearly show that the higher C−O stretching frequencies in nonclassical carbonyls are caused only by electrostatic effects and not by σ-donation.[170,180] The authors investigated the
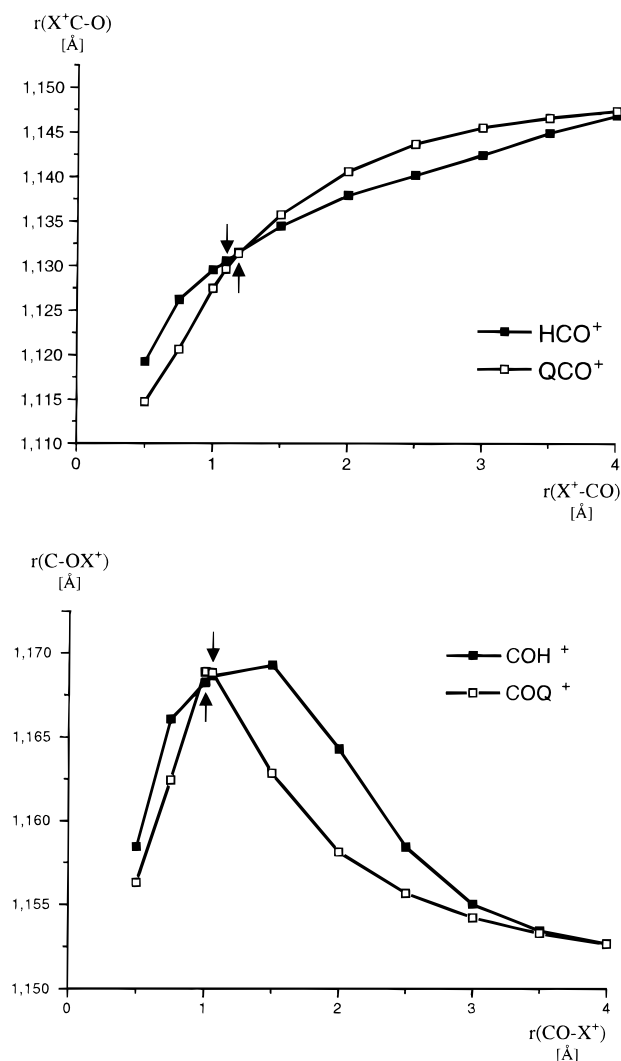

Figure 20. Calculated change in the C−O bond length when a proton or a positive charge Q^+ approches CO (top) from the carbon end or (bottom) from the oxygen end. (Reproduced with permission from ref 170. Copyright 1997 American Chemical Society.)

changes which take place when a proton H^+ or a point charge Q^+ are attached to CO. Figure 20 shows the alteration in the C−O distance when H^+ or Q^+ approaches CO from the carbon or oxygen end.[170] There are two important conclusions which can be drawn from Figure 20. (a) The change in the C−O distances at the energy minimum points are nearly the same when a proton or a point charge is attached. (b) The C−O bonds in HCO^+ and QCO^+ are shorter than in free CO, but they are longer in COH^+ and COQ^+. Hence, the C−O bond shortening and bond stretching is mainly an electrostatic effect which has nothing to do with the formation of a bond. The bond lengthening in COH^+ and COQ^+ is strong evidence against the antibonding nature of the 5σ orbital of CO, because σ-donation into the HOMO should also lead to shorter bonds when the positively charged species is attached at the oxygen end.

LFFS analyzed the change in the polarization of the C−O-localized molecular orbitals (LMOs) when H^+ or Q^+ are attached.[170] They found that the LMOs become less polarized in HCO^+ and QCO^+ and more polarized in COH^+ and COQ^+ than in CO. This is
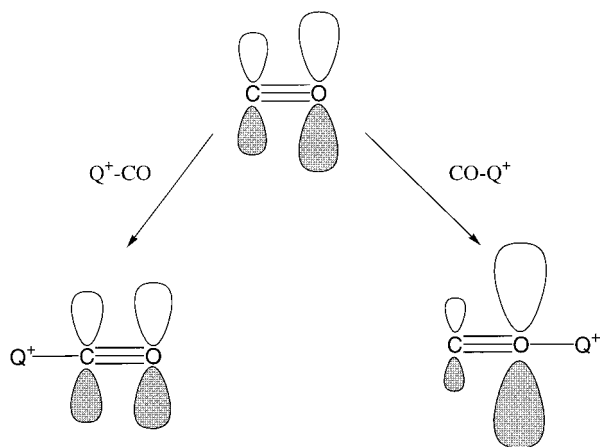
Figure 21. Schematic representation of the change in the polarization of the π orbital of CO when a positive charge becomes attached to the carbon or the oxygen atom. The same effect is found for the σ orbital. (Reproduced with permission from ref 170. Copyright 1997 American Chemical Society.)

Figure 22. Plot of the calculated $TM \leftarrow L$ back-donation in $TM(CO)_5L$ (TM = Cr, Mo, W; L = CO, SiO, CS, N_2, NO^+, CN^-, NC^-, HCCH, CCH_2, CH_2, CF_2, H_2) given by the CDA method and the change of the $TM-CO_{trans}$ bond length (in Å) relative to $TM(CO)_6$. (Reproduced with permission from ref 194. Copyright 1996 American Chemical Society.)

schematically shown in Figure 21. The change in the polarization leads to stronger C−O covalent bonding in HCO^+ and QCO^+, while the covalent character is weaker in COH^+ and COQ^+. A more even distribution of the bonding π electrons between C and O was already suggested as the reason for the bond strengthening in CO^+.[191] The papers of GK[180] and LFFS[170] show that this model is supported by a detailed analysis of the electronic structure of carbonyls.

The bonding aspects of CO as a σ donor ligand in coordination chemistry have been discussed by Aubke and Wang (AW) in a review published in 1994.[192] While the authors suggested that the C−O stretching frequencies should be a better probe for the role of $OC \leftarrow TM$ π-back-bonding than the C−O bond length, because they are more sensitive to subtle changes in the C−O bond order, they recognized that the increase in the C−O stretching mode above the value in free CO is difficult to satisfactorily explain by the removal of electron density from the alleged antibonding 5σ HOMO of CO. They speculated that rehybridization involving the 4σ and 5σ MO may be responsible for the shift of the vibrational mode. AW wrote "It is hoped that sound theoretical work... will continue and will provide an appropriate supplement to the synthetic and spectroscopic work described in this review".[192] The papers of GK[180] and LFFS[170] are a direct answer to this.

The change in the C−O stretching frequency is also frequently used as a probe to investigate the $L \leftarrow TM$ π-back-donation in complexes where the ligand L is trans to CO. It is argued that ligands which are weaker π acceptors than CO lead to enhanced $OC \leftarrow TM$ π-back-donation and thus to a lower C−O_{trans} stretching mode. The measured C−O wavenumbers are then taken as direct evidence for the strength of the $L \leftarrow TM$ π-back-donation. The correlation between $\nu(C-O)$ and the nature of the $(OC)TM-L_{trans}$ bond has been investigated in a theoretical study of $H(PR_3)_2RuL(CO)$ complexes by Poulton, Sigalas, Polting, Streib, Eisenstein, and Caulton (PSPSEC).[193] The authors come to the conclusion that "the variation in π-effects alone is not sufficient to account for
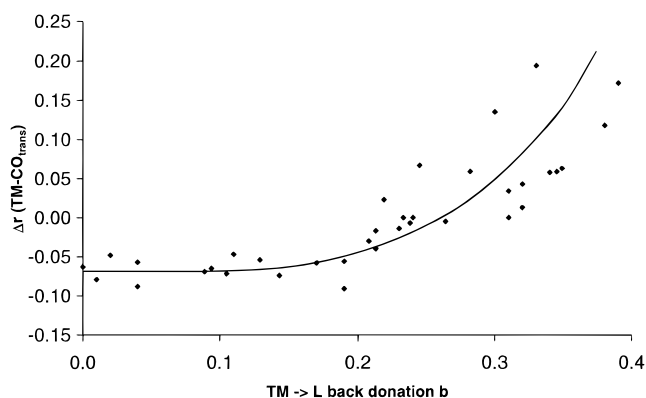
the ranking of the CO frequencies... the σ effect is also involved". In light of the papers of GK[180] and LFFS,[170] it should be added that electrostatic interactions may also play a role. Ehlers, Dapprich, Vyboishchikov, and Frenking (EDVF)[194] investigated the correlation of the vibrational frequency $\nu(C-O)_{trans}$ with the $L \leftarrow TM$ π-back-donation for a large number of group-6 complexes $(CO)_5TM-L$ (TM = Cr, Mo, W) where many ligands L are valence-isoelectronic with CO (L = SiO, CS, N_2, NO^+, CN^-, NC^-, HCCH, CCH_2) with the CDA method. Other small ligands L = CH_2, CF_2, H_2 were also included in the work. A plot of the $L \rightarrow TM$ σ-donation did not show any correlation with $\nu(C-O)$, but the $L \leftarrow TM$ π-back-donation correlates reasonably well with the C−O stretching mode (Figure 22). A closer examination of the data, however, shows that a higher or lower value of $\nu(C-O)$ does *not* necessarily indicate stronger or weaker π-acceptance of L. It becomes clear that σ-bonding and particularly charge interactions[170,180] also have a significant influence on the C−O stretching frequency. As a caveat we want to stress that it is more legitimate to expect a correlation between the bonding situation and the force constants rather than the vibrational frequencies, as it has been done by GK[180] and by LFFS.[170]

Numerous other high-level theoretical studies about TM carbonyls which focus on accurate calculations of properties such as geometries, bond energies, vibrational frequencies, NMR chemical shifts, etc., have been published in the past decade.[195−205] Although these works are important for the understanding of the molecules, they address other questions than the nature of the chemical bond and, thus, shall not be discussed in this review.

V.2. Carbene Complexes and Higher Homologues

The nature of the chemical bond between a transition metal and a carbene fragment CR_2 quickly drew the attention of theoreticians soon after the first stable TM carbene complex was reported in 1964.[206] Because of the size of the molecules, early theoretical studies of the bonding situation have been performed using qualitative MO models and semiempirical

calculations.[207] Carbene complexes became particularly interesting for theoretical analyses of the bonding situation when experimental studies suggested that there are *two* categories of TM carbene complexes which show very different properties. One category comprises the "Fischer-type" complexes,[208] which are characterized by electrophilic reactivity of the carbene ligand. Stable Fischer complexes have a π-donor group X at the carbene ligand which is bound to a TM in a low oxidation state. The second class comprises the "Schrock-type" complexes,[209,210] which have nucleophilic carbene ligands typically with hydrogen, alkyl, or aryl groups but no π-donor substituents at the carbene carbon atom. Schrock complexes have TMs in a high oxidation state. Although many TM carbene complexes can easily be identified to belong into one of the two categories, there are species which make it difficult to classify them as Fischer or Schrock complexes. In particular, dihalocarbene complexes may exhibit either nucleophilic or electrophilic behavior at the carbene center, which shows that there is not a strict separation of the two classes of carbene complexes.[211]

Ab initio calculations of real TM carbene complexes have not been published before the 1980s. The electronic structures of the Fischer carbene complexes $(CO)_5Cr-CH(OH)$ and $(CO)_4Fe-CH(OH)$ and the Schrock complex $H_2(CH_3)Nb-CH_2$ were the subject of two theoretical studies by Nakatsuji et al.[212,213] Although the calculations were carried out at a rather low level of theory by the present standard (assumed geometries, HF calculations with minimal basis sets), the results gave interesting insight into the differences between the bonding situation of the two classes of compounds. It was suggested that the different reactivity of the carbene ligands of Fischer and Schrock complexes is not caused by the charge distribution but rather by the shape of the frontier orbitals. The nucleophilic or electrophilic reactivity of the carbene ligands should be orbital controlled and not charge controlled.[212,213] The HOMO of H_2-$(CH_3)Nb-CH_2$ has a maximum coefficient at the $C_{carbene}$ atom, and the LUMO has the largest coefficient at Nb.[213] The Fischer carbene complexes $(CO)_5Cr-CH(OH)$ and $(CO)_4Fe-CH(OH)$, in contrast, have LUMOs with large coefficients at the $p(\pi)$ AO of the carbene ligand, which explains the electrophilic behavior of the compounds.[212]

The most successful bonding model which explains the different properties of Fischer and Schrock carbene complexes L_nTM-CR_2 uses the singlet and triplet states of the fragments CR_2 and L_nTM as building blocks for the respective compounds. This model, which has been suggested by Taylor and Hall (TH)[214] and by Rappé, Carter, and Goddard (RCG),[215−219] is now generally accepted as the best description for the binding interactions in the two classes of compounds. The idea behind it is related to the dichotomic bonding model for alkene complexes that was suggested in 1952 by Dewar[53] and by Chatt and Duncanson (DCD).[54] The DCD model has also proven to be very helpful for other classes of TM compounds. This will become obvious from the other sections in this review. Figure 23 schematically
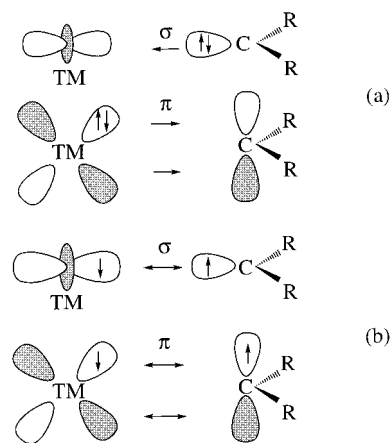

Figure 23. Schematic representation of the dominant orbital interactions in (a) Fischer-type carbene complexes and (b) Schrock-type carbene complexes.

shows the essential features of the bonding picture. The TM−carbene bond in Fischer complexes is described in terms of donor−acceptor interactions between a $(^1A_1)$ singlet carbene and a singlet metal fragment $R_2C \rightarrow TML_n$ and π-back-donation $R_2C \leftarrow TML_n$. This is similar to the bonding model for the TM−CO bond (Figure 8). The TM−carbene bond in Schrock complexes is described as a covalent bond between a $(^3B_1)$ triplet carbene and a triplet metal fragment. Since the latter model does not employ donor−acceptor interactions between the metal and the carbene, the more appropriate name for the Schrock complexes is TM alkylidenes.

It has become common to explain the properties of TM carbene complexes in terms of the bonding model shown in Figure 23. It is not our goal to discuss all aspects of the correlation between chemical behavior and the bonding situation of the compounds. We only want to point out that the electronic ground state of a carbene immediately shows the preference for the different binding interactions with a TM. Carbenes like methylene and dialkylcarbenes which have a triplet gound state will preferentially form covalent bonds with triplet metal fragments, while carbenes with π-donor groups which favor a singlet ground state will preferentially engage in donor−acceptor interactions with TM fragments in their singlet state. In particular, dihalocarbenes, which have singlet ground states and large singlet → triplet excitation energies,[222,223] are constrained to donor−acceptor bonding.[211] It should be noted that the term "covalent bonding" for the type of interactions shown in Figure 23a does not mean that covalent bonding is absent in donor−acceptor bonds which are shown in Figure 23b. Chemical bonds of both types may have contributions from covalent interactions and electrostatic interactions. The terms covalent bonding and donor−acceptor bonding only refer to the different bonding models shown in Figure 23. Other less common expressions for the bonding models are shared electron interactions and closed-shell interactions, respectively.[108] Another name for a donor−acceptor bond is the term dative bond.[224]

The bonding model shown in Figure 23 has been examined in two papers by Cundari and Gordon (CG) which made an important contribution to the under-
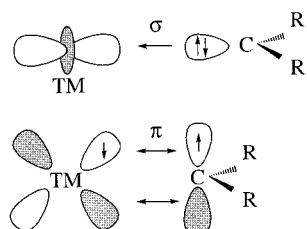
Figure 24. Schematic representation of the resonance structure |2110> which was found in ref 225 to be equally important as the resonance form |1111> shown in Figure 19b for the description of high-valent carbene complexes.

standing of the TM−carbene bond.[225,226] The work of CG can be considered as an attempt to quantify the bonding concept of TH[214] and RCG.[215−219] CG suggest a multiconfigurational (MC) picture for the metal−carbene bond, where the electron distribution is described by several possible configurations ("resonance structures") out of which the configurations depicted in Figures 23a,b are two possible forms. CG estimated the relative weight of each configuration in the wave function. First, the authors calculated the high-valent TM alkylidenes $H_2TM−CH_2$ (TM = Ti, Zr, Hf), $H_3TM−CH_2$ (TM = Nb, Ta), $(OH)_2(NH)$-$TM−CH_2$ (TM = Mo, W), and $(OH)_2(CH)Re−CH_2$ at the HF level of theory.[225] The bond lengths obtained this way should be rather accurate, because HF geometries of high-valent TM compounds are usually in good agreement with experiment.[28] Second, single-point calculations at the 4-orbital 4-electron FORS (full optimized reaction space)[228] level using the HF-optimized geometries yielded a wave function containing delocalized MOs which were transformed into localized orbitals via the Boys localization procedure.[97] In the final step of the analysis, the authors used the localized MOs (LMOs) as a basis for a 4 × 4 CI calculation which generated 20 spin-adapted configurations for all possible electron distributions among the σ- and π-bonding orbitals of the metal and the carbene carbon atom. The coefficients of the 4 × 4 CI were then used to estimate the weight of each resonance structure.

The results of the σπ-MC/LMO/CI analysis by CG91[225] essentially support the bonding model for high-valent TM alkylidenes suggested by TH[214] and RCG.[215−219] The contribution of the resonance structure shown in Figure 23b was for all compounds either the largest or the second largest and roughly 3 times larger than that in the configuration shown in Figure 23a. The authors use a notation which subsequently shows the occupation of the σ (C) π (C) π (TM) σ (TM) orbitals depicted in Figure 23, i.e., Figure 23a gives the |2020> configuration and Figure 23b gives the |1111> configuration. Another configuration which was equally important as that in Figure 23b is |2110> shown in Figure 24. It is a "nucleophilic" resonance form, because it shows an electron distribution $L_nTM^+−CR_2^-$ where the carbene ligand carries a negative charge, while the configurations shown in Figure 23 depict neutral resonance forms. It was found that the nucleophilic configurations account for roughly one-half of all contributions to the ground-state wave function of the TM alkylidenes and that the neutral resonance forms contribute with ∼45%. Only 5% of the wave function is given by the electrophilic configuration. This is in agreement with the experimental observation that the carbene ligands of TM alkylidenes react mostly as nucleophiles.

The second paper of CG92[226] focused on the effect of ligand and substituent modification on the TM−alkylidene bond. The authors used the same σπ-MC/LMO/CI method for the analysis of the bonding situation in substituted alkylidenes L_nTMCR_2 with TM = Ti, Zr, Hf, Nb, and Ta. They found that the intrinsic nature of the metal−carbon double bond can typically be changed only within certain limits by modification of the electronegativity of L and R. Significant changes are effected in three other ways: (i) variation of the metal, (ii) introduction of highly electropositive substituents R like Li, (iii) use of π-donor substituents at the carbene group. The latter conclusion is in agreement with experimental observations, particularly for dihalocarbene complexes. CG92[226] found that variation of the halogen atom at the carbene group may change the reactivity from a more nucleophilic to a more electrophilic behavior. This effect was suggested to be related to the extent of π-back-bonding from halogen to carbon and, thus, to the change in the TM → CR_2 π-back-donation.[211] This finding and the results of the bonding analysis of CG show that the classification of a TM carbene complex according to the model shown in Figure 23 sketches two extreme cases and that the real bonding situation is a continuum which is described by mixing several resonance forms. The resonance structure |2110> shown in Figure 24, which was found to be the most important one besides the |1111> configuration (Figure 24), has one σ donor acceptor bond and one π-type covalent bond. Nucleophilic and electrophilic reactivity of the carbene center can be shifted in either direction by changing the substituents at the carbene groups, without triggering a fundamental change in the bonding situation. This can be achieved without that the formal oxidation state of the metal changes, which obscures a general correlation between oxidation state and bonding model of a complex.

CG also analyzed the TM−SiR_2 bond in two subsequent studies using the same methods as for the carbene complexes.[229,230] In the first paper the authors investigated the positively charged species TM−SiH_2^+ (TM = Sc, Ti, V, Cr, Mn, Fe, Co, and Ni) and compared them with the analogous carbene complexes TM−CH_2^+. They also presented results for the series Cr−EH_2^+ (E = C, Si, Ge, Sn). SiH_2 has a ($^1A_1$) singlet ground state which is 16.8 kcal/mol lower in energy than the ($^3B_1$) triplet excited state.[227] It could be expected that the |2020> configuration (Figure 23a) plays a larger role in silylene complexes than in the analogous methylene complexes, because CH_2 has a ($^3B_1$) triplet ground state which is 9.6 kcal/mol lower than the ($^1A_1$) excited state.[231−234] CG found that the MC/LMO/CI wave functions of the early TM−SiH_2^+ compounds with TM = Sc, Ti, V, Cr, Mn have large contributions only from the dominant |1111> configuration (analogous to Figure 23b) and

from the second largest $|2110\rangle$ resonance form (Figure 24), while $|2020\rangle$ (Figure 23a) and the other 17 configurations are negligible.[229] The early transition metals have a high-spin ground state and do not have filled π-type d orbitals in the complexes. The resonance form $|2020\rangle$ is therefore not significant. On the other hand, for the series $FeSiH_2^+$, $CoSiH_2^+$, $NiSiH_2^+$, the contribution of the $|2020\rangle$ configuration becomes increasingly important and eventually turns into the dominant term. The analogous carbene complexes $TMCH_2^+$ show a much smaller change in the resonance structure contributions, which are always dominated by the $|1111\rangle$ and $|2110\rangle$ configurations. The $|2020\rangle$ resonance form only becomes important in the most electron-rich carbene complex $NiCH_2^+$, but the $|1111\rangle$ and $|2110\rangle$ forms are still the largest ones.[229] A remarkably constant mixture of configurations was found for $Cr-EH_2^+$ complexes, which are nearly invariant to the modification of the ligand atom E from carbon to tin. The $|1111\rangle$ configuration always contributes with $\sim 50\%$, $|2110\rangle$ has $\sim 35\%$, while the remaining 18 resonance form are negligible.

CG used the insight into the nature of the interactions between bare TM ions and silylene to propose strategies for designing a high-valent TM silylidene complex analogous to Schrock-type alkylidenes.[230] All TM silylene complexes which could be isolated until now are low-valent (Fischer-type) complexes with TM−Si donor−acceptor bonds. CG calculated silylene complexes $H_nTM-SiR^1R^2$ with TM = Ti, Zr, Hf, Nb, and Ta, where R^1 and R^2 are H, Cl, Me, or SiH_3.[230] The authors did not calculate the TM−Si bond dissociation energies, but from the TM−Si force constant, it was concluded that electron-withdrawing substituents at TM or Si increase the thermodynamic stability of the complex. CG used the same methodology as before[225,226,229] in order to analyze the TM−Si bonding situation. For all complexes they found that the configurations $|1111\rangle$ and $|2110\rangle$ are the most important contributors to the MC/LMO/CI wave function.[230]

The bonding in high-valent (Schrock-type) TM silylene complexes $(CH_3)H_2Nb-SiR_2$ (R = H, OH) and a comparison with Fischer-type silylene complexes $(CO)_4Fe-SiR_2$ and $(CO)_5Cr-SiR_2$ (R = H, OH) was the focus of a theoretical study by Nakatsuji, Hada, and Kondo (NHK).[235] The geometries of the compounds were optimized at the HF level. The geometry of $(CH_3)H_2Nb-SiH_2$ was also calculated using the SAC (symmetry-adapted cluster) method.[236] The analysis of the bonding situation was carried out by inspection of the molecular orbitals and by the Mulliken population analysis. NHK predicted that nucleophiles and electrophiles should both attack $(CH_3)H_2Nb-SiR_2$ at the Nb atom, because the frontier orbitals have the largest coefficient at the niobium atoms. The possibility of nucleophilic attack at silicon was not excluded, however, because the LUMO also has a large coefficient at Si. Electrophiles should attack $(CO)_5Cr-SiR_2$ at the chromium atom and nucleophiles at Si.[235]

The electronic structure of Fischer-type carbene complexes and higher homologues $(CO)_5Mo-EH_2$ (E

= C, Si, Ge, Sn) was the subject of a theoretical study of Márquez and Sanz (MS92a).[237] The geometries were first optimized at the HF level of theory, followed by optimization of the Mo-E distance at the CASSCF level while keeping the rest of the geometrical variables frozen. The calculated Mo-E bond dissociation energies with respect to the fragments in the singlet state, which were obtained at this level of theory, gave the order C $\gg$ Si > Ge $\approx$ Sn. Inspection of the bonding situation with the help of the Mulliken population analysis showed that the donor−acceptor model given in Figure 23a is a valid description for the four molecules. The Mo-E π-bond polarization increases toward Mo from Mo−C to Mo−Sn. The σ donor orbital at E has more s-character for the heavier elements. The same authors (MS92b) also examined the bonding situation in Schrock-type complexes Mo−EH_2 (E = C, Si, Ge, Sn), which were optimized at the (8/8) CASSCF level.[238] The metal−ligand interactions were found to be best described with the bonding model shown in Figure 23b, i.e., with an open-shell (^7S) state for Mo and ($^3B_1$) for EH_2 yielding the $^5B_1$ ground state of $MoEH_2$. The Mo-E bond orders become smaller from Mo−CH_2 (1.447) to Mo−SnH_2 (0.936). The Mo-E bond energies with respect to the high-spin state of EH_2, which is not the ground state for SiH_2, GeH_2, SnH_2, show the order C > Si $\approx$ Ge $\approx$ Sn. The calculated bond energies were only one-half of the bond energies which were found for the Fischer-type complexes $(CO)_5Mo-EH_2$.[237] The enhancement of the Mo−EH_2 bond through carbonylation of Mo also became obvious from the calculated Mo−EH_2 force constants, which are are clearly higher in the case of $(CO)_5Mo-EH_2$ than for Mo−EH_2, particularly for the carbene complexes.[238]

Chemical bonding in Fischer-type carbene complexes and in higher homologues has been the subject of three theoretical studies at the DFT level by Ziegler et al.[239−241] The first paper by Jacobsen, Schreckenbach, and Ziegler (JSZ)[239] focused on the importance of nonlocal density corrections and relativistic effects on the geometries and bond energies of $(CO)_5MCH_2$ (M = Cr, Mo, W). The second paper by Jacobsen and Ziegler (JZ95)[240] reported the trends in the structure and bonding of carbene and silylene complexes $(CO)_5CrER_2$ with ER_2 = CH_2, CF_2, CCl_2, CMe_2, $CMe(OMe)$, SiH_2, SiF_2, $SiCl_2$, $SiMe_2$, and $SiMe(OMe)$. The authors analyzed the Cr−EH_2 interactions between the singlet fragments $(CO)_5Cr$ and ER_2 at the frozen geometries of the complexes using the ETS method. It was found that the silylene complexes have lower metal−ligand bond energies than the respective carbene complexes. The ETS analysis showed that the main difference between the two classes of compounds is the Cr−ER_2 π-bond strength, which is very weak in the silylene complexes. This explains why the latter compounds exhibit a Lewis-acidic behavior of the SiR_2 group, which frequently leads to base-stabilized silylene complexes $L_nTM-SiR_2(D)$ where D is an electron donor.[242,243]

JZ95 estimated the σ and π bond strength of the Cr−CR_2 and Cr−SiR_2 bonds using the calculated values of the ETS method for the σ- and π-orbital

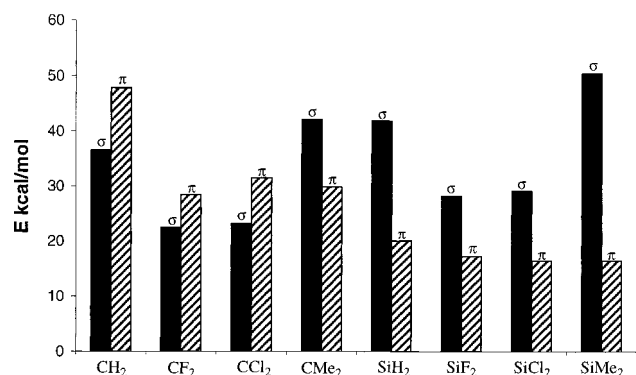**Figure 25.** Calculated σ-bond strengths and π-bond strengths of various $(CO)_5Cr=ER_2$ complexes. (Reproduced with permission from ref 240. Copyright 1995 American Chemical Society.)

interactions $E_{orb}(\sigma)$ and $E_{orb}(\pi)$ and the values for the "steric" interactions $E°$, which is the sum of the Coulombic interactions and Pauli repulsion.[240] The latter term could not be broken down into σ and π contributions. Jacobsen and Ziegler argued that the major contribution to the "steric" interactions should come from the lone-pair σ orbital of ER_2 and, thus, should be combined with $E_{orb}(\sigma)$ to give the reduced σ-bond strength of the Cr-ER_2 bonds $E'(\sigma)$.[240,241] This means that the $E'(\sigma)$ values underestimate the contribution of the σ-bond strength, because the Pauli repulsion is completely considered as a σ-type interaction. Figure 25 shows the diagram of the calculated reduced σ-bond strengths and π-bond strengths of the carbene and silylene complexes.[240] It becomes obvious that the carbene complexes have significantly higher π-bond strengths than the silylene complexes, whereas the latter have even slightly higher reduced σ-bond strengths than the former.

The third paper by Jacobsen and Ziegler (JZ96)[241] investigated the chemical bonding in $(CO)_5Cr-EH_2$ (E = C, Si, Ge, Sn) and $(CO)_5TM-CH_2$ (TM = Mo, W, Mn$^+$). The most remarkable difference among the complexes $(CO)_5Cr-EH_2$ (E = C, Si, Ge, Sn) was found to be the drop in the Cr-E π bond strength. The calculated π-orbital interactions of the Cr-CH_2 bond using the ETS method is more than twice as strong as that for the SiH_2 species, which has a comparable π-bond strength to the GeH_2 and SnH_2 complexes. The difference in π-bond strength also manifests in geometric parameters such as in the Cr-CO_{trans} bond lengths, which are clearly longer in the carbene complexes due to weaker Cr-CO_{trans} π-back-donation than in the higher homologues. The calculated reduced σ-bond strength of the Cr-CH_2 bond was reported to be lower than that for the Cr-SiH_2 bond, while the Cr-GeH_2 and Cr-SnH_2 bonds have slightly smaller $E'(\sigma)$ values than Cr-CH_2.[241] The differences in the σ and π interactions of the Cr-EH_2 bonds were explained with the orbital energies of the HOMO and LUMO of EH_2. The energy levels of the HOMO and particularly the LUMO of the heavier EH_2 ligands with E = Si, Ge, Sn are higher than with CH_2, which leads to significantly weaker π-interactions with the $Cr(CO)_5$ fragment while the σ-interactions should become higher. The authors point out that the overlap between the π-symmetric

frontier orbitals of $Cr(CO)_5$ and EH_2 cannot be used to explain the trend of the orbital interactions $E_{orb}(\pi)$ because the values for the overlap integrals change only slightly from CH_2 to SnH_2. This is another manifestation of the fact that the energy match of the interacting bonding electrons of two fragments is more important for the bond energy than the orbital overlap.[5]

The breakdown of the energy contributions to the $(CO)_5TM-CH_2$ bonds for TM = Cr, Mo, W, Mn$^+$ reported by JZ96[241] showed the trend Mn$^+$ < Cr $\approx$ Mo < W for the π-bond strength. The lower $E_{orb}(\pi)$ value for Mn$^+$ was explained by the authors with the positive charge of the metal, which leads to much lower lying frontier orbitals. The Mn$^+$ molecule also has the lowest σ-bond strength of the four carbene complexes. The higher π-bond strength of the tungsten complex was explained with the relativistically destabilized d orbital, which therefore rises in energy leading to stronger interaction with the empty p(π) carbene orbital.

A comparative theoretical study of the structures and bonding in Schrock-type and Fischer-type tungsten carbene complexes has recently been published by Vyboishchikov and Frenking (VF98a).[244] The authors calculated the geometries and bond energies of the low-valent complexes $(CO)_5W-CR_1R_2$ with the ligands CH_2, CF_2, CHF, CH(OH) (**1**−**4**) and the high-valent complexes X_4W-CH_2 with X = F, Cl, Br, I, OH (**5**−**9**) and F_4W-CF_2 (**10**). They also investigated the negatively charges species $F_5W-CH_2^-$ and $F_5W-CF_2^-$ (**11**−**12**). The geometries were optimized at the HF and MP2 levels of theory, and the TM−carbene bond dissociation energies were predicted at CCSD(T) using the MP2-optimized structures. The analysis of the bonding situation was carried out with the help of the NBO and CDA partitioning schemes and with Bader's topological analysis of the electron density distribution, which is also known as AIM (atom-in-molecules) method.[108]

The most important results about the tungsten−carbene bonding situation, which are shown in Table 12, can be summarized as follows. The W−C bonds of the low-valent complexes **1** − **4** are significantly longer (by ~ 0.2 Å) than the bond distances in the high-valent complexes **5**−**10**. The anionic complexes **11**−**12** have intermediate W−C bond lengths. The metal−carbene distances *cannot* be used to estimate the bond dissociation energy D_e of the complexes into the fragments L_nTM and CR_1R_2 in their electronic ground state. For example, the CCSD(T) value of F_4W-CH_2 (**5**) is $D_e = 118.2$ kcal/mol, but for F_4W-CF_2 (**10**) it is only $D_e = 57.5$ kcal/mol, although **5** and **10** have similar W−C bond lengths. The large difference between the D_e values can be explained with the electronic ground state of the carbene ligand, which has a strong influence on the strength of the metal−carbene bond. CF_2 has a $^1A_1$ ground state. The first excited $^3B_1$ state of CF_2 is 56.7 kcal/mol higher in energy.[245] Since the $^3B_1$ state of CF_2 is the electronic reference state in the carbene complex **10**, it follows that the actual interaction energy between F_4W, which has a triplet ground state, and CF_2 is 114.2 kcal/mol. The much higher value agrees with

Table 12. Analysis of the $L_nW=CR_2$ Carbene Bonds in Low-Valent (Fischer-type) Complexes 1−4 and High-Valent (Schrock-type) Complexes 5−12[a]

molecule	no.	R^b	D_e^c	AIM[d]		NBO[e]				CDA[f]		
				H_b	P	%W	$q(W)$	$q(CR_2)$	$p(\pi)$	$d(W \leftarrow CR_2)$	$b(W \rightarrow CR_2)$	Δ
$(CO)_5W(CH_2)$	**1**	2.031	78.9	−0.382	1.18	24.5 (σ)	−0.41	−0.13	0.67	0.314	0.282	0.016
						62.9 (π)						
$(CO)_5W(CF_2)$	**2**	2.057	60.6	−0.256	0.93	28.2 (σ)	−0.57	0.04	0.67	0.369	0.219	0.027
$(CO)_5W(CHF)$	**3**	2.029	80.0	−0.355	1.10	22.7 (σ)	−0.48	−0.04	0.67	0.324	0.268	0.017
						67.3 (π)						
$(CO)_5W(CH(OH))$	**4**	2.088	75.0	−0.272	0.93	28.0 (σ)	−0.54	0.13	0.61	0.417	0.177	0.032
$F_4W(CH_2)$	**5**	1.860	118.2	−0.940	1.71	38.8 (σ)	2.41	−0.38	1.20	0.013	−0.084	0.380
						33.8 (π)						
$F_4W(CF_2)$	**6**	1.892	57.5	−0.793	1.54	34.8 (σ)	2.32	−0.33	1.13	0.440	0.223	0.351
						39.3 (π)						
$Cl_4W(CH_2)$	**7**	1.850	75.3	−0.973	1.82	41.5 (σ)	1.06	−0.24	1.11	−0.031	−0.058	0.416
						48.6 (π)						
$Br_4W(CH_2)$	**8**	1.851	74.2	−0.956	1.85	41.1 (σ)	0.63	−0.24	1.10	−0.014	−0.074	0.406
						42.4 (π)						
$I_4W(CH_2)$	**9**	1.844	70.5	−0.978	1.87	41.1 (σ)	0.27	−0.25	4.09	0.343	−0.044	0.423
						45.7 (π)						
$(OH)_4W(CH_2)$	**10**	1.886	108.0	−0.831	1.67	30.1 (σ)	2.10	−0.40	1.17	0.016	−0.069	0.396
						33.3 (π)						
$F_4W(CH_2)$	**11**	1.934	101.3	−0.702	1.48	27.7 (σ)	2.45	−0.63	1.19	0.451	0.234	−0.006
						42.7 (π)						
$F_4W(CF_2)$	**12**	1.966	62.8	−0.530	1.57	24.4 (σ)	2.34	−0.54	1.12	0.440	0.223	0.005
						40.9 (π)						

[a] Taken from ref 244. [b] Bond lengths calculated at MP2 [Å]. [c] Bond dissociation energies at CCSD(T) [kcal/mol]. [d] Energy density at the bond critical point H_b [Hartree/Å^3], covalent bond order P. [e] Polarity of the $W-C_{carbene}$ bond in %W, partial charges $q(W)$ and $q(CR_2)$, population of the $p(\pi)$ A of $C_{carbene}$. [f] Donation d, back-donation b, rest term Δ.

the short W−C bond distance. However, neither the bond dissociation energies nor the interaction energies of low-valent and high-valent carbene complexes can be correlated with the W−C interatomic distances, because the chemical bonding in the two classes of complexes is caused by different types of interactions. The calculated D_e values and W−C interaction energies of $(CO)_5W-CH(OH)$ (75.0 kcal/mol) and Cl_4W-CH_2 (75.3 kcal/mol) are nearly the same but the W−C distances differ by more than 0.2 Å.[244]

The analysis of the W−C bonding situation in **1−12** given by VF98a strongly supports the bonding model of TH[214] and RCG[215−219] shown in Figure 23.[244] The CDA results for the W−C interactions indicate that the bonding in the low-valent complexes **1−4** can be interpreted in terms of donor−acceptor interactions and that the $W \leftarrow CR_1R_2$ σ-donation is larger than the $W \rightarrow CR_1R_2$ π-back-donation. The neutral high-valent complexes **5−10** have large values for the rest term, which gives the contribution that arises from mixing of unoccupied orbitals of the two fragments. This unphysical result indicates that the bonds are not formed by donor−acceptor interactions but rather by covalent interactions between open-shell fragments. The CDA results for the negatively charged complexes $F_5W-CH_2^-$ (**11**) and $F_5W-CF_2^-$ (**12**), however, suggest that the W−carbene bonds of these high-valent species may also be considered as donor−acceptor complexes, because the rest term is ∼0. Thus, the formal valency of a transition metal may not automatically indicate the type of metal−carbene bonding. A similar situation has been described by Pidun and Frenking (PF),[115,116] who analyzed the chemical bonding in TM alkene and alkyne complexes in terms of metallacyclic structure or donor−acceptor interactions with the CDA method. PF found that the

neutral compound $Cl_4W(HCCH)$ has a metallacyclic structure with two W−C 2c−2e bonds, while the negatively charged molecule $Cl_5W(HCCH)^-$ can be discussed as a donor−acceptor complex. More details are given in the section about alkyne complexes.

The NBO data and the topological analysis of the electron density distribution reported by VF98a[244] showed significantly different results between the low-valent complexes **1−4** and the high-valent species **5−12** (Table 12). The population of the formally empty $p(\pi)$ AO of the carbene carbon atom of **1−4** was calculated to be much lower (0.61−0.67 e) than that of **5−12** (1.09−1.20). The $W-CR_1R_2$ π bond of **1−4** was found to be more polarized toward the tungsten end, while in the high-valent complexes **5−12** it was more polarized toward the carbon end. The bond order for the W−carbene bonds in the low-valent complexes **1−4** is only between 0.93 and 1.18, while it is much higher (1.48−1.87) in **5−12**. This clearly shows a higher double-bond character in the W-carbene bonds and more π-charge at the carbene carbon atoms for the high-valent carbene complexes compared with the low-valent species, which is in agreement with the electrophilic and nucleophilic reactivity of the carbene ligands of the latter and former complexes, respectively. The partial charges of the carbene ligands of the two classes of compounds are not very different though. The complexes **1−4** have carbene ligands that are nearly neutral, while the carbene ligands of **5−10** carry small negative charges between −0.24 and −0.40. This is because the W-carbene σ bonds of the high-valent complexes **5−10** are more polarized toward carbene than those of **1−4**.

The difference in the electronic structure between the two types of compounds and the anisotropic electron deficiency at the carbene carbon center of
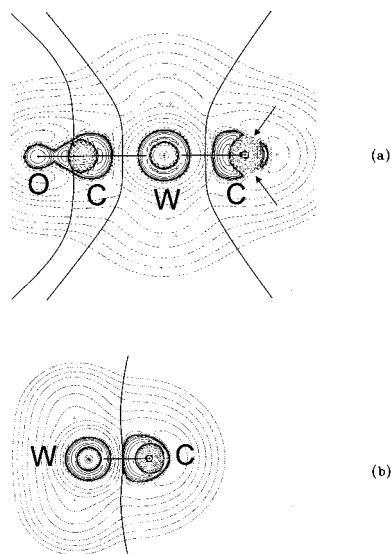
Figure 26. Contour line diagrams of the Laplacian distribution $\nabla^2\rho(\mathbf{r})$ in the plane perpendicular to the plane of the carbene ligand of (a) $(CO)_5W-CH_2$, (b) Cl_4W-CH_2. Dashed lines indicate charge depletion ($\nabla^2\rho(\mathbf{r}) > 0$); solid lines indicate charge concentration ($\nabla^2\rho(\mathbf{r}) < 0$). The solid lines connecting the atomic nuclei are the bond paths; the solid lines separating the atomic nuclei indicate the zero-flux surfaces in the plane. The arrows in a show the holes in the valence sphere of the carbene ligand that are prone to attack by a nucleophilic agent. (Reproduced with permission from ref 244. Copyright 1998 Wiley-VCH.)

the high-valent species becomes visible when the Laplacian distribution in the π-plane of the carbene ligands are compared. Figure 26 shows the contour line diagrams of **4** and **5**. The low-valent Fischer complex **4** has an area of charge depletion (dashed lines) in the direction of the $p(\pi)$ orbitals of the carbene carbon atom. There are "holes" in the electron concentration, which are visible signs for the direction of a possible nucleophilic attack. They are indicated by arrows in Figure 26. In contrast to the Fischer carbene **4**, the carbene carbon atom of the Schrock complex **5** is shielded by a continuous area of charge concentration, which protects the atom from nucleophilic attack. Another difference was found when the energy values at the W-carbene bond critical points H_b, which indicate the degree of covalent character of a bond,[128] were compared (Table 12). The H_b values of **5**–**12** have significantly larger negative numbers than those of **1**–**4**, which suggests that the W-carbene bonds of the high-valent complexes have a much higher covalent character than those of the low-valent compounds.

A particular class of TM carbene complexes is formed when the ligand is a N-heterocyclic carbene $C(N_{cyc}N')$. Examples of N-heterocyclic carbene complexes have been known since 1968, when Öfele[246] and Wanzlick[247] reported the first syntheses of such compounds. Spectroscopic studies lead to the suggestion that unlike in typical Fischer-type carbene complexes, there is little TM $\rightarrow C(N_{cyc}N')$ π-back-donation in these complexes.[248] The synthesis of the first stable N-heterocyclic carbene imidazol-2-ylidene by Arduengo[249] revitalized experimental studies of the complexes, particularly since it was found that they may be used as homogeneous catalysts.[220] The

bonding properties of complexes of the group-11 metal chlorides TMCl (TM = Cu, Ag, Au) with the N-heterocyclic carbene imidazol-2-ylidene and the related silylene and germylene have been the subject of a theoretical study at the MP2 and CCSD(T) levels of theory by Boehme and Frenking (BF).[221] The metal–ligand interactions were analyzed with the NBO and CDA partitioning scheme and with the topological analysis of the electron density distribution. The results of BF may be summarized as follows.

The TM–$X(N_{cyc}N')$ (X = C, Si, Ge) bonds are rather strong, i.e., between 56.5 and 82.5 kcal/mol for the carbene complexes, 37.4 and 64.1 kcal/mol for the silylene complexes, and 29.9 and 49.4 kcal/mol for the germylene complexes. The bond strengths show the trends Au > Cu > Ag and C > Si > Ge for TM and X, respectively. The TM–X bonds are largely ionic, but the covalent contributions are not negligible. The covalent bond orders of the TM–X bonds are between 0.45 and 0.59 for the carbenes, 0.61 and 0.76 for the silylenes, and 0.49 and 0.62 for the germylenes. The donor–acceptor interactions are mainly caused by TM ← X σ-donation, while TM → X π-back-donation is very small. The population of the $p(\pi)$ orbital of X becomes higher in the complexes, but this is caused by enhanced N → X π-donation of the nitrogen lone pairs, which strengthens the aromatic character of the imidazol-2-ylidene rings.[221]

The main reason for the stability of the N-heterocyclic carbenes is the N → $C_{carbene}$ π-donation, which is enhanced through cyclic delocalization.[250,251] However, neither aromatic delocalization nor a cyclic structure is necessary for a carbene to become isolable. Even acylic diaminocarbenes $C(NR_2)_2$ with large alkyl groups have been synthesized.[252] A recent theoretical study at the MP2 level by Beste, Krämer, Gerhard, and Frenking (BKGF)[253] investigated the structure and bonding situation in the mono- and bis-carbene complexes $F_4Ti[C(NH_2)_2]_n$ and $Cl_4Ti[C(NH_2)_2]_n$ ($n = 1, 2$). The calculations predict that the titanium halides may bind one or two carbene ligands with nearly the same binding energy. The calculated bond energies were lower than in the case of the group-11 carbene complexes but still rather high (38–45 kcal/mol). The Ti–C bonds have a strongly ionic character. The covalent bond orders are only between 0.39 and 0.44.[253]

V.3. Carbyne Complexes

The nature of the chemical bonding in TM complexes which have a formal metal–carbon triple bond $L_nTM\equiv CR$ has received much less attention by theoreticians than TM carbene complexes $L_nTM=CR_2$. The still rather young history of TM carbyne complexes shows some parallels to the chemistry of carbene complexes. The same two authors who introduced two different classes of carbene complexes were also the first to show that the same dichotomy exists for carbyne complexes. In 1973, Fischer et al. reported the synthesis of $Br(CO)_4W(CMe)$.[254] Five years later, Schrock succeeded in isolating $CpCl(PMe_3)MeTa(CPh)$.[255] Although the distinction between the two types of compounds into low-valent

(Fischer-type) carbyne complexes and high-valent (Schrock-type) alkylidyne complexes is less clear-cut than in the case of carbene complexes, it has become a useful model to explain the differences in the chemical behavior of Fischer and Schrock carbyne complexes. Generally, the carbyne ligand of Fischer complexes reacts electrophilic, while Schrock alkylidene complexes usually exhibit nucleophilic reactivity at the carbyne center.[210,256−259] An important difference between Fischer-type carbene and carbyne complexes is that the latter compounds do not need a π-stabilizing substituent R at the carbyne ligand L_nTMCR in order to become isolable.

Most previous theoretical studies of TM carbyne complexes have been carried out at a semiempirical level of theory and, thus, shall only briefly be reviewed. Three papers from the group of Fenske analyzed the TM≡CR triple bond in neutral and positively charged low-valent (Fischer-type) carbyne complexes using Fenske−Hall[260] approximate SCF calculations.[261] The calculations gave strong σ and degenerate or nearly degenerate π bonds between chromium, manganese, iron, and the CR ligand. The authors concluded that the carbyne ligand is a stronger π acceptor than CO and that the carbyne carbon atom accumulates negative charge.[261b] The TM≡CR π bond remains nearly degenerate when R = phenyl or NH_2.[261a,b] This result was taken as evidence that in aminocarbynes the contribution of the Lewis structure $L_nTM≡C−NR_2$ is much more important than that of $L_nTM=C=NR_2$. The same result was found in an independent study of aminocarbyne complexes at the EHT level by Schubert et al.[262]

The first ab initio treatment of a TM carbyne complex was published in 1984 by Ushio, Nakatsuji, and Yonezawa (UNY)[213] who reported SCF calculations of $(CO)_5CrCH^+$ and *trans*-$Cl(CO)_4CrCH$ with partial geometry optimization of the carbyne ligand. The optimized Cr−CH distances compared quite well with the experimental results. The Mulliken population analysis gave negative partial charges for the carbyne carbon atoms in both the neutral and the cationic complex, which is in agreement with the semiempirical work. The problems of UNY[213] to calculate a reasonable Cr−CH bond energy at the SCF level inspired Poblet, Strich, West, and Bénard (PSWB)[263] to carry out the first ab initio study of a TM carbyne complex which includes correlation energy. The authors found that *trans*-$Cl(CO)_4CrCH$ is unbound at the SCF level with regard to dissociation into the neutral fragments $Cl(CO)_4Cr$ and CH. Calculations at the CASSCF level gave a Cr−CH BDE of 115 kcal/mol,[263] which is the experimental value for the triple-bond energy of VCH^+ in the gas phase.[264] Analysis of the CASSCF wave functions showed that the degenerate Cr−C π bond is essentially nonpolar, while the σ bond is clearly polarized toward the carbon end, which leads to a partial negative charge at the carbyne ligand.[263]

The insight into the chemical bond of TM carbyne complexes which was gained from theoretical calculations has been reviewed in 1988 by P. Hofmann.[265] The author presented a qualitative MO model for the
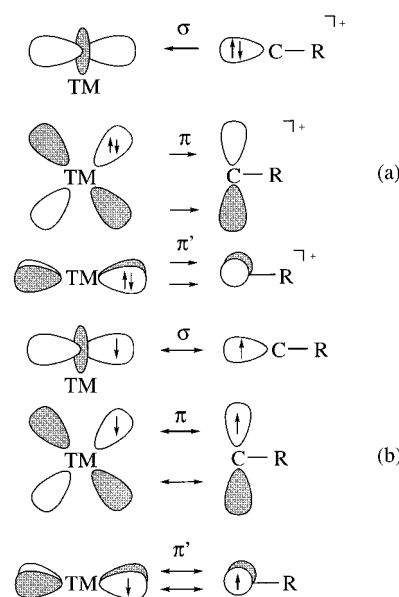

Figure 27. Schematic representation of the dominant orbital interactions in (a) Fischer-type carbyne complexes and (b) Schrock-type carbyne complexes.

chemical bonding in carbyne complexes $L_nTM≡CR$ which is based on orbital interaction diagrams between different fragments L_nTM and CR. The discussion of the Tm≡C triple bond in terms of donor−acceptor interactions between closed-shell fragments leads to a somewhat arbitrary decision for choosing the electronic structure of the metal and ligand fragments, because CR and L_nTM are open-shell species. Hofmann has chosen L_nTM^- and CR^+ as interacting fragments, where CR^+ has a doubly occupied σ orbital which serves as a donor orbital and a doubly degenerate empty p(π) AO at carbon which serves as an acceptor orbital (Figure 27a). Hofmann's choice leads to a model for the orbital interactions in carbyne complexes which is similar to the donor−acceptor model for TM complexes with the isoelectronic group-13 diyl ligands ER (E = B−Tl, Figure 40) and carbonyl complexes (Figure 8). An alternative breakdown of carbyne complexes in closed-shell species leads to L_nTM^{3+} and CR^{3-}, which has been used by other authors to discuss the TM≡C bond.[210] However, it seems that the choice made by Hofmann is more useful because it is in better agreement with the actual charge distribution in carbyne complexes.

Theoretical studies of TM carbyne complexes have been in a dormant stage for a decade after Hofmann's review appeared in 1988.[256] Very recently, Vyboishchikov and Frenking (VF98b) reported the results of HF and MP2 calculations of 13 low-valent (Fischer-type) and 13 high-valent (Schrock-type) tungsten carbyne complexes.[266] The geometries of the 26 compounds were completely optimized, and the W≡C BDEs of seven complexes were calculated at the CCSD(T) level of theory using MP2-optimized geometries. The main focus of the paper of VF98b, which was the sequel of an analogous investigation of tungsten carbene complexes,[244] was the analysis of the bonding situation in the carbyne complexes using the NBO, CDA, and AIM methods.
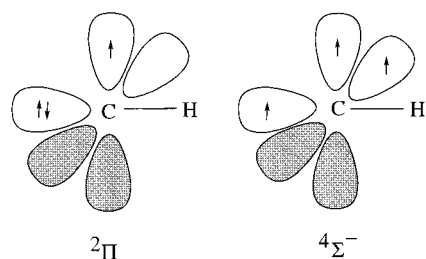
$^2\Pi$ $^4\Sigma^-$

Figure 28. Schematic representation of the $^2\Pi$ ground state and the $^4\Sigma^-$ first excited state of CH.

VF98b have used the same closed-shell fragments L_nTM^- and CR^+ as a model for the orbital interactions in the Fischer-type complexes as P. Hofmann chose.[256] They also used a similar dichotomy of bonding models for high- and low-valent carbynes which had been suggested for carbene complexes by Taylor and Hall[214] and by Rappé, Carter, and Goddard[215−219] and which had proven to be very helpful for the interpretation of the $L_nW=CR_2$ bond.[244] Figure 27a shows the dominant orbital interactions in low-valent carbyne complexes, which has $L_nTM^- \leftarrow CR^+$ σ-donation and degenerate $L_nTM^- \rightarrow CR^+$ π-back-donation. The $TM\equiv C$ triple bond in the high-valent complexes has an electron-sharing σ bond and a degenerate π bond between the neutral fragments L_nTM and CR in the respective electronic quartet state (Figure 27b). A quartet state is probably the electronic ground state for many L_3W fragments.[267] CH has a $^2\Pi$ ground state, but the electronically excited $^4\Sigma^-$ state (Figure 28) is only 15.9 kcal/mol higher in energy.[268] VF98b suggested that there should be a correlation between the excitation energy of a carbyne ligand from the $^2\Pi$ ground state to the $^4\Sigma^-$ excited state with the $TM\equiv CR$ BDE in Schrock-type carbyne complexes.[266] Carbynes with a high excitation energy should have a lower BDE than carbynes which have a low excitation energy.

Table 13 summarizes the most important results of the seven tungsten carbyne complexes for which the $W\equiv CR$ BDEs have been calculated by VF98b.[266] A comparison with the results of the tungsten carbene complexes (Table 12) gives insights into the

differences between the bonding situation in $L_nW\equiv$ CR and $L_nW=CR_2$ complexes. The $W\equiv CR$ triple bonds are significantly shorter and stronger than related $W=CR_2$ double bonds. A comparison of the calculated BDEs of the three carbyne complexes $Cl_3W(CR)$ with R = H (D_e = 154.5 kcal/mol), F (D_e = 111.7 kcal/mol), and NH_2 (D_e = 104.9 kcal/mol) with the $^2\Pi \rightarrow ^4\Sigma^-$ excitation energies of CR supports the proposed bonding model for the Schrock-type carbyne complexes. The excitation energies of CH, CF, and CNH_2 are 15.9,[268] 61.3,[269] and 78.2 kcal/mol,[270] respectively.

The most important results of the bonding analysis which are given in Table 13 can be summarized as follows. The NBO data show that the Fischer- and Schrock-type carbyne complexes have $W-C$ σ bonds that are strongly polarized toward the carbon atom. The complexes have degenerate or nearly degenerate π bonds which are less polar than the σ bonds. The $W\equiv C$ π bond in the aminocarbyne complex **18** remains nearly degenerate, which supports earlier suggestions[261a,b,262,265] in favor of a $W\equiv C-NR_2$ bonding situation. The carbyne ligand is nearly neutral in the Fischer complexes but carries a small negative charge in the Schrock complexes. The formally empty $p(\pi)$ AOs of the carbyne carbon atom in the Fischer complexes are significantly occupied with 1.6−1.7 electrons, while the Schrock complexes have an even larger population of 1.9−2.0 electrons. The $W\equiv CR$ covalent bond orders are rather high. They are between 1.7 and 2.1 in the Fischer complexes and between 2.3 and 2.5 in the Schrock complexes. The strongly covalent character of the tungsten−carbyne bonds also becomes evident by the calculated energy densities at the bond critical point $H(\mathbf{r}_c)$, which have large negative values. The CDA analysis indicates strong $L_nW^- \rightarrow CR^+$ π-back-donation. However, this was calculated with respect to negatively charged metal fragments and positively charged carbyne ligands, which necessarily leads to strong back-donation. More important are the CDA results for the rest term. The large deviation of the calculated numbers from zero for the Schrock carbyne complexes indicates that the molecules are not true donor−

Table 13. Analysis of the $L_nW\equiv CR$ Carbyne Bond in Low-Valent (Fischer-type) Complexes 13−15 and High-Valent (Schrock-type) Complexes 16−19[a]

molecule	no.	R^b	$D_e{}^c$	AIM[d]		NBO[e]				CDA[f]		
				H_b	P	%W	q(W)	$q(CR_2)$	$p(\pi)$	d(W ← CR_2)	b(W → CR_2)	Δ
$Br(CO)_4W(CH)$	**13**	1.843	133.9	−0.708	1.97	29.5 (σ) 61.9 (π)	−0.24	−0.07	1.64	0.403	0.753	−0.029
$Br(CO)_4W(CF)$	**14**	1.854	105.0	−0.536	1.79	27.6 (σ) 64.4 (π)	−0.38	0.04	1.67	0.500	0.742	0.112
$Br(CO)_4W\{C(NH_2)\}$	**15**	1.849	95.2	−0.597	1.80	27.7 (σ) 53.1 (π)	−0.33	0.12	1.65	0.524	0.726	0.069
$Cl_3W(CH)$	**16**	1.761	154.5	−1.127	2.52	29.9 (σ) 60.4 (π)	1.06	−0.22	1.90	0.061	0.267	0.621
$Cl_3W(CF)$	**17**	1.767	111.7	−0.902	2.33	26.2 (σ) 63.5 (π)	0.98	−0.15	1.89	0.014	0.212	0.618
$Cl_3W\{C(NH_2)\}$	**18**	1.757	104.9	−1.031	2.43	35.7 (σ) 55.8 (π)	1.04	−0.13	1.99	0.017	0.213	0.554
$Cl_4W(CH)$	**19**	1.764	176.5	−1.129	2.48	36.3 (σ) 52.0 (π)	0.95	−0.26	1.92	−0.016	0.339	0.381

[a] Taken from ref 266. [b] Bond lengths calculated at MP2 [Å]. [c] Bond dissociation energies at CCSD(T) [kcal/mol]. [d] Energy density at the bond critical point H_b [Hartree/Å³], covalent bond order P. [e] Polarity of the $W-C_{carbene}$ bond in %W, partial charges q(W) and $q(CR_2)$, population of the $p(\pi)$ A of $C_{carbene}$. [f] Donation d, back-donation b, rest term Δ.

acceptor complexes but normal covalently bound molecules.[266]

V.4. Alkene π-Complexes and Higher Homologues

The same dichotomy of bonding models for TM–ligand interactions which has proven to be very helpful for understanding the bonding situation in carbene and carbyne complexes in terms of donor–acceptor interactions or shared-electron bonding is also found in the theoretical literature about the structure and bonding of TM complexes with alkene ligands. Alkene complexes were actually the first example of TM compounds for which Dewar, Chatt, and Duncanson suggested the model of synergistic ligand → TM σ-donation and ligand ← TM π-back-donation (Figure 29a).[53,54] The σ-donation arises from
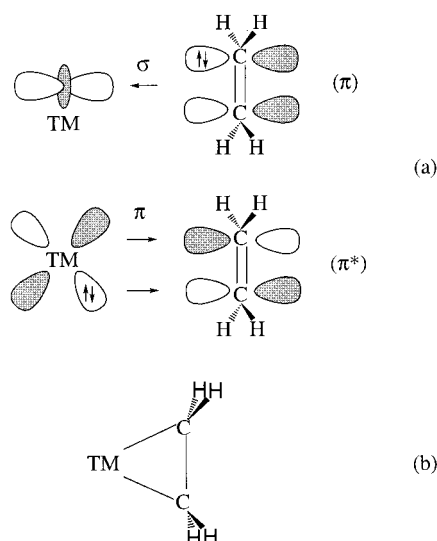
Figure 29. Schematic representation of the bonding models for TM–olefin complexes: (a) DCD model of donor–acceptor interactions and (b) metallacyclopropane.

the occupied π-MO of the alkene, which has σ-symmetry in the complex, while the π-back-donation occurs through charge donation from the occupied d_{xz} MO of the metal to the vacant π^* orbital of the olefin. The alternative bonding model has two electron-sharing σ bonds between the metal and the carbon atoms which leads to a description of the molecule as a metallacyclopropane (Figure 29b).

There have been early studies at the semiempirical and ab initio HF level using fixed geometries to investigate the question of π complex vs metallacycle in TM ethylene complexes.[271–273] The first theoretical study at a more reliable level was published by Steigerwald and Goddard (SG) in 1985.[274] They optimized the geometry of $Cl_2Ti(C_2H_4)$, which was used as model for $Cp^*_2Ti(C_2H_4)$, at the GVB level. It was found that the calculated C–C bond length (1.46 Å), which is in good agreement with the experimental value for $Cp^*_2Ti(C_2H_4)$, corresponds more to a single bond than to a double bond. The analysis of the optimum valence-bond orbitals for the Ti–C and C–C bonds gave two Ti–C σ bonds between a d orbital on Ti and a p orbital on each carbon. It also gave a C–C σ bond but no C–C π bond. SG concluded

that $Cl_2Ti(C_2H_4)$ and $Cp^*_2Ti(C_2H_4)$ are metallacycles, not π-complexes.[274] The authors also analyzed the VB wave function of a $Cl_2Ti(C_2H_4)$ π-complex, which was calculated by restricting the GVB calculations so that there is a C=C double bond and an electron lone pair which occupies a metal d orbital with the proper symmetry for Ti → C_2H_4 π-donation. The restricted GVB calculations gave a geometry of $Cl_2Ti(C_2H_4)$ which has a significantly shorter C–C bond (1.375 Å) than the metallacyclic form. The π-complex was found at the GVB–CI level to be 14.8 kcal/mol higher in energy than the metallacycle.[274] The authors proposed three rules for the factors which influence the formation of a metallacyclic form or a π-complex. Donor–acceptor-type complexes are more likely to be formed when (i) the metal has low-lying electronic states with doubly occupied d orbitals; (ii) the C=C π bond is strong; (iii) the metal–carbon σ bond is strong.

Rule i was supported by a theoretical study by Sodupe, Bauschlicher, Langhoff, and Partridge (SBLP),[275] who calculated the bonding of the first-row TM ions Sc^+–Cu^+ to ethylene at the MCPF level of theory using HF-optimized geometries. Analysis of the metal AO population in the electronic ground state of the C_{2v} equilibrium structures showed that only in $Sc(C_2H_4)^+$ and $Ti(C_2H_4)^+$ the metal ion inserts into the C=C π bond which leads to a metallacyclic form, while the later TM ions V^+–Cu^+ give electrostatically bound π-complexes. The difference in the bonding type does not lead to significantly different bond energies. $Sc(C_2H_4)^+$ and $Ti(C_2H_4)^+$ were calculated with bond dissociation energies D_e = 24.8 and 24.2 kcal/mol, respectively. The other $TM(C_2H_4)^+$ species have bond energies between D_e = 16.1 (Mn^+) and 37.6 kcal/mol (Ni^+). $Sc(C_2H_4)^+$ and $Ti(C_2H_4)^+$ clearly do have longer C–C bond lengths than the other $TM(C_2H_4)^+$ complexes, however.[275]

The chemical bonds in $Cu(C_2H_4)$ and $Cu(C_2H_4)^+$ have recently been investigated at the CCSD(T) level of theory using MP2-optimized geometries by Böhme, Wagener, and Frenking (BWF).[276] The neutral complex has a very weak Cu–C_2H_4 bond (D_e = 4.2 kcal/mol), while the positively charged species $Cu(C_2H_4)^+$ has a much stronger bond with a bond energy D_e = 43.9 kcal/mol. The analysis of the electronic structure using the NBO and AIM methods showed that the weak metal–ligand bonding in $Cu(C_2H_4)$ is caused by dispersion forces, while the strong interactions in $Cu(C_2H_4)^+$ are mainly caused by electrostatic attraction with only negligible covalent contributions. An interesting result was found by the topological analysis of the electron density distribution. There is a bond path from the Cu^+ cation to the midpoint of the C=C bond in $Cu(C_2H_4)^+$, but there are no Cu^+–C bond paths (Figure 30). It follows that $Cu(C_2H_4)^+$ has a T-shaped electronic structure. Although the bonding interactions in the neutral complex are much weaker than in the cation, there are two Cu–C bond paths and a ring critical point in $Cu(C_2H_4)$ (Figure 30). The topology of the electron density distribution of $Cu(C_2H_4)$ has a cyclic structure. This does not mean that $Cu(C_2H_4)$ should be considered as a true metallacylic compound in the sense of the bonding

$Cu(C_2H_4)$

(a)

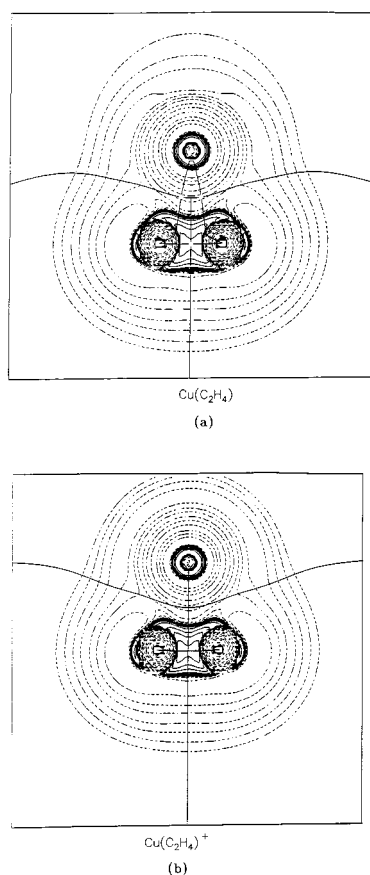$Cu(C_2H_4)^+$

(b)

Figure 30. Contour line diagrams of the Laplacian distribution $\nabla^2\rho(r)$ of (a) $Cu(C_2H_4)$ showing a cyclic structure and (b) $Cu(C_2H_4)^+$ showing a T-shaped structure. (Reproduced with permission from ref 276. Copyright 1996 Elsevier Science S.A.)

description shown in Figure 29b, because there are no genuine Cu–C chemical bonds in the molecule. It is interesting to note that the much stronger Cu^+–C_2H_4 attraction is not revealed by the shape of the Laplacian distribution, which is very similar to that of the weakly bound $Cu(C_2H_4)$ (Figure 30).[276]

A somewhat different conclusion about the nature of the chemical bond in $Cu(C_2H_4)^+$ was made by Hertwig, Koch, Schröder, Schwarz, Hrusak, and Schwerdtfeger (HKSSHS),[277] who also investigated the heavier analogues $Ag(C_2H_4)^+$ and $Au(C_2H_4)^+$ at the MP2, CCSD(T), and DFT levels. The authors used the EDA method in order to gain insight into the TM^+–C_2H_4 bond. HKSSHS suggested that the interaction of all three metal cations with ethylene shows large covalent contributions which stem mainly from $TM^+ \leftarrow C_2H_4$ σ donor interactions, while $TM^+ \rightarrow C_2H_4$ π-back-bonding is weaker but still important.[277] For example, the analysis of the DFT total binding interactions in $Cu(C_2H_4)^+$ (−62.9 kcal/mol) gave large stabilizing contributions of σ-bonding (−39.9 kcal/mol) and π-back-bonding (−21.5 kcal/mol). However, the sum of all *stabilizing* orbital interactions (−68.8 kcal/mol) is compensated by the *destabilizing* Pauli repulsion, which comes from the interactions of the occupied orbitals (96.1 kcal/mol). Thus, the covalent interactions in $Cu(C_2H_4)^+$ given by the sum of the occupied–occupied and occupied–unoccupied orbital interactions are actually repulsive, and the metal–

ligand bonding according to the EDA results is only caused by the electrostatic term (−90.8 kcal/mol).[277] The same holds true for $Ag(C_2H_4)^+$ and $Au(C_2H_4)^+$, which are more weakly and strongly bound than $Cu(C_2H_4)^+$, respectively. It is interesting to note that HKSSHS[277] found in their AIM calculations the onset of a cyclic form for the bond paths of $Cu(C_2H_4)^+$, while BWF[276] found a T-shaped structure (Figure 30). The difference is probably caused by the different theoretical level. The bond critical points of the Cu–C bonds found by HKSSHS almost coincide with the ring critical point.

Chemical bonding in olefin complexes of group 10 elements Ni, Pd, Pt has been the focus of several theoretical studies. The first ab initio work was carried out in 1981 by Kitaura, Sakaki, and Morokuma (KSM),[278] who analyzed the bonding situation in $(PH_3)_2Ni(C_2H_4)$ using the EDA partitioning scheme. KSM found that the $Ni \rightarrow (C_2H_4)$ π-back-donation contributes much more to the nickel–olefin bonding than the $Ni \leftarrow (C_2H_4)$ σ-donation. The absolute values of the donor–acceptor interactions were much smaller, however, than the electrostatic attraction between the metal and the ethylene ligand. They also found that substitution of PH_3 by NH_3 greatly strengthens the $Ni \rightarrow (C_2H_4)$ π-back-donation. Although this study was carried out only at the HF level with small basis sets using fixed geometries that were taken from experimental results, the main conclusion of the study was supported by later investigations. In 1985 Ziegler reported a bonding analysis of neutral and positively charged $(PH_3)_2TM(C_2H_4)^q$ for TM = Ni, Pd, Pt, Co^+, Rh^+, and Ir^+ using the LCAO–HFS method in conjunction with his ETS partitioning scheme.[279] The author found that, at the HFS level, the energy contribution of the $TM \rightarrow (C_2H_4)$ (TM = Ni, Pd, Pt) π-back-donation is more than 3 times higher than the $TM \leftarrow (C_2H_4)$ σ-donation.[279] The latter term becomes larger in the positively charged complexes $(PH_3)_2TM(C_2H_4)^+$ ($TM^+ = Co^+$, Rh^+, Ir^+), but it is still less important than the $TM^+ \rightarrow (C_2H_4)$ π-back-donation. However, the importance of the π-back-donation seems to be exaggerated at the HFS level. The same energy partitioning scheme was later employed by Li, Schreckenbach, and Ziegler (LSZ)[280] for the bonding analysis of the olefin complexes $(PH_3)_2Pt(C_2H_4)$ and $(CO)_4Os(C_2H_4)$ using relativistic and nonrelativistic NL-DFT calculations. LSZ showed that the nonrelativistic energy contributions of the $Pt \rightarrow (C_2H_4)$ π-back-donation to the Pt–ethylene bonding are higher (42 kcal/mol) than $Pt \leftarrow (C_2H_4)$ σ-donation (30 kcal/mol) but not by a factor of 3. Relativistic contributions increase the two values from 42 to 48 kcal/mol and from 30 to 32 kcal/mol, respectively.[280]

The chemical bonding of the $(PH_3)_2Pt$ fragments to the C=C double bonds of fullerene has been investigated in two theoretical studies at the HF level of theory. The metal binds to the strained hexagonal C=C bond shared by two six-membered rings.[281−285] Koga and Morokuma (KM)[286] optimized the geometry of $(PH_3)_2Pt(\eta^2\text{-}C_{60})$ with a small-core ECP and a valence basis set of DZ quality for Pt and 3-21G for the other atoms. The results were compared with the bonding situation in $(PH_3)_2Pt(C_2H_4)$, which was found
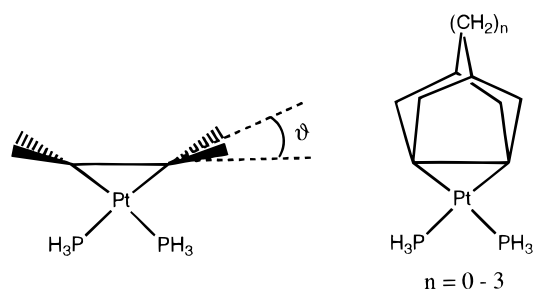
Figure 31. Pt−olefin complexes with strained olefines as ligands which were investigated in refs 288 and 290.

to have a weaker Pt−olefin BDE than $(PH_3)_2Pt(\eta^2$-$C_{60})$. KM used the Mulliken population analysis and the Boys orbital localization method in order to analyze the bonding situation. The authors concluded that there is a much larger Pt → olefin π-back-donation in $(PH_3)_2Pt(\eta^2$-$C_{60})$ than in $(PH_3)_2Pt(C_2H_4)$. The amount of charge donation from the metal fragment to the olefin in the former complex is about 3 times larger than in the latter. The Boys localization method gave two Pt−C σ bonds, and the C−C bond of the PtC_2 fragment was stretched by 0.128 Å from 1.367 Å in free C_{60} to 1.495 in the complex. It was suggested that the PtC_2 moiety should be considered as a metallacyclopropane.[286]

The second paper by Bo, Costas, and Poblet (BCP)[287] reported theoretical results for the single and multiple metal complexes $[(PH_3)_2TM]_n(\eta^2$-$C_{60})$ (TM = Pd, Pt; n = 1, 2, 6). The basis set used in this HF study was larger than that in the work of KM. The bonding situation was examined with the Mulliken population analysis and with the AIM method. BCP found that the interaction between the metal fragment and C_{60} is basically local. They also found a substantial $(PH_3)_2TM \rightarrow C_{60}$ charge donation in the complexes, which increases substantially when n becomes larger. Inspection of the metal d-occupation revealed a correlation with the charge transfer, which indicates that the electron flow occurs via TM → C_{60} π-back-donation. The TM−C_{60} bond energies and charge donation of the Pd complexes were found to be smaller than for the Pt analogues.[287]

The interaction of the $Pt(PH_3)_2$ fragment with the strained olefins shown in Figure 31 has been the subject of two theoretical studies. Morokuma and Borden (MB)[288] calculated the ethylene complex $(PH_3)_2Pt(C_2H_4)$ with constrained values for the pyramidalization angle v (Figure 31) in order to model the complex with the strained olefin with n = 1. The geometries were optimized at the HF level, and the energies were calculated at MP2. It was found that the Pt−C_2H_4 BDE in the model complex with v = 60.6°, which is the experimental value for the real compound,[289] is significantly higher than in optimized $(PH_3)_2Pt(C_2H_4)$. Inspection of the Mulliken population analysis revealed that there is enhanced Pt → (C_2H_4) π-back-donation in the geometrically constrained olefin, which is given as an explanation for the stronger bond. MB[288] also investigated the barrier for internal rotation of the $(PH_3)_2Pt$ fragment in the olefin complexes. It was found that the rotational barrier also becomes higher when v becomes larger but not nearly as large as the increase in the olefin

binding energy. This is because the Pt → (C_2H_4) π-back-donation in the transition state also becomes higher when the olefin is strained.[288]

The $Pt(PH_3)_2$(olefin) complexes with the strained olefins shown in Figure 31 with n = 0−3 have recently been calculated at the B3LYP level of theory using an ECP for Pt with a DZP-quality valence basis set and 6-31G(d) basis sets for the other atoms by Uddin, Dapprich, Frenking, and Yates (UDFY).[290] The authors also calculated the complexes $(PH_3)_2Pt$-(C_2H_4) with constrained pyramidalization angles v in order to see if these are good models for the actual compounds. The bonding situation was analyzed with the NBO and the CDA partitioning schemes. It was found that the Pt → olefin π-back-donation increases while the Pt ← olefin σ-donation remains nearly constant from n = 3 to 0. There is a nearly linear correlation of the pyramidalization angle θ (Figure 31) and the ratio of donation/back-donation.[290]

The nature of the chemical bonding in high-valent and low-valent tungsten complexes with side-on bound π ligands has been investigated by Pidun and Frenking (PF95)[291] using Cl_4WL and $(CO)_5WL$ (L = HCCH, C_2H_4, CO_2, CS_2, CH_2O) as examples. The geometries were optimized at the HF and MP2 levels, and the W−L bond energies were calculated at CCSD(T). The calculations showed that the WCl_4L complexes have significantly shorter W−L bond lengths than the $(CO)_5WL$ analogues. The topological analysis of the electron density distribution showed the electronic structure of the π ligands in the high-valent compounds Cl_4L to be much more distorted with respect to the free ligands than in the low-valent complexes $(CO)_5WL$. However, calculations of the W−L bond dissociation energy with respect to the fragments in the electronic ground state, i.e., triplet WCl_4, singlet $W(CO)_5$, and singlet L, showed that the BDEs of $(CO)_5WL$ are always higher than those of Cl_4WL except for L = C_2H_4. $Cl_4W(CO_2)$ and Cl_4W-(CS_2) were even predicted to be thermodynamically unstable species. This was explained by PF95 with the different bonding situation in the two classes of compounds.[291] The compounds Cl_4WL are metallacycles, which have two electron-sharing σ bonds bonds between Cl_4W and L. The rather low or even vanishing thermodynamic stabilization arises from the fact that the excitation energy necessary to promote the ligands from the singlet ground state to the bond-forming triplet state is rather high.

The analysis of the bonding situation using the AIM method showed that the partial charges of the ligands L are not as different between the two classes of compounds as one might expect.[291] Significant differences were found, however, for the energy density at the W−L bond critical points H_b, which have negative numbers in the Cl_4WL complexes while H_b is ∼0 in the $(CO)_5WL$ complexes.[291] This indicates covalent W−L bonds in the former complexes and closed-shell interactions in the latter.[128] The W−L covalent bond orders according to Cioslowski and Mixon[125] are much higher in Cl_4WL than in $(CO)_5WL$. Strong evidence for a qualitatively different bonding situation also came from the CDA results. The

$(CO)_5WL$ complexes gave "normal" values for the W ← L σ-donation, W → L π-back-donation, and the W ↔ L repulsive polarization. CDA calculations of Cl_4-WL using closed-shell fragments WCl_4 and L nearly always gave *negative* values for the donation and back-donation. Even more revealing was the result that the rest term Δ, which gives the mixing of the vacant orbitals of the fragments, had large contributions for the occupied orbitals of the Cl_4WL compounds. The latter are clearly metallacyclic compounds, while the $(CO)_5WL$ species are donor–acceptor complexes.

The result that ethylene is more strongly bound than acetylene in the complexes $(CO)_5WL$ while the opposite trend was predicted for the Cl_4WL compounds prompted Pidun and Frenking (PF96)[115] to analyze the bonding situation in olefin and alkyne complexes in more detail. The authors also calculated the negatively charged complexes $Cl_5W(C_2H_4)^-$ and $Cl_5W(C_2H_2)^-$ at the same level of theory as in the previous work.[291] PF96 compared not only the bonding of high- and low-valent tungsten complexes, but also the difference of the binding interactions between ethylene and acetylene complexes. It was found that the negatively charged complexes $Cl_5W(C_2H_4)^-$ and $Cl_5W(C_2H_2)^-$ are borderline cases between metallacyclic compounds and donor–acceptor complexes.[115] Details of this work will be reviewed in the following section about alkyne complexes. A summary of their work about the difference in the chemical bonding between high-valent and low-valent TM complexes has recently been presented by the authors.[116]

Complexes with ligands of the heavy-atom analogues of ethylene have received much less attention by theoreticians than olefin complexes. There are only two ab initio studies which focus on the chemical bonding in silene and disilene complexes. Sakaki and Ieki (SI) calculated the Pt complexes Cl_3PtL^- and $(PH_3)_2PtL$ (L = C_2H_4, SiH_2CH_2, and Si_2H_4).[292] The geometries were partially optimized at the HF, MP2, MP3, and MP4 levels of theory. The Mulliken population analysis was employed for the examination of the bonding situation. In both Pt(0) and Pt(II) complexes, the d(π)-orbital population of Pt decreases upon coordination of L with the order L = C_2H_4 < SiH_2CH_2 < Si_2H_4, which means that the Pt → L π-back-donation becomes stronger from ethylene to silaethylene and disilaethylene. The Pt ← L σ-donation also increases with the same trend. This is because the π HOMO raises in energy and the π^* LUMO lowers in energy in the order L = C_2H_4 < SiH_2CH_2 < Si_2H_4. The same order is found for the Pt–L bond energies, which are higher in Cl_3PtL^- than in $(PH_3)_2PtL$. The difference density maps of the molecular orbitals were used by SI[292] to analyze the extent of donor–acceptor interactions in the compounds. The authors suggest that the Pt–L bonds in the ethylene complexes of Pt(0) and Pt(II) and in the disilene complex of Pt(II) should be considered as donor–acceptor bonds, while the disilene complex of Pt(0) should be considered as metallacyclic compound.

The bonding situation in the disilene complexes $Cl_3Pt(Si_2H_4)^-$ and $(PH_3)_2Pt(Si_2H_4)$ has also been studied by Cundari and Gordon (CG).[293] CG calculated the geometries of the two compounds and those of $Cl_2TM(SiH_2H_4)$ (TM = Ti, Zr, Mo, W) at the HF level using an ECP for Pt with a valence basis set of DZ quality and 3-21G(d) basis sets for the other atoms. The calculated Si–Si force constants k_{SiSi} were taken as an indicator of the nature of the TM–SiH_2H_4 interactions. The authors suggest that the Pt(0) complexes more closely resemble a metallacyclopropane, while the Pt(II) species are more like a donor–acceptor complex. However, the difference between the two coordination modes of disilene was found to be smaller than that for ethylene in the respective Pt(0) and Pt(II) complexes.[293] For Cl_2TM-(Si_2H_4) (TM = Ti, Zr, Mo, W) it was found that the compounds with Zr and W are more like metallacycles than the Ti and Mo compounds.

V.5. Alkyne π-Complexes and Higher Homologues

The chemical bonding in TM alkyne complexes can be discussed in a similar way as for the TM alkene complexes, i.e., the bonding may be considered either to arise from donor–acceptor interactions between the alkyne ligand and the TM or as a metallacyclic compound as shown for alkene complexes in Figure 29. The major difference between alkene and alkyne complexes is the fact that the alkyne ligand has a second occupied π orbital orthogonal to the TMC_2 plane denoted as $\pi_\perp$ which may engage in TM–alkyne bonding (Figure 32). Thus, alkynes may be 2- or
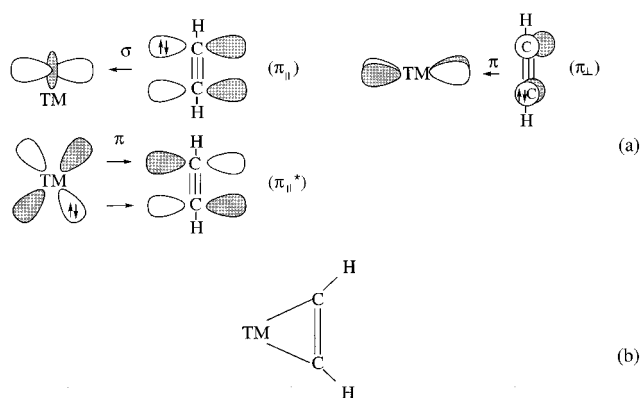
Figure 32. Schematic representation of the bonding models for TM–alkyne complexes: (a) Donor–acceptor interactions of the metal with the in-plane $\pi_\parallel$ and $\pi_\parallel^*$ orbitals and the out-of-plane $\pi_\perp$ orbital of the ligand; (b) metallacyclopropyne.

4-electron donors. On the other hand, the $\pi_\perp^*$ orbital cannot be a second π-acceptor orbital, because there is no d function which has the proper symmetry to interact with the orbital. The participation of the alkyne out-of-plane $\pi_\perp$ orbital besides the in-plane $\pi_\parallel$ MO in the metal–alkyne bonding was suggested very early.[294] Semiempirical calculations at the EHT level showed that both the in-plane and out-of-plane π orbitals of alkynes may be involved in the TM–ligand bonding, depending on the symmetry of the complex.[295] Several more quantitative theoretical studies

have been carried out to clarify the role of the alkyne $\pi_\perp$ orbital in the chemical bonding of TM alkyne complexes. Thus, three major topics arise in the analysis of TM alkyne complexes: (a) Metallacyclic vs donor−acceptor bonding; (b) Participation of the π orbitals of the alkyne in the binding interactions; (c) Difference between alkene and alkyne complexes.

Sodupe and Bauschlicher (SB) presented the results of a complete first- and second-row TM sweep of the ground and low-lying excited states of TM-$(C_2H_2)^+$ compounds (TM$^+$ = Sc$^+$−Cu$^+$ and Y$^+$−Ag$^+$) at the MCPF level using HF-optimized geometries.[296] Only structures with C_{2v} symmetry were considered in the investigation. The ground states of the alkyne complexes of the early TMs Sc$^+$−V$^+$ and Y$^+$−Nb$^+$ compounds were found to be metallacyclic compounds where the metal ion inserts into the in-plane $\pi_\parallel$ bond of acetylene. This conclusion was based on the significant alteration in the geometry of the acetylene ligand in the TM(C$_2$H$_2$)$^+$ complexes of the early TMs. The C−C distance increases significantly compared to free acetylene, and the C−C−H bond angle deviates by more than 30° from linearity. The ligand geometries in the complexes of the later TM ions Cr$^+$−Cu$^+$ and Mo$^+$−Ag$^+$ in the electronic ground state were not very different from free acetylene. The chemical bonding in these complexes is mainly caused by electrostatic attraction.[296]

The bonding situation of the first TM row acetylene complexes TM(C$_2$H$_2$)$^+$ was compared with the ethylene complexes TM(C$_2$H$_4$)$^+$ in a theoretical study by Sodupe, Bauschlicher, Langhoff, and Partridge (SBLP).[275] The covalently bound ethylene complexes of Sc$^+$ and Ti$^+$ have much lower BDEs than the respective acetylene complexes. The binding energies of the ethylene systems were calculated to be 16−19 kcal/mol lower than the corresponding binding energies of the acetylene complexes.[275,296] This was explained with the weaker π bond of acetylene, which facilitates the insertion of the metal ion.[275] The same reasoning was used to explain why the ground state of V(C$_2$H$_2$)$^+$ is covalently bound while V(C$_2$H$_4$)$^+$ is held together by electrostatic attraction. A significant contribution of the $\pi_\perp$ orbital to the TM$^+$−C$_2$H$_2$ bonding was dismissed, because the overlap of the out-of-plane orbitals was found to be very small.[296] The TM$^+$−ligand BDEs of the electrostatically bound acetylene complexes were found to be slightly lower than those of the respective ethylene complexes by 1−3 kcal/mol. This was explained by the larger polarizability of ethylene compared with acetylene.[275] The second TM row atoms have significantly higher BDEs in the covalently bound acetylene complexes than the first TM row elements. This was attributed to the more diffuse valence d orbitals and the smaller d−d exchange energy for the second-row ions.[296] Since the strength of the electrostatically bound complexes depends on the metal−C$_2$H$_2$ distance and, thus, on the size of the metal ion, the binding energy was found to be larger for most first-row TM ions than for the analogous second-row ions.[296]

The conclusion that the main interaction between Cu$^+$ and Ag$^+$ and acetylene is of electrostatic nature has also been reached in a theoretical study at the
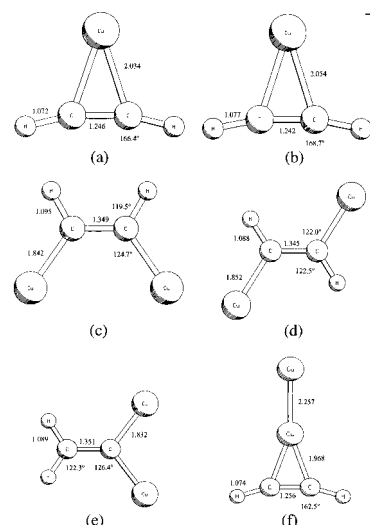

Figure 33. Geometry optimized energy minimum structures at the MP2 level of (a) Cu(C$_2$H$_2$), (b) Cu(C$_2$H$_2$)$^+$, (c) *cis*-Cu$_2$(C$_2$H$_2$), (d) *trans*-Cu$_2$(C$_2$H$_2$), (e) 1,1-Cu$_2$(C$_2$H$_2$), (f) Cu−Cu(C$_2$H$_2$). (Reproduced with permission from ref 276. Copyright 1996 Elsevier Science S.A.)

CIPSI level by Miralles-Sabater, Merchán, Nebot-Gil, and Viruela-Martin (MMNV).[297] The chemical bonding in the copper−acetylene molecules shown in Figure 33 has recently been analyzed at the MP2 level by Böhme, Wagner, and Frenking (BWF).[276] The Cu$^+$−C$_2$H$_2$ bond strength which was calculated at the CCSD(T) level is higher (D_e = 40.6 kcal/mol) than that in the work of SB[296] and MMNV,[297] but the NBO results and the topological analysis of the electron density distribution supported the classification of the bond as electrostatic in nature. The AIM calculations showed a T-shaped structure for Cu(C$_2$H$_2$)$^+$ with a bond path from the copper atom to the midpoint of the C−C bond of the acetylene ligand, which is similar to Cu(C$_2$H$_4$)$^+$ (Figure 30). The metal−ligand bond strength of the neutral compound Cu(C$_2$H$_2$), which is held together only by weak dispersion forces, was found to be much lower (D_e = 2.3 kcal/mol) than that in the ion. BWF pointed out that the geometries of Cu(C$_2$H$_2$)$^+$ and Cu(C$_2$H$_2$) do not reveal the drastically different bond energies.[276] Figure 33a,b shows that the Cu−C distance in the neutral complex (2.034 Å) is even shorter than in the ion (2.054 Å) and that the C−C bond lengths and the C−C−H angles in the two compounds are nearly the same.

Some unexpected results were found for the system Cu$_2$(C$_2$H$_2$). The copper atoms may insert into one of the π bonds of acetylene and form Cu−C σ bonds, which leads to compounds that can be considered as trans, cis, and vicinal dicopper-substituted ethylenes (Figure 33c−e). However, the lowest lying energy minimum structure of the system Cu$_2$(C$_2$H$_2$) was found by BWF to be a C_{2v}-symmetric π complex of acetylene with Cu$_2$ oriented orthogonal to the C−C axis (Figure 33f).[276] The BDE of Cu$_2$(η^2-C$_2$H$_2$) at CCSD(T) yielding acetylene and Cu$_2$ is D_e 14.9 kcal/mol,[298] which is clearly higher than the BDE of Cu-(C$_2$H$_2$), D_e = 2.3 kcal/mol. The NBO analysis of the bonding situation in (C_{2v}) Cu$_2$−C$_2$H$_2$ showed that the directly bound copper atom Cu1 carries a large positive charge (0.35 e) while the distant copper atom

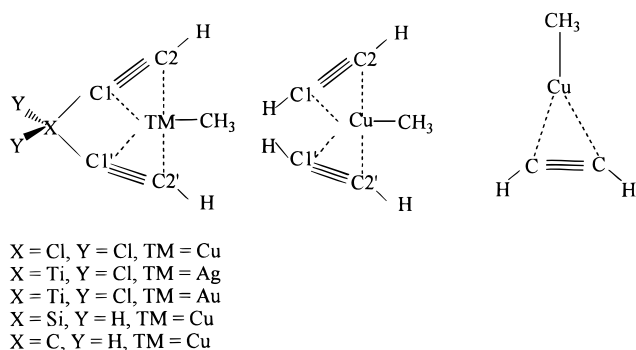**Figure 34.** Tweezer-like copper–alkyne complexes which were studied in ref 299.

X = Cl, Y = Cl, TM = Cu
X = Ti, Y = Cl, TM = Ag
X = Ti, Y = Cl, TM = Au
X = Si, Y = H, TM = Cu
X = C, Y = H, TM = Cu

Cu2 has a negative partial charge (-0.28 e). Thus, the enhanced copper–acetylene binding in the dicopper complex $Cu_2(C_2H_2)$ can be explained by induced dipole interactions.[276] The AIM calculations gave a cyclic structure for the $Cu1C_2$ moiety with two $Cu1-C$ bond paths and a ring critical point. The energy density values at the $Cu1-C_2$ bond critical points of $Cu_2(C_2H_2)$ were more negative than in case of $Cu(C_2H_2)$, which indicates the onset of a covalent $Cu-C$ bond in the former compound. The charge polarization in the Cu_2 moiety leads to stronger $Cu-Cu$ binding in $Cu_2(C_2H_2)$ than in free Cu_2. The BDE of the $Cu-Cu$ bond of the acetylene complex at the CCSD(T) level is $D_e = 56.8$ kcal/mol, while free Cu_2 has $D_e = 44.2$ kcal/mol.[298]

The chemical bonding of $CuCH_3$ with one and two alkyne ligands has been investigated by Kovács and Frenking (KF) at the B3LYP level of theory using an ECP for the metal with valence basis sets up to TZP quality.[299] The goal of this work was to achieve an understanding for the bonding situation of tweezer-like compounds of the transition metals copper, silver, and gold where the tricoordinate metals bind to two alkyne ligands (Figure 34). The electronic structures were analyzed with the NBO method and the topological analysis of the electron density distribution. Complexes with Cp_2Ti bridges have been synthesized, and X-ray structure analyses have been reported.[117−121]

The most important results of the bonding analysis can be summarized as follows.[299] The $TMCH_3$ moiety is a Lewis base in the complexes $Y_2X(CCH)_2TMCH_3$ which donates ~0.4–0.5 electrons to the bisalkyne tweezer, which behaves like a Lewis acid. The transition metals Cu, Ag, Au are highly positively charged ($\sim$+1 e) in these compounds, while the methyl groups carry a higher negative charge than in free $TMCH_3$. The bonding between the transition metals and the bisalkyne ligands is largely ionic in character. The role of the bridging $TiCl_2$ moiety in the tweezer complexes is a 2-fold one. It serves to position the alkyne groups in a proper position for tricoordination around the group-11 metals and enhances the Lewis acidity of the ligands, which explains why the tweezer complexes with $TiCl_2$ bind the $TMCH_3$ molecules much stronger than the complexes with SiH_2 and CH_2 bridges. The calculated partial charges, the shape of the Laplacian distribution, and the bond-path topology suggest that the group-11 atoms Cu, Ag, Au are primarily bound to the carbon atoms C2

and C2′ of the alkyne ligands (Figure 34).[299]

The theoretical studies of KSM,[278] Ziegler,[279] and LSZ[280] which were reviewed in the section about alkene complexes also gave results about the bonding situation in the group-11 alkyne complexes $(PH_3)_2$-$TM(C_2H_2)$ (TM = Ni, Pd, Pt). The HF calculations of KSM[278] predict that the Ni–acetylene bond in $(PH_3)_2$-$Ni(C_2H_2)$ is slightly stronger than the Ni–ethylene bond in $(PH_3)_2Ni(C_2H_4)$. The bonding analysis was carried out with the EDA method. It was found that in both complexes the Ni $\rightarrow$ (π)ligand back-donative interactions are stronger than the Ni $\leftarrow$ (π)ligand donor interactions. The calculated electrostatic attraction was much higher, however, than the sum of the donor–acceptor orbital interactions.[278] More recent theoretical studies which include correlation energy supported the main conclusion of the SCF study. Ziegler analyzed the bonding situations in the acetylene complexes $(PH_3)_2TM(C_2H_2)$ (TM = Ni, Pd, Pt) and $(PH_3)_2TM(C_2H_2)^+$ (TM = Co, Rh, Ir) using HFS calculations in conjunction with the ETS method and compared them with the analogous ethylene complexes.[279] He found that the contribution of the TM $\rightarrow$ C_2H_2 π-back-donation to the bond energy in the neutral molecules and to a lesser extent in the positively charged complexes is much higher than the TM $\leftarrow$ C_2H_2 donation. The more recent work of LSZ[280] about the bonding interactions in $(PH_3)_2Pt(C_2H_2)$ and the analogous ethylene complex, which was carried out at the NL-DFT level of theory, also reported a higher contribution of back-donation over donation but only by a factor of 1.5. Unfortunately, both studies did not give the bonding contributions of the electrostatic interactions. The HFS calculations of Ziegler[279] predicted that from the six compounds $(PH_3)_2TM(C_2H_2)$ (TM = Ni, Pd, Pt) and $(PH_3)_2TM$-$(C_2H_2)^+$ (TM = Co, Rh, Ir), the acetylene ligand of the nickel complex should be more strongly bound than the respective ethylene ligand, while in the remaining five complexes acetylene would be more weakly bound than ethylene. The results may not be correct. The later work of LSZ[280] at the NL-DFT level gave a slightly higher BDE for $(PH_3)_2Pt-(C_2H_2)$ than for $(PH_3)_2Pt-(C_2H_4)$.

A recent theoretical study by Hyla-Kryspin, Koch, Gleiter, Klettke, and Walther (HKGKW)[300] about nickel acetylene complexes gave the results of a bonding analysis of $(PH_3)_2Ni(C_2H_2)$, $Ni(C_2H_2)_2$ and the binuclear complex $Ni_2(C_2H_2)_3$, which has two terminal and one bridging acetylene ligands which bind to the two nickel atoms (Figure 35). The results were important because qualitative models about the stability of TM complexes were compared with the results of accurate quantum chemical calculations. The geometries were optimized at the B3LYP level, and the bonding situation was analyzed with the NBO partitioning scheme. A qualitative fragment MO analysis of the mononuclear complexes which considers the symmetry requirements for the possible donor–acceptor interactions showed that in the tetragonal form **a** of $Ni(C_2H_2)$ and in the planar form **b** of $(PH_3)_2Ni(C_2H_2)$ there are four occupied ligand MOs which can interact with four empty Ni orbitals. Indeed, these forms were found to be minima on the

Ni(C₂H₂)₂ (tetragonal)
NIMAG=0
0.0 kcal/mol

Ni(C₂H₂)₂ (planar)
NIMAG=4
37.8 kcal/mol

(PH₃)₂Ni(C₂H₂) (tetragonal)
NIMAG=3
26.8 kcal/mol

(PH₃)₂Ni(C₂H₂) (planar)
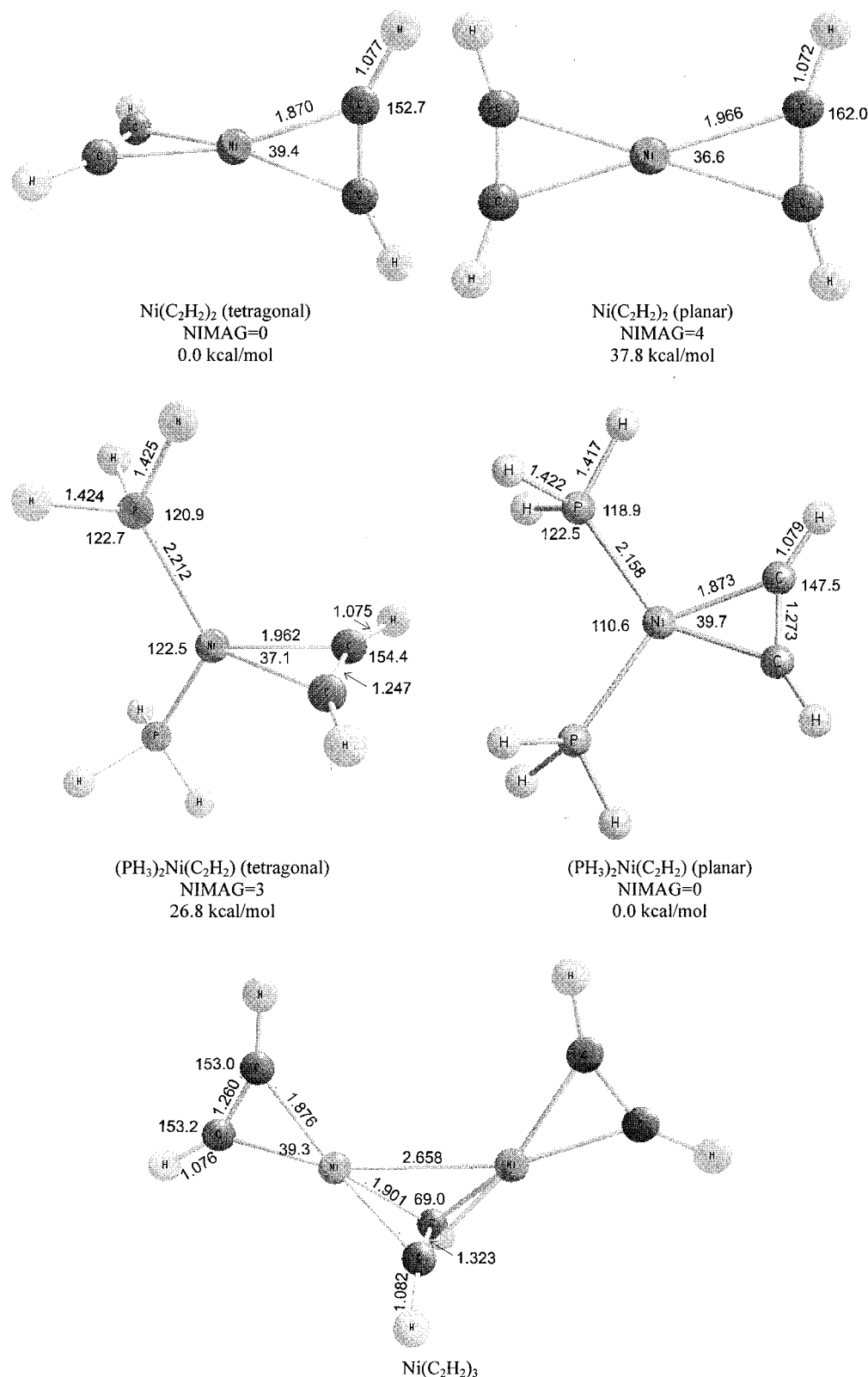NIMAG=0
0.0 kcal/mol

Ni(C₂H₂)₃

Figure 35. B3LYP-optimized structures of nickel–acetylene complexes. Bond distances in Å, angles in degrees. (Reproduced with permission from ref 300. Copyright 1998 American Chemical Society.)

potential energy surfaces, while the planar form **b** of Ni(C₂H₂) and the tetragonal form **a** of (PH₃)₂Ni-(C₂H₂), which are formal 16 VE complexes, are higher-order sadle points.[300] Thus, the acetylene ligand should be considered as a 4-electron donor in both complexes, and the stable forms of the two compounds should formally be considered as 18 VE

species. This means that the in-plane $\pi_\parallel$ *and* the out-of-plane $\pi_\perp$ orbitals of acetylene should engage to a similar extent in the nickel–acetylene interactions. However, inspection of the orbital populations given by the NBO method shows that the out-of-plane $\pi_\perp$ orbital of the terminal acetylene ligand is much less depopulated than the in-plane $\pi_\parallel$ MO.[300] The NBO

analysis indicates that within symmetry-permitted Ni $\leftarrow$ ligand donation, only the Ni 4s AO is effectively populated, which suggests a 12 valence electron configuration for Ni. However, energy calculations of the reaction $NiL_2 + L \rightarrow NiL_3$ with L = CO, PH_3, C_2H_2 reported by HKGKW show that acetylene leads to a much higher degree of saturation than CO and PH_3, which indicates that the out-of-plane $\pi_\perp$ MO of acetylene is engaged in the metal–ligand binding interactions.[300] It seems possible that the NBO method does not give an accurate account of the Ni–acetylene interactions, because the valence p functions of the TMs are treated as Rydberg orbitals.[300] The occupancy-weighted orthogonalization procedure of the standard NBO method minimizes the occupation of the TM valence p orbitals, which might lead to an underestimation of the importance of the out-of-plane $\pi_\perp$ orbital. It would be interesting to see the results of an energy decomposition analysis which is not biased against particular orbital contributions. The bridging acetylene ligand in $Ni_2(C_2H_2)_3$ on the other hand was found to contribute to the bonding with each of the two π systems with approximately the same amount of energy as one π system of the terminal acetylene.[300]

The nature of the chemical bond in TM alkyne complexes where the metal is in a high or low oxidation state has been the topic of several quantum chemical studies of the Frenking group. The first paper by Stegmann, Neuhaus, and Frenking (SNF) focused on the alkyne complexes $X_4TM(C_2H_2)$, $X_5TM(C_2H_2)^-$ and $F_4TM(C_2F_2)$ (X = F, Cl; Y = Mo, W).[301] The neutral complexes with the respective vinylidene ligands CCH_2 and CCF_2 were also studied. The HF-optimized geometries were in very good agreement with experimental values. The bonding analysis using the NBO and AIM methods gave a straightforward answer about the nature of the TM–alkyne bonds. The NBO results show two metal–carbon σ bonds which are slightly polarized toward the carbon end. The alkyne ligands carry only a small partial charge, which may either be positive or negative. The hybridization of the TM–C bonds has largely d character. The topological analysis of the electron density distribution gave a cyclic structure for the alkyne complexes. The energy density at the bond critical points of the TM–C bonds suggests a significant covalent contribution to the binding interactions. The calculated molecules are unequivocally metallacyclic compounds with the formal oxidation state +VI for the metal.[301] A similar conclusion was drawn by Nielson, Boyd, Clark, Hunt, Metson, Rickard, and Schwerdtfeger (NBCHMRS) in a theoretical study at the HF and MSX$_\alpha$ level of theory of $Cl_5W(C_2H_2)^-$, $Cl_3(PH_3)_2W(C_2H_2)$, and $Cl_2(PH_3)_3W(C_2H_2)$.[302] The authors interpreted the calculated charge distribution and orbital population in favor of a high oxidation state of the metal. It was suggested that the acetylene–tungsten interactions are best described by a covalent bonding mechanism involving σ- and π-type overlaps.

A theoretical study of tungsten complexes in high and low oxidation states with side-on bound π ligands by Pidun and Frenking (PF95)[291] gave surprising

Table 14. Charge Decomposition Analysis of W–Ethylene and W–Acetylene Complexes in Their MP2 Geometries (Donation *d*, Backdonation *b*, Repulsive Part *r*, and Rest Term Δ)[a]

molecule	d	b	r	Δ
$Cl_4W(C_2H_2)$	0.057	−0.140	−0.189	0.382
$Cl_4W(C_2H_4)$	−0.263	−0.194	−0.318	0.351
$Cl_5W(C_2H_2)^-$	0.308	0.234	−0.760	−0.048
$Cl_5W(C_2H_4)^-$	0.041	0.138	−0.900	−0.045
$(CO)_5W(C_2H_2)$	0.297	0.165	−0.391	−0.004
$(CO)_5W(C_2H_4)$	0.225	0.148	−0.422	−0.025

[a] Taken from ref 115.

results about acetylene and ethylene complexes, which led the authors to carry out another investigation (PF96)[115] that focused on a comparison of the bonding of acetylene in $Cl_4W(C_2H_2)$, $Cl_5W(C_2H_2)^-$, and $(CO)_5W(C_2H_2)$ with the respective ethylene complexes (Figure 36). The geometry optimizations were carried out at the HF and MP2 levels of theory, while the bond energies were predicted using CCSD(T). The CDA partitioning scheme was used for the bonding analysis. The π-bonded ligands of the high-valent W(VI) compounds $Cl_4W(C_2H_2)$, $Cl_5W(C_2H_2)^-$, $Cl_4W(C_2H_4)$, and $Cl_5W(C_2H_4)^-$ have much shorter W–C bond lengths than the respective low-valent W(0) complexes $(CO)_5W(C_2H_2)$ and $(CO)_5W(C_2H_4)$, but the latter molecules have a significantly higher or at least comparable BDE. Another puzzling result reported by PF96 concerns the relative BDEs of the acetylene and ethylene ligands in the investigated complexes.[115] It was found that $W(CO)_5$ binds ethylene stronger than acetylene, while the opposite trend was reported for the complexes with WCl_4 and WCl_5^- (Figure 36). An explanation for the peculiar results and insight into the binding mechanism was given by the CDA results which are shown in Table 14.

The CDA results for the low-valent compounds show that $(CO)_5W(C_2H_2)$ and $(CO)_5W(C_2H_4)$ can be considered to be donor–acceptor complexes, because the value for the rest term Δ is essentially zero. The amount of $(CO)_5W \leftarrow (C_2H_n)$ donation is larger than the $(CO)_5W \rightarrow (C_2H_n)$ back-donation for both π ligands.[115] A larger donation than back-donation has been found in another CDA study by Ehlers, Dapprich, Vyboishchikov, and Frenking (EDVF) for the low-valent TM acetylene complexes $(CO)_5TM(C_2H_2)$ (TM = Cr, Mo, W) and $(CO)_3TM(C_2H_2)$ (TM = Ni, Pd, Pt).[194] The CDA results of PF96[115] clearly demonstrate that the neutral high-valent compounds $Cl_4W(C_2H_2)$ and $Cl_4W(C_2H_4)$ should not be described as donor–acceptor complexes because the value for the rest term Δ is significantly different from zero (Table 14). The CDA results suggest that the neutral W(VI) complexes should be considered as metallacyclic compounds with two electron-sharing W–C σ bonds, which is in agreement with the interpretation of the bonding situation in $Cl_4W(C_2H_2)$ based on the NBO and AIM analysis reported by SNF[301] The rather low BDEs of $Cl_4W(C_2H_2)$ and $Cl_4W(C_2H_4)$, which do not correlate with the very short W–C interatomic distances, were explained by PF96[115] with the high excitation energies ($\sim$100 kcal/mol) that are necessary to promote the acetylene and ethylene ligands from the electronic ground state to the triplet state.

$Cl_4W(C_2H_2)$ $D_e=36.6$ kcal/mol

$Cl_4W(C_2H_4)$ $D_e=12.1$ kcal/mol

$Cl_5W(C_2H_2)^-$ $D_e=22.3$ kcal/mol

$Cl_5W(C_2H_4)^-$ $D_e=8.5$ kcal/mol

$(CO)_5W(C_2H_2)$ $D_e=35.3$ kcal/mol
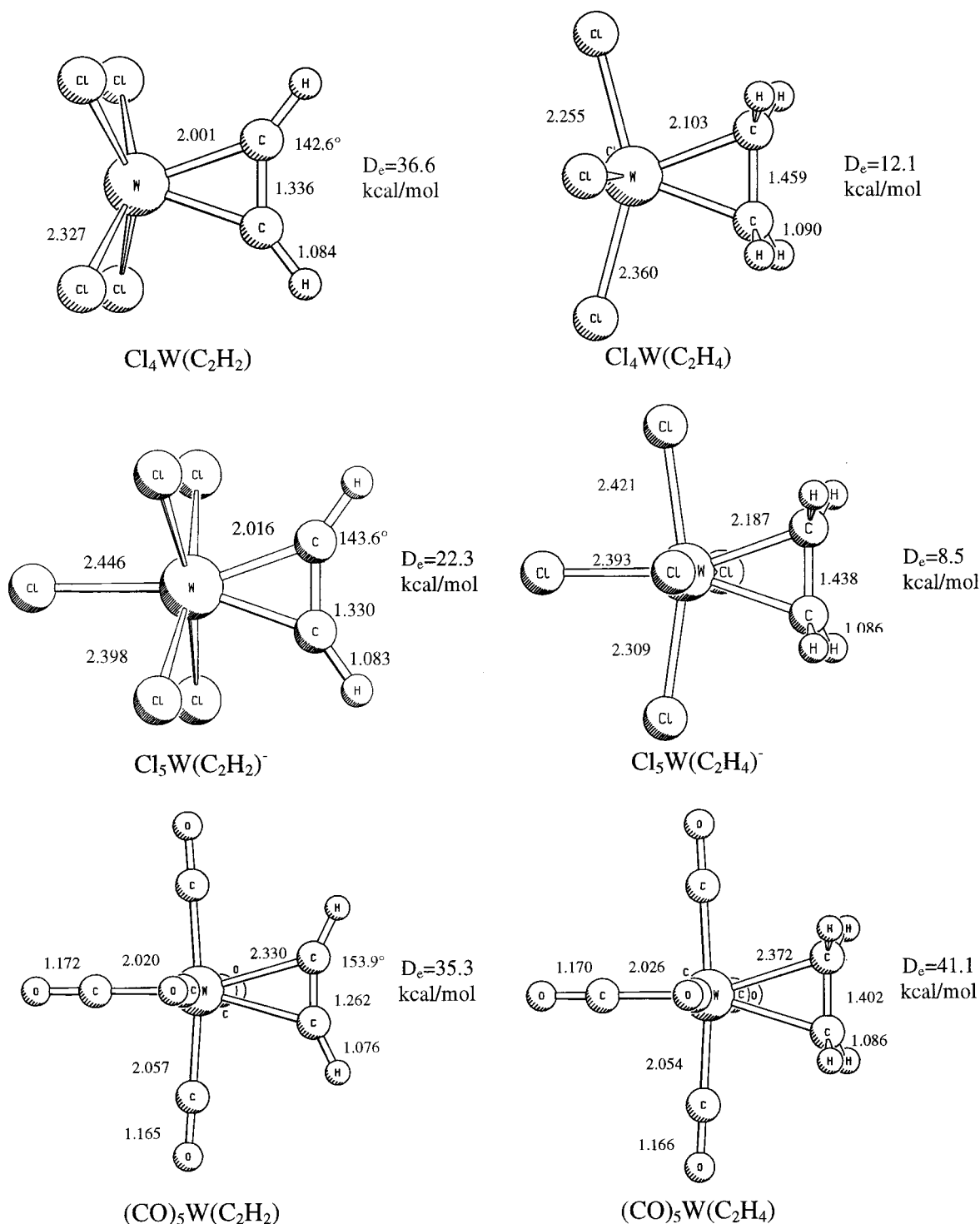
$(CO)_5W(C_2H_4)$ $D_e=41.1$ kcal/mol

Figure 36. MP2-optimized geometries of ethylene and acetylene complexes in high and low oxidation states. Bond distances in Å, angles in degrees. Ligand BDEs D_e were calculated at CCSD(T). (Reproduced with permission from ref 115. Copyright 1996 Elsevier Science S.A.)

In the triplet states there are two unpaired electrons at the carbon atoms which then can form two 2c−2e bonds with triplet WCl_4. The higher BDE of acetylene than ethylene in $Cl_4W(C_2H_n)$ was explained with the hybridization at the carbon atom, while the stronger donor−acceptor bond of ethylene compared to acetylene in $(CO)_5W(C_2H_n)$ was explained with the higher lying HOMO and lower lying LUMO of the former ligand.[115]

An interesting result was given by the CDA method for the negatively charged high-valent compounds $Cl_5W(C_2H_2)^-$ and $Cl_5W(C_2H_4)^-$.[115] Table 14 shows that the values for the metal−ligand donation and back-donation are positive and that the rest term is very small and can be considered as ∼0. According to the CDA results, both compounds may thus be discussed as donor−acceptor complexes. The rather large values for the repulsive polarization term explain why the BDEs of the π ligands in the negatively charged complexes are rather small. Metal → (π)ligand back-donation is now clearly larger than metal ← (π)ligand donation in $Cl_5W(C_2H_4)^-$, while in $Cl_5W(C_2H_2)^-$ the

$d(W \leftarrow C_2H_2)$	~0.0	0.222	0.260
$b(W \rightarrow C_2H_2)$	0.282	~0.0	~0.0
$r(W \leftrightarrow C_2H_2)$	~0.0	-0.375	~0.0

$d(W \leftarrow C_2H_2)$	0.326	~0.0	~0.0
$b(W \rightarrow C_2H_2)$	~0.0	~0.0	0.195
$r(W \leftrightarrow C_2H_2)$	-0.194	-0.272	~0.0
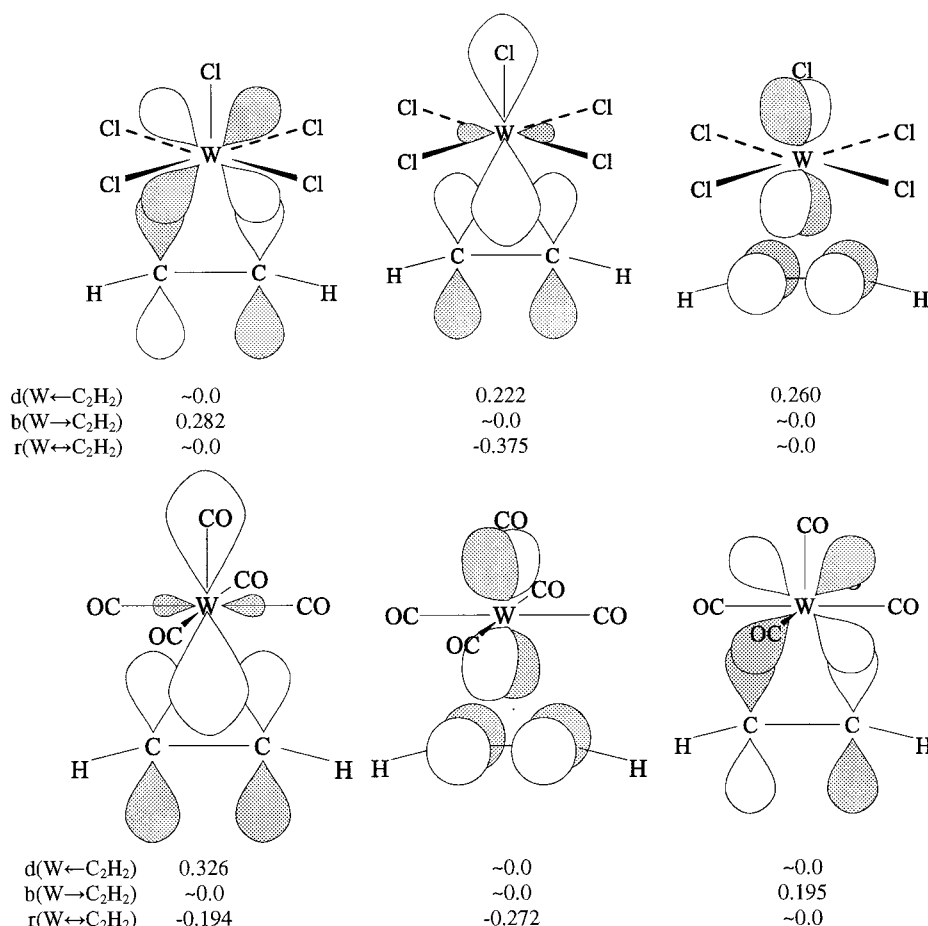
Figure 37. Dominant orbital interactions in $Cl_5W(HCCH)^-$ and $(CO)_5W(HCCH)$ as revealed by the CDA.)Reproduced with permission from ref 115. Copyright 1996 Elsevier Science S.A.)

acetylene ligand is still a stronger donor than acceptor. Inspection of the orbital contributions to the donation and back-donation in the complexes $(CO)_5W$-(C_2H_2) and $Cl_5W(C_2H_2)^-$ revealed a qualitative difference of the $W \leftarrow C_2H_2$ donation between the two complexes. Figure 37 schematically shows the most important complex orbitals for the metal−acetylene interactions. There is only one dominant orbital for the $(CO)_5W \leftarrow C_2H_2$ donation, which involves the in-plane $\pi_{||}$ orbital (a_1 symmetry) of the acetylene ligand. In the case of $Cl_5W(C_2H_2)^-$, however, there are *two* dominant orbitals for the acetylene $\rightarrow$ metal donation, which involve the (a_1) in-plane $\pi_{||}$ orbital and the (b_2) out-of-plane $\pi_\perp$ orbital of acetylene. Thus, acetylene is a two-electron donor in $(CO)_5W(C_2H_2)$ but a four-electron donor in $Cl_5W(C_2H_2)^-$.[115]

The same authors have later shown (PF97)[116] that the bonding analysis of $Cl_5W(C_2H_2)^-$ may also lead to a description of the bonding situation in terms of two covalent 2c−2e bonds between tungsten and carbon, which is similar to the bonding description in $Cl_4W(C_2H_2)$. AIM calculations of the two compounds showed that the Laplacian distributions are very similar to each other. The contour line diagrams in the $W(C_2H_2)$ bonding region of $Cl_4W(C_2H_2)$ and $Cl_5W(C_2H_2)^-$ are practically indistinguishable, and the energy values at the W−C bond critical points suggest comparable covalent contributions to the binding interactions.[116] The very similar results of the topological analysis of the electron density dis-

tribution let it seem questionable whether the binding situation should be described with qualitatively different models. PF97 called $Cl_5W(C_2H_2)^-$ a borderline case, where the donor−acceptor model and the model of covalent bonding may both be applied.

An important contribution to the question concerning the bonding properties of acetylene as two-electron or four-electron donor in TM complexes has recently been made in a paper by Decker and Klobukowski (DK).[303] The authors calculated the first BDEs of CO in $TM(CO)_5$ and $(CO)_4TM(C_2H_2)$ with TM = Fe, Ru, Os at the NL-DFT level using a variety of different functionals in order to find out the reason for the CO labilizing effect of the alkyne ligand, which strongly accelerates the substitution of CO. Previous theoretical studies suggested that ligands with additional π-donor groups may stabilize the electron deficiency at the metal which occurs in a dissociative substitution reaction.[304,305] DK analyzed the electronic structure of $TM(CO)_5$, $TM(CO)_4$, $(CO)_4TM$-(C_2H_2), and $(CO)_3TM(C_2H_2)$ with the CDA partitioning scheme and with the AIM method.[303] The CDA calculations showed that in the saturated 18 VE complex $(CO)_4TM(C_2H_2)$, the acetylene ligand is a two-electron donor, with only the $\pi_{||}$ orbital donating to the metal. In the complex $(CO)_3TM(C_2H_2)$, however, both π orbitals of acetylene donate electron density to the metal, thereby making acetylene formally a four-electron donor. This result was supported by AIM calculations, which show that the
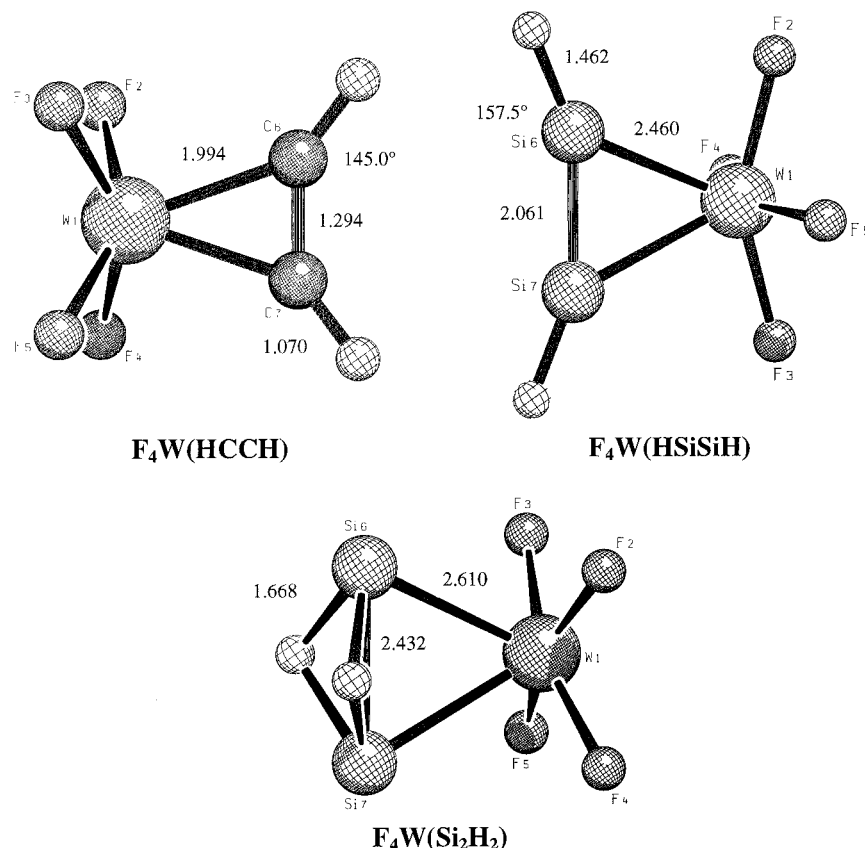
Figure 38. HF-optimized geometries of $F_4W(HCCH)$, $F_4W(HSiSiH)$, and $F_4W(Si_2H_2)$. (Reproduced with permission from ref 306. Copyright 1995 American Chemical Society.)

$TM-C_{acetylene}$ bonds strengthen when CO is removed from $(CO)_4TM(C_2H_2)$. The trend of the CO labilization for the metals Fe, Ru, Os was explained in terms of the orbital energy gap for the $TM \leftarrow C_2H_2$ back-donation between the $\pi_\perp$ orbital of C_2H_2 and the metal acceptor orbitals.[303]

Theoretical studies of TM complexes with heavy-atom analogues of alkynes as ligands are nearly a white spot in computational chemistry. This may be due to the fact that TM complexes with the formula $L_nTM(\eta^2\text{-RXYR}')$, where X, Y is a group-14 atom Si–Pb, are not known yet. The only theoretical study about this class of compounds was published by Stegmann and Frenking (SF) in 1996.[306] The authors optimized at the HF level the geometries of isomers with the formula $F_4W(CSiH_2)$ and $F_4W(Si_2H_2)$. Bond energies of the compounds were predicted using CCSD(T). The bonding analyses were carried out with the NBO and AIM methods. The complex with the π-bonded disilaacetylene ligand shown in Figure 38 was found at CCSD(T) to be the energetically lowest lying structure of the $F_4W(Si_2H_2)$ isomers. The complex with the doubly hydrogen bridged Si_2H_2 ligand is 10.1 kcal/mol higher in energy. This was a surprising result because the butterfly form of free Si_2H_2 at the same level of theory is 14.2 kcal/mol more stable than the HSiSiH form, which has a trans arrangement of the hydrogen atoms.[306] This means that the tungsten–silicon bonds of $F_4W(\eta^2\text{-HSiSiH})$ should be very strong. Indeed, calculations at the CCSD(T) level showed that the disilaacetylene ligand is as strongly bound as acetylene in $F_4W(\eta^2\text{-HCCH})$. The NBO analysis of $F_4W(\eta^2\text{-HSiSiH})$ gave two

nonpolar W–Si σ bonds (50.7% at the tungsten end). The covalent bond order is rather large (1.13), which suggests some π-bonding contributions to the W–Si bonds. The AIM calculations also indicated significantly covalent W–Si bonds. The W–Si bonds of the complex with the π-bonded butterfly form of the Si_2H_2 ligand (Figure 38) were clearly polarized toward the tungsten end (64.6% at W) and the bond order is lower (0.73). The complex with the π-bonded HCSiH ligand is also a minimum on the potential energy surface (Figure 38). However, the isomeric form with a silavinylidene ligand $F_4WC(SiH_2)$ was found to be 9.9 kcal/mol lower in energy. The NBO analysis of $F_4W(\eta^2\text{-HSiCH})$ showed W–C and W–Si σ bonds but also a W–C π bond. SF suggested that $F_4W(\eta^2\text{-HSiCH})$ might therefore alternatively be considered as a tungsten alkylidene complex with an additional W–Si bond.[306]

V.6. TM Complexes with Group-13 Ligand Atoms E = B, Al, Ga, In, Tl

The chemistry of TM complexes with group-13 ligand atoms E = B–Tl has been the subject of intensive experimental studies in the last couple of years, which was highlighted by several spectacular syntheses of stable compounds with $TM-ER_n$ bonds that have not been known before. The recent experimental progress in the field has been summarized and discussed in several reviews.[307–311] Stable TM compounds have been synthesized where the group-13 atoms bind to the metal in different binding modes (Figure 39). One class of compounds has ER_3 ligands
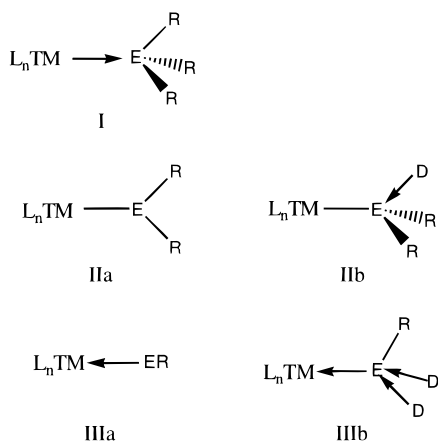
Figure 39. Different binding modes of TM complexes with group-13 ligand atoms E.

that behave as a Lewis acid with electron-rich TMs in donor−acceptor complexes $L_nTM \rightarrow ER_3$ (**I**). Another group of complexes (**IIa**) has terminal σ-bonded ER_2 ligands which may become additionally stabilized by a donor ligand D at the ER_2 ligand in $L_nTM-ER_2(D)$ (**IIb**). A third class of compounds has ligands ER where the group-13 atom has the formal oxidation state I. The diyl ligand ER behaves like a Lewis base in complexes $L_nTM \leftarrow ER$ (**IIIa**). The dicoordinated element E is often stabilized by further donor groups D in complexes $L_nTM-ER(D)_2$ (**IIIb**), but examples for **IIIa** are known where the complex L_nTM-ER is stable without additional ligands at ER. Numerous experimental studies focused on TM complexes with boron ligands,[307−309] but much work has also been carried out with group-13 ligand atoms aluminum, gallium, and indium.[310] TM complexes with TM−Tl bonds are scare and much more unstable than the lighter group-13 homologues.[311]

The synthesis of stable TM compounds particularly with group-13 diyl ligands ER led to intensive discussions of the bonding situation in the compounds. Accurate theoretical studies which addressed the nature of the $TM-ER_n$ were not available until very recently. The need for such investigations became clear when the discussion about the bonding situation in the complex $(CO)_4Fe-GaAr^*$ ($Ar^* = 2,6-(2,4,6-$ triisopropylphenyl)-phenyl)[312] triggered a controversial discussion[313] about the question of whether the Fe−Ga bond should be considered as a triple bond[312] or a single bond.[314] Recent theoretical work addressed the bonding situation in this[315] and related compounds.[316] It is clear, however, that theoretical investigations of the nature of TM−E bonds with group-13 elements E are still underdeveloped. Much work has to be done to elucidate the bonding features in this field.

Most of the theoretical work has focused on the bonding situation in group-13 diyl complexes L_nTM- ER. Figure 40 shows the principle donor−acceptor orbital interactions in TM−ER bonds. The qualitative picture is similar to the situation in TM−CO bonds (Figure 8) and in the TM−CR carbyne bonds of Fischer-type complexes (Figure 27). There is donation from the σ-symmetric electron lone pair of ER into a σ-symmetric empty orbital of TM, and there is also back-donation from π-symmetric filled d orbitals of
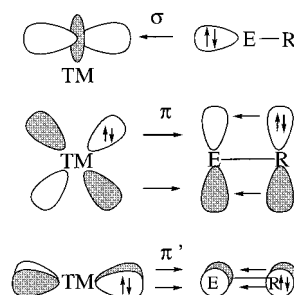

Figure 40. Schematic representation of the dominant orbital interactions in TM complexes with diyl ligands ER where E is a group-13 atom and R has two occupied p(π) lone-pair orbitals.

the TM into the degenerate p(π) orbitals of E. The p(π) orbitals of E in free ER are vacant if R has no filled π-symmetric orbitals, but they become partly filled by $E \leftarrow R$ π donation if R has π-symmetric lone-pair orbitals. It becomes clear that the size of the TM $\rightarrow$ ER π-back-donation and the $E \leftarrow R$ π-donation should be important for the nature of the TM−ER bond and, thus, for the reactivity of L_nTM-ER complexes toward attack by a nucleophilic agent.

V.6.1. Complexes with Ligands BF, BO⁻ and BNH₂

The chemical bonding of BR ligands as alternatives to CO has been investigated in three recent theoretical studies at the nonlocal DFT level of theory.[187,188,317] The calculated bond energies of several neutral and positively charged carbonyl complexes $(CO)_nTM-BF$ and $(CO)_nTM-BNH_2$ showed that the TM−BF and TM−BNH₂ bonds have much higher bond dissociation energies than the TM−CO bonds in the corresponding homoleptic carbonyl complexes TM-$(CO)_{n+1}$.[187,317] Inspection of the frontier orbitals of valence isoelectronic BR, CO, and N₂ showed that the major changes are the rise in the energy level of the lone-pair HOMO in the order $AB = BO^- > BNH_2 > BF > CO > N_2$ while the π-symmetric LUMO changes very little in energy (Figure 41). Since the TM−AB bond energy shows the same trend as the orbital energy of the HOMO of AB, it can be suspected that the contribution of the $TM \leftarrow AB$ σ-donation to the total bond energy may be higher for the borylene ligands than for CO and N₂. An energy decomposition analysis using the ETS method showed that this assumption is correct.[187] The contribution of the π-back-donation to the dissociation energy of several $(CO)_nTM-ER$ (R = F, NH₂, O⁻) and $(CO)_n-$ TM−CO complexes remains nearly constant for the neutral ligands, but the contribution of the σ-donation increases strongly with the trend $CO < BF < BNH_2 < BO^-$. Because the same trend is found for the bond dissociation energies, it was concluded that the *differences* in the bond strengths and the high thermodynamic stability of the borylene complexes are mainly caused by $TM \leftarrow ER$ σ-donation. The negatively charged ligand BO⁻ plays a special role, because the negative charge shifts the energy levels of the HOMO and the LUMO upward (Figure 41). This makes BO⁻ a poor π acceptor and a very good σ donor.

The authors point out that while the higher lying HOMO of BR leads to thermodynamic stabilization
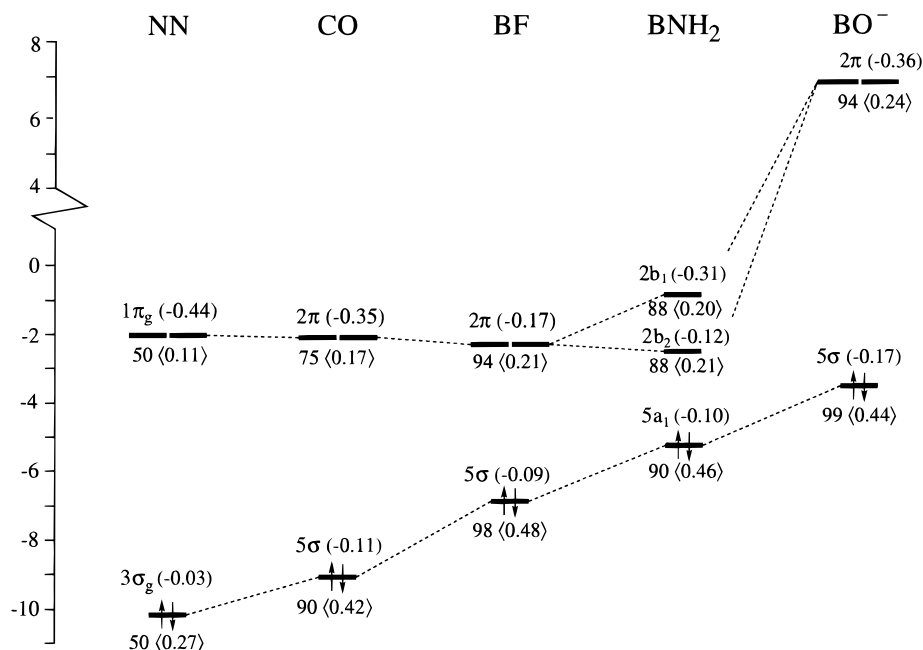
Figure 41. Valence orbital energies (eV) of AE systems N_2, CO, BF, BNH_2, and BO^- given by BP86 calculations. Below each level the percentage of atom A character is indicated and the overlaps with the relevant $Fe(CO)_4$ frontier orbital are quoted in angular brackets. Above each level the Mulliken overlap population is given in parentheses. (Reproduced with permission from ref 187. Copyright 1998 Wiley-VCH.)

of the L_nTM-BR complexes, the smaller HOMO–LUMO gap (Figure 41) and the buildup of positive charge yields low kinetic stability.[187] It was suggested that ligands BNR_2 with bulky substituents R may provide steric protection which might lead to stable borylene complexes that can be isolated. Indeed, the X-ray structure of the complex $(CO)_5W-BN(SiMe_3)_2$ has been reported in the meantime.[318] Another possible strategy for improving the kinetic stability is the binding of the ligand BR in a bridging position between binuclear fragments such as $Fe_2(CO)_8$ or $Mn_2(Cp)_2(CO)_4$. The authors analyzed the orbital interactions in $Fe_2(CO)_8-(BR)$ and $Mn_2(Cp)_2(CO)_4-(BR)$ and came to the conclusion that the binuclear fragments have just the right frontier orbitals to yield a better σ/π balance of the TM–BR interactions.[187] The difference between the TM–ER and TM–CO σ/π balance was suggested to be the main reason for the different kinetic stability between carbonyl complexes and borylene complexes.[187,188,317]

The change in the E–R stretching frequency of CO, BF, BNH_2, and BO^- between the free ligands and the complexes $(CO)_5Cr-ER$ was also investigated.[187] A related study of the same principle authors analyzed the change in the E–R stretching frequencies of N_2, CO, BF, and SiO between the free ligands and the complexes $(CO)_4Fe-ER$ and $Fe(ER)_5$.[188] It was found that the stretching frequencies of the borylene ligands BR and that of SiO are higher in the complexes than in the free ligands, while N_2 and CO have lower stretching modes. The results were explained in terms of orbital population of the antibonding π^* LUMO of ER via TM $\rightarrow$ ER π-back-donation and orbital depopulation of the σ-type HOMO of ER via TM $\leftarrow$ ER donation. The Mulliken population analysis gives negative values for the overlap population of the HOMO of N_2, CO, SiO, BF, BNH_2, BO^-, i.e., the orbitals should have an antibonding charac-

Table 15. ETS Decomposition Analysis of the $Fe(CO)_4$–AB Bonding in C_{3v} and C_{2v} $Fe(CO)_4AB$ (AB = N_2, CO, BF, SiO)^a

energy term	$(CO)_4Fe-AB$ (ax)				$(CO)_4Fe-AB$ (eq)			
	NN	CO	BF	SiO	NN	CO	BF	SiO
ΔE_σ	−26.9	−45.8	−80.4	−58.7	−26.0	−42.0	−78.7	−48.7
ΔE_π	−26.6	−42.8	−46.5	−31.7	−27.0	−45.6	−53.7	−34.0
ΔE_{orb}	−53.5	−88.6	−126.9	−90.4	−53.0	−87.6	−132.4	−82.7
ΔE^b	25.3	35.0	46.9	44.5	28.1	37.7	54.7	37.5
BDE^b	−18.1	−42.3	−67.9	−35.6	−19.0	−42.3	−66.7	−39.7

^{a} Taken from ref 188. Values are given in kcal/mol. ^{b} Bond dissociation energy.

ter.[187,188] The contribution of the TM $\rightarrow$ ER π-back-donation and TM $\leftarrow$ ER σ-donation are balanced for ER = CO and N_2 and the population of the strongly antibonding π^* orbital could then lead to higher E–R stretching frequencies. The σ-HOMO of BR is much higher in energy (Figure 41) than that of N_2 and CO, and the larger contribution of the TM $\leftarrow$ ER σ bonding dominates the orbital interactions yielding a shift of the E–R stretching mode toward higher wavenumbers. An alternative explanation for the change toward higher C–O wavenumbers in *non-classical* carbonyls[181−183] has been given by other authors.[170,180] The explanation considers the change in the polarization of the E–R bonding orbitals toward a more equal distribution when ER becomes bound to a strongly electron withdrawing atom as the reason for the frequency shift (Figure 21). The details are discussed in the section about TM carbonyl complexes.

Table 15 shows the results of the energy decomposition analysis of the axial and equatorial isomers of $(CO)_4Fe-ER$ (ER = N_2, CO, BF, SiO). It becomes obvious that the Fe $\leftarrow$ ER σ-donation and Fe $\rightarrow$ ER π-back-donation are balanced for CO and N_2, while the complexes with BF and SiO have stronger

contributions from Fe ← ER σ-donation than from Fe → ER π-back-donation. The stabilizing orbital interactions ΔE_{orb} in the equatorial isomer of (CO)$_4$Fe–BF are larger than in the axial isomer, but the higher value for the repulsive ΔE° term makes the equatorial form slightly less stable than the axial form. The opposite result is found for (CO)$_4$Fe–SiO. The axial form of (CO)$_4$Fe–SiO has a larger ΔE_{orb} value than the equatorial form, but the latter isomer is predicted to be more stable than the former because of a lower value for the repulsive ΔE° term. Unfortunately, the authors did not give the values for the separate contributions of the charge interactions ΔE_{els} and the Pauli repulsion $\Delta E_{\mathrm{Pauli}}$ but only the sum of the two terms ΔE°.

V.6.2. Complexes (CO)$_5$W–AlR and (CO)$_5$W-ER(NH$_3$)$_2$ (R = H, Cl)

The bonding situation of TM complexes with the heavier group-13 diyl ligands AlH and AlCl with and without additional donor ligands has recently been investigated in a combined experimental/theoretical study by Fischer et al.[319] Calculations at the MP2 level of theory were carried out for (CO)$_5$W–AlR and (CO)$_5$W–AlR(NH$_3$)$_2$ (R = H, Cl), and the electronic structure was analyzed with the NBO and CDA methods and with the topological analysis of the electron density distribution. The bonding situation in the donor-stabilized complexes (CO)$_5$W-ECl(NH$_3$)$_2$ was studied for the whole series of group-13 elements E = B–Tl.[194]

The most important results can be summarized as follows. The W−E bonds are mainly held together by electrostatic forces between the negatively charged tungsten and the positively charged ligand atoms E (Table 16). The covalent bond orders P(W−E) are very low, which indicates only weak covalent bonding. The amount of W ← E donation is higher than W → E π-back-donation, but the latter is not negligible. The donor-free complexes (CO)$_5$W–AlR exhibit a higher degree of W → E π-back-donation than the NH$_3$-stabilized species (CO)$_5$W–AlR(NH$_3$)$_2$.

The theoretically predicted W−E bond dissociation energies of (CO)$_5$W-ECl(NH$_3$)$_2$ show the trend B > Al > Ga ≈ In > Tl. The MP2 values for the W−E

bond energies are probably too high but not very much.[320] At the same level of theory, for example, the first dissociation energy of a CO ligand from W(CO)$_6$ is D_e = 52.9 kcal/mol[320,322] while the experimental value is 44 ± 2 kcal/mol.[323] Thus, the calculated W−E bond energies indicate that the bonds are rather strong. An interesting observation was made about the influence of the donor ligands NH$_3$ on the bond length and bond energy of the W−AlR (R = H, Cl) bonds. The donor-free complexes (CO)$_5$W–AlR have significantly *shorter* W−AlR bonds than the donor-stabilized (CO)$_5$W–AlR(NH$_3$)$_2$ complexes, but the bond dissociation energies of the latter are 30−35 kcal/mol *higher* than the former (Table 16). The stronger binding in (CO)$_5$W–AlR(NH$_3$)$_2$ can neither be explained by the calculated partial charges at W and Al nor by enhanced W−Al covalent bonding. Rather, there is a substantial change in the hybridization of the donor lone-pair orbital at Al which has a much higher %p character in (CO)$_5$W−AlR(NH$_3$)$_2$ than in (CO)$_5$W−AlR (Table 16). A higher p character raises the energy of the donor orbital and makes it more diffuse. This leads to a larger charge transfer Δq (CO)$_5$W ← AlR(NH$_3$)$_2$ at longer W−Al distances compared with Δq (CO)$_5$W ← AlR, which can be seen from the calculated partial charges at the W(CO)$_5$ fragment.

V.6.3. Complexes (CO)$_4$Fe–ER (R = Cp, N(SiH$_3$)$_2$, Ph) and (CO)$_5$W–EN(SiH$_3$)$_2$

Weiss et al.[159] reported in 1997 the first TM complex with a terminal group-13 diyl ligand (CO)$_4$Fe−AlCp* that could be isolated and characterized spectroscopically and by X-ray structure analysis. The axial AlCp* ligand exhibits an η^5-bonded Cp* substituent. There is a nearly linear arrangement of Fe, Al, and the midpoint of the Cp* ring. The authors also reported quantum chemical investigations at the MP2 level of the bonding situation in the related model compound (CO)$_4$Fe–AlCp. The NBO data show that the Fe−Al bond has a significant ionic character. The iron atom has a large negative charge, and the Al atom carries a large positive charge. The CDA data indicate substantial Fe ← Al σ-donation and much less Fe → Al π-back-donation.[159]

Table 16. NBO and CDA Bonding Analysis of (CO)$_5$W−AlR and (CO)$_5$W−ER(NH$_3$)$_2$ (E = B−Tl, R = H,Cl) at MP2^a

molecule	R(W−E) (Å)	D_e, (W−E) (kcal/mol)	D_e, (E−N)^b (kcal/mol)	q(W)	q(W(CO)$_5$)	q(E)	P(W−E)	donation (M → L)	back-donation (M → L)	%s (l.p.)
(CO)$_5$WAlH(NH$_3$)$_2$	2.605	100.9	64.0	−0.67	−0.93	1.09	0.37	0.474	0.271	23.0 (0.824)
								0.643^c	0.069^c	
(CO)$_5$WAlCl(NH$_3$)$_2$	2.575	93.1	65.2	−0.72	−0.90	1.24	0.40	0.356	0.280	23.9 (0.807)
								0.679^c	0.056^c	
(CO)$_5$WAlH	2.482	70.0		−0.93	−0.64	1.07	0.60	0.399	0.301	62.5 (0.868)
(CO)$_5$WAlCl	2.481	58.4		−0.94	−0.58	1.13	0.59	0.370	0.301	64.1 (0.824)
AlH(NH$_3$)$_2$			33.1			0.32		0.453	−0.019	77.5 (1.94)
AlCl(NH$_3$)$_2$			30.5			0.54		0.489	−0.009	84.0 (1.94)
AlH						0.60				91.5 (1.96)
AlCl						0.68				93.8 (1.95)
(CO)$_5$WBCl(NH$_3$)$_2$	2.349	119.6		−0.53	−0.63	0.19	0.42	0.196	0.095	35.2 (1.225)
(CO)$_5$WGaCl(NH$_3$)$_2$	2.586	70.9		−0.73	−0.72	1.07	0.44	0.434	0.213	18.3 (0.748)
(CO)$_5$WInCl(NH$_3$)$_2$	2.731	70.5		−0.71	−0.77	1.18	0.42	0.449	0.207	19.8 (0.760)
(CO)$_5$WTlCl(NH$_3$)$_2$	2.800	47.8		−0.70	−0.61	1.08	0.42	0.411	0.114	36.2 (0.908)

^{a} Taken from ref 319. W−E bond distances, W−E and E−N bond dissociation energies, NBO partial charges q, Wiberg bond indices P, CDA donation and back-donation, hybridization of the lone-pair donor orbital at atom E given by the s contribution (occupancies in parentheses). ^{b} Dissociation energy of two NH$_3$ ligands. ^{c} Al−N bond.
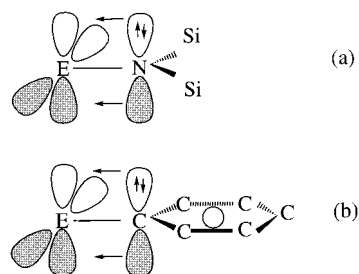
Figure 42. Schematic representation of the dominant orbital interactions in TM complexes with diyl ligands (a) $EN(SiR_3)_2$ and (b) E(phenyl) where E is a group-13 atom.

The nature of the $(CO)_4Fe-ER$ bonding has recently been analyzed for different groups R at the DFT (BP86) level of theory by Uddin, Boehme, and Frenking (UBF).[316] The results gave interesting insight into the Fe−ER interactions, because the groups R varied from good π donors (Cp), medium π donors ($N(SiH_3)_2$), to poor π donors (Ph). The latter two ligands have also different π interactions with the in-plane and out-of-plane $p(\pi)$ orbitals of E (Figure 42), which makes it possible to study the differences between the Fe → ER π-back-donation into the two orbitals. Experimental geometries were available for $(CO)_4Fe-ER$ complexes with the related substituents R = Cp*,[159,324,325] $N(SiMe_3)_2$,[318] and Ar* (Ar* = 2,6-(2,4,6-triisopropylphenyl)phenyl),[312] which showed that the calculated geometries are quite accurate.[316] The most important results are summarized in Table 17.

The calculated Fe−ER bond dissociation energies for the different elements E show the same trend B > Al > Ga ≈ In > Tl, which has also been found for the W−E bonds of $(CO)_5W-ECl(NH_3)_2$. The trend of the $(CO)_4Fe-ER$ bond energies for different substituents R is Cp < $EN(SiH_3)_2$ < Ph, except for the AlN-$(SiH_3)_2$ and AlCp complexes which have nearly the same bond energy (Table 17). Most complexes have

the ER ligand in the axial position, but the differences between the axial and equatorial isomers were in all cases very small (<2 kcal/mol).[316]

The calculated data led to the following conclusion about the Fe-E bonding interactions: The bonds are mainly held together by Coulombic attraction between the negatively charged Fe and the strongly positively charged group-13 atoms. The covalent contributions to the bonding are rather small. This is indicated by the calculated bond orders, which show less than an Fe-E single bond. The Fe−ER bond orders are in most cases even lower than the Fe−CO bond orders (Table 17). The size of the Fe → ER π-back-donation which is given by the increase in the π charge at E Δq_π (E) shows for all compounds a regular trend for the atoms E: B > Al > Ga > In > Tl, while the trend for the Fe ← ER σ-donation exhibits an irregular behavior. The extent of Fe → ER π-back-donation *relative* to the Fe ← ER σ-donation varies significantly for the different groups R. The largest Fe → ER back-donation is found for the weakest π donor Ph, while the ligands ECp have the smallest Fe → back-donation, which is an expected result. It is interesting to note that the ligands EN-$(SiH_3)_2$ attract nearly as much π charge from Fe as EPh, although the amino substituent is a better π donor than phenyl. This is due to the electronegative nitrogen atom which withdraws electronic charge from the atom E by lowering the energy level of the acceptor orbitals and, thus, enhances the acceptor strength of the ligand. An interesting observation was made about the nonequivalent $p(\pi)$ acceptor orbitals of $EN(SiH_3)_2$ (Figure 42). The in-plane $p(\pi)$ AO of boron and aluminum, which are nearly empty in the free ligands, clearly become more highly populated in the complexes than the out-of-plane $p(\pi)$ orbitals (Table 17). The results for the complexes $(CO)_5W-EN(SiH_3)_2$, which are not given here, show the same trends as the complexes $(CO)_4Fe-EN(SiH_3)_2$.

Table 17. Calculated Fe−E Bond Dissociation Energies D_e, NBO and CDA Data of $(CO)_4-Fe-ECp$, $(CO)_4-Fe-EN(SiH_3)_2$, and $(CO)_4-Fe-EPh$ at BP86[a,b]

E	isomer	D_e	$q[Fe(CO)_4]$	$q(Fe)$	$q(E)$	$p_x(E)^f$	$p_y(E)^f$	$p_z(E)$	$\Delta q_\pi(E)^{d,e}$	$\Delta q_\sigma(E)^{d,e}$	$P(Fe-E)$	$P(Fe-CO)^c$
					Complexes $(CO)_4-Fe-ECp$							
B	ax	77.99	−0.51	−0.56	0.32	0.51	0.51	0.71	−0.40	+0.67	0.48	0.70
Al	ax	53.12	−0.67	−0.58	1.18	0.29	0.29	0.26	−0.30	+0.87	0.48	0.69
Ga	ax	32.89	−0.46	−0.51	0.96	0.27	0.27	0.21	−0.24	+0.61	0.49	0.77
In	ax	33.86	−0.53	−0.49	1.06	0.25	0.25	0.19	−0.19	+0.64	0.48	0.78
Tl	eq	17.11	−0.30	−0.51	0.81						0.32	0.73
					Complexes $(CO)_4-Fe-EN(SiH_3)_2$							
B	eq	85.83	−0.31	−0.58	0.59	0.39	0.48	0.61	−0.60	+0.68	0.65	0.62
Al	eq	52.98	−0.57	−0.63	1.23	0.20	0.30	0.21	−0.37	+0.81	0.51	0.63
Ga	ax	39.68	−0.53	−0.56	1.14	0.24	0.20	0.19	−0.31	+0.69	0.53	0.71
In	ax	38.92	−0.57	−0.53	1.21	0.21	0.17	0.16	−0.27	+0.70	0.50	0.73
Tl	ax	25.35	−0.46	−0.48	1.07	0.18	0.14	0.13	−0.21	+0.49	0.44	0.79
					Complexes $(CO)_4-Fe-EPh$							
B	ax	102.77	−0.36	−0.59	0.65	0.41	0.34	0.65	−0.63	+0.83	0.76	0.57
Al	eq	63.60	−0.66	−0.62	1.20	0.15	0.30	0.27	−0.40	+0.87	0.50	0.63
Ga	ax	55.03	−0.63	−0.56	1.12	0.21	0.18	0.24	−0.34	+0.76	0.52	0.68
In	ax	53.24	−0.67	−0.53	1.16	0.18	0.16	0.23	−0.29	+0.75	0.49	0.70
Tl	ax	42.52	−0.60	−0.50	1.04	0.15	0.14	0.19	−0.25	+0.61	0.44	0.74

[a] Taken from ref 316. D_e is given in kcal/mol. [b] Partial charges q, p-orbital population, difference of the π-population and the σ-charges of the atom E between the complexes and the free ligands Δq_π and Δq_σ, Wiberg bond indices P, charge donation d, and back-donation b. [c] CO_{ax} trans to ECp; CO_{eq} in case of the equitorial isomer. [d] Calculated using the frozen geometries in the complexes. [e] Negative number indicates higher electronic charge, and positive number indicates less electronic charge in the complex than in the free ligand. [f] $p(\pi)$ AO of atom E; p_x denotes the out-of-plane and p_y denotes the in-plane $p(\pi)$ orbitals of element E in the case of the $EN(SiH_3)_2$ and EPh complexes.

The W−E bond energies are slightly lower than the Fe-E dissociation energies, but the W → $EN(SiH_3)_2$ π-back-donation was calculated to be significantly smaller than the Fe → $EN(SiH_3)_2$ π-back-donation.[316]

In summary, it can be concluded that the $(CO)_n$TM−ER bonds have a dominant ionic character. The amount of TM → ER π-back-donation, which depends strongly on the nature of R, may become as large as the TM ← ER σ-donation, but the total contributions of the covalent interactions to the TM−ER bonds are less than that of a single bond.

V.6.4. Complexes $TM(ECH_3)_4$ (TM = Ni, Pd, Pt)

The compounds $Ni[InC(SiCH_3)_3]_4$ and $Ni[GaC-(SiCH_3)]_4$ which were synthesized by Uhl et al. were the first examples of homoleptic group-13 complexes that could be isolated and characterized spectroscopically by X-ray structure analysis.[326,327] They were also the first examples where more than one diyl ligand is bound to the same transition metal. It would be interesting to know the differences of the chemical bonding between $TM(ER)_4$ and $(CO)_n$TM−ER. The nature of the chemical bond in $TM(ECH_3)_4$ complexes (TM = Ni, Pd, Pt) has been studied recently at the DFT (B3LYP) level of theory by Uddin and Frenking.[316,327] Table 18 summarizes the most important results.

Table 18. Calculated TM−E Bond Dissociation Energy D_e and NBO Data of $TM(ECH_3)_4$ at B3LYP[a,b]

E	D_e	q[TM(ER)₃]	q(TM)	q(E)	Δq_π(E)[c,d]	Δq_σ(E)[c,d]	P(TM−E)
			Complexes Ni(ECH₃)₄				
B	83.80	0.04	0.16	0.31	−0.72	+0.55	0.56
Al	55.64	−0.10	−0.48	0.76	−0.60	+0.62	0.52
Ga	43.15	−0.07	−0.30	0.67	−0.50	+0.47	0.51
In	45.44	−0.14	−0.44	0.72	−0.56	+0.57	0.53
Tl	28.39	−0.08	−0.30	0.64	−0.42	+0.38	0.52
			Complexes Pd(ECH₃)₄				
B	67.46	0.02	0.20	0.30	−0.70	+0.52	0.60
Al	46.02	−0.10	−0.50	0.77	−0.50	+0.53	0.44
Ga	33.43	−0.11	−0.40	0.70	−0.44	+0.44	0.43
In	37.42	−0.18	−0.59	0.77	−0.44	+0.60	0.45
Tl	19.88	−0.13	−0.46	0.69	−0.34	+0.35	0.42
			Complexes Pt(ECH₃)₄				
B	82.68	0.05	0.35	0.24	−0.76	+0.52	0.68
Al	57.32	−0.16	−0.69	0.80	−0.56	+0.62	0.48
Ga	43.34	−0.15	−0.60	0.72	−0.48	+0.50	0.47
In	46.79	−0.16	−0.81	0.79	−0.48	+0.56	0.48
Tl	26.20	−0.13	−0.69	0.71	−0.40	+0.43	0.46

[a] Taken from ref 316. D_e is given in kcal/mol. [b] Partial charges q, difference of the π-charges and the σ-charges of the atom E between the complexes and the free ligands Δq_π and Δq_σ, Wiberg bond indices P. [c] Calculated using the frozen geometries in the complexes; identical values have been found in the free ligands for all complexes of Ni, Pd, and Pt. [d] Negative number indicates higher electronic charge, and positive number indicates less electronic charge in the complex than in the free ligand.

There is a very high degree of TM → ECH_3 π-back-donation in the TM−E bonds of $TM(ECH_3)_4$, which is in most cases even higher than the TM ← ECH_3 σ-donation. This becomes obvious by the large increase in the p(π) population of the elements E given by Δq_π (E). The p(π) AOs of E in the free ligands ECH_3 are nearly empty.[316] Despite the large back-donation, however, the calculated bond orders P(TM−E) are very small (<0.7), which indicates that the

covalent contributions to the TM−E bonding of the homoleptic diyl complexes are as low as in the carbonyl complexes $(CO)_n$TM−ER. The calculated partial charges for the atoms TM and E suggest weaker charge attraction between TM and E in $TM(ECH_3)_4$ than in $(CO)_n$TM−ER (compare Tables 17 and 18). The boron complexes $TM(BCH_3)_4$ even have positive charges at TM and B, which could be taken as evidence for charge repulsion. This conclusion is not justified. The electronic charge distribution is very anisotropic, and two atoms carrying a positive partial charge do not necessarily repel each other. For example, the electrostatic interactions in $TM(CO)_6{}^{n+}$ between the positively charged metals Re^+, Os^{2+}, Ir^{3+}, and CO, which has a positive partial charge at the carbon end, are strongly attractive (see Tables 8 and 10). The magnitude of the Coulombic attraction between TM and E in $TM(ECH_3)_4$ still needs to be investigated by an energy decomposition analysis.

Table 18 shows that the theoretically predicted TM−E bond dissociation energies are very high. The calculated bond energies may be compared with the values for the first CO dissociation energies of $TM(CO)_4$, which are 25 kcal/mol for $Ni(CO)_4$ and <10 kcal/mol for $Pd(CO)_4$ and $Pt(CO)_4$.[194,322] The diyl ligands are much more strongly bound in the homoleptic complexes than CO. It is interesting to note that the TM−ER bond energies for each element TM have the same trend as the TM → ER π-back-donation B > Al > Ga ≈ In > Tl. It seems that the trend of the L_nTM−ER bond dissociation energies does not depend on the nature of R, TM, and L.

V.6.5. Chemical Bonding in Boryl Complexes L_nTM–BR_2

Although TM boryl complexes have been calculated in several theoretical studies of the reaction mechanism of various boration reactions,[328−333] accurate theoretical investigations which address the nature of the chemical bond in TM compounds L_nTM−ER_2 are still in an infant stage. The TM−ER_2 bond is a covalent (shared electron) bond and not a donor−acceptor bond as in the diyl complexes with ligands ER. Figure 43 shows that the formally empty p(π)
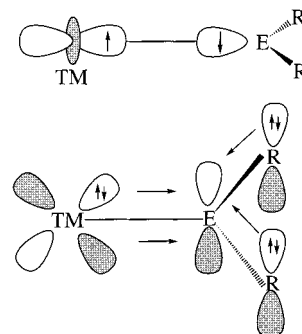

Figure 43. Schematic representation of the dominant orbital interactions in TM complexes with ligands ER_2 where E is a group-13 atom and R has p(π) lone-pair electrons.

AO of the atom E may electronically be stabilized by π-donation from the group R, besides the TM → ER_2

π-donation from the metal. Experimental efforts which focused mainly on boryl complexes L_nTM-ER_2 showed that the nature of R indeed has a strong influence on the stability of the compounds.[307,308] Pioneering efforts in this field have been made by early contributions of Nöth and Schmid.[334–338] More recent advances have been reported in the work of Braunschweig,[339] Hartwig,[340,341] Roper,[342] and others.[307,308] Boryl complexes are particularly stable with the cyclic ligands Bcat (cat = catecholate; $1,2\text{-}O_2C_6H_4$) and Bpin (pin = pinacolato; $OCMe_2CMe_2O$). The impact of the π-bonding contributions on the stability of the molecules is not completely understood yet. A recent review about TM boryl complexes came to the conclusion that "Thus, the importance of π-bonding effects involving the metal atom in these compounds has not yet been fully resolved".[343]

An important theoretical contribution to the understanding of the chemical bonding in boryl complexes was made by Rablen, Hartwig, and Nolan (RHN), who measured the heats of reaction for oxidative addition of catecholborane to the complex $(CO)(PPh_3)_2ClIr$ yielding the boryl complex *trans,cis*-$(CO)(PPh_3)_2Cl(H)Ir-Bcat$.[344] The authors used high-level calculations of B–H and B–C bond dissociation energies and the measured heats of formation to obtain the first estimate of a transition-metal–boryl bond energy. The authors note that the BDE value for the Ir–B bond $D_o = 66$ kcal/mol greatly exceeds the 35 kcal/mol bond energy for the Ir–Me bond in *trans*-$(CO)(PPh_3)_2(Cl)(Me)(I)Ir$. RHN compared the Ir–Me, Ir–H, and Ir–Bcat BDEs in Vaska-type complexes with the bonding in the respective H–X compounds and came to the conclusion that "π-interactions need not be invoked to explain the large metal-boron BDE".[344] They pointed out that π-bonding in iron and tungsten boryl complexes had been suggested in experimental studies by Hartwig, because the conformation of the solid-state structures could be explained in terms of TM $\rightarrow$ BR_2 π-donation.[340,341] The energy of this π bond in catechol-substituted boryl systems was found to be small, however, because the rotational barrier is not very high.

The nature of the chemical bonding between neutral and positively charged bare TM atoms and BH_2 in TM^q-BH_2 (TM = Sc, Co, Rh, and Ir; $q = 0, +1$) was investigated at the CASSCF, MR–SDCI+DC, and various DFT levels by Musaev and Morokuma (MM).[345] The authors calculated also $Rh-B(OH)_2$ and $Rh-B(OH)_2^+$. The trend of the $TM-BH_2$ binding energies for the neutral and cationic systems was calculated $Sc^q < Co^q < Rh^q < Ir^q$. The positively charged compounds have stronger TM^+-BH_2 bonds than the neutral $TM-BH_2$ species for TM = Sc, Co, and Ir, while the Rh^+-BH_2 bond is clearly stronger than the $Rh-BH_2$ bond. All these trends were explained in terms of the low-lying electronic states of the bare TM atoms and cations and the relativistic effects.[345] Unlike the work of RHN,[344] MM came to the conclusion that π interactions between the metal and the boryl groups are important for the $TM-BH_2$ bond.[345] Two reasons were given which led to the conclusion. First, the calculated TM–B binding ener-

gies for Sc^+ and Sc, which have no doubly occupied $d(\pi)$ orbitals, are smaller than those for Co^+ and Co by 3.5 and 14.2 kcal/mol. Second, the TM–B bond was found to be weaker than the TM–H and TM–Me bonds. The compounds $Rh-B(OH)_2$ and $Rh^+-B(OH)_2$ were calculated with slightly higher BDEs than $Rh-BH_2$ and Rh^+-BH_2, respectively.[345]

The question of the relative importance of R $\rightarrow$ B and TM $\rightarrow$ B π-donation in $Pd-B(OH)_2$ and $Pt-B(OH)_2$ has been addressed in a theoretical study by Sakaki and Kikuno (SK) in the context of calculating the addition reaction of R_2B-BR_2 to $TM(PH_3)_2$ (R = H, OH; TM = Pd, Pt).[333] The authors found that the difference between the $Pt-BH_2$ and $Pt-B(OH)_2$ bond energies is much smaller than the difference between H_2B-BH_2 and $(OH)_2B-B(OH)_2$ bond energies. This was interpreted in terms of easier π delocalization of the $d(\pi)$ electrons of Pt into the $p(\pi)$ AO of boron compared to HO $\rightarrow$ B π-donation. SK also suggested that the $d(\pi)$ electrons of Pd less easily delocalize to the $p(\pi)$ AO of boron than those of Pt, due to the lower energy of the Pd d orbitals.[333] This was given as an explanation for the finding that the $Pd-B(OH)_2$ bond energy is similar to the $Pd-SiH_3$ BDE. We want to point out that the conclusions about the importance of TM $\rightarrow$ BR_2 π-bonding in the theoretical studies of MM[345] and SK[333] were based only on the comparison of the bond strength of different compounds without an explicit analysis of the bonding situation in the boryl compounds being carried out. The possibility that other factors than π-bonding may be responsible for the differences in the binding interactions was not explored.

The nature of the chemical bond and the strength of the $Os-BR_2$ bond dissociation energies of different boryl ligands has recently been studied by Giju, Bickelhaupt, and Frenking (GBF).[346] These authors calculated the structures and bond energies of the 16 and 18 valence electron (VE) complexes $(PH_3)_2Cl(CO)Os-BR_2$ and $(PH_3)_2Cl(CO)_2Os-BR_2$ with $BR_2 = BH_2$, BF_2, $B(OH)_2$, $B(OHC=CHO)_{cyc}$, and Bcat at the B3LYP/II level of theory.[346] Figure 44 shows the optimized geometries of the complexes with the ligand Bcat. GBF analyzed the bonding situation of the boryl complexes using the NBO partitioning scheme.[346] The most important results are shown in Tables 19 and 20. Table 19 shows that the Os–B bond dissociation energies are very high. They are much higher than the calculated dissociation energy of one CO from $Os(CO)_5$ ($D_e = 42.9$ kcal/mol).[194,322] The high Os–B bond energies arise partly from electrostatic interactions between the negatively charged osmium and the positively charged boron (Table 19). Note that the positive charge at boron in the BH_2 complexes is much lower than in the other complexes. This suggests weaker $Os-BH_2$ charge attraction than in the other boryl complexes. However, covalent Os–B bonding also appears to be very strong. The calculated bond orders for the Os–B bonds of the 16 VE complexes are rather large (0.856–1.074). Note that the highest bond order is found for the BH_2 complexes. The bond orders suggest that the 16 VE complexes have an Os–B single bond. The Os–CO bonds still have higher bond orders
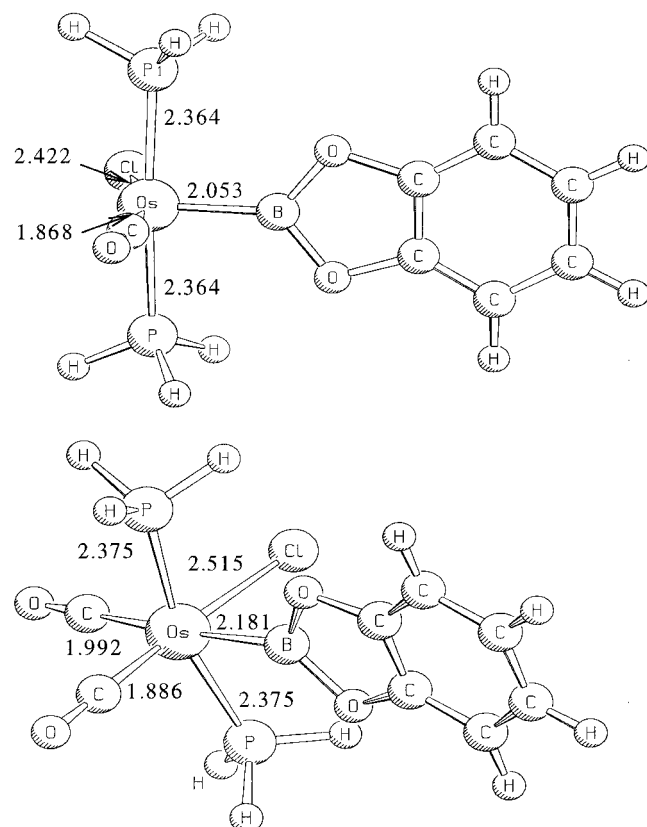
Figure 44. 16 VE and 18 VE osmium complexes with boryl ligands which have been studied in ref 346.

than the Os−B bonds, while the Os−P and Os−Cl bonds have significantly lower bond orders. The Os−B bonds are only weakly polarized toward the osmium end. The hybridization at Os is between sd^2 and sd^3. Table 20 shows that the total charge transfer between the boryl ligand and the osmium fragment $q([Os] \leftarrow [B])$ in the 16 VE complexes is small, which is in agreement with the weakly polarized Os−B bond. The Os → B π-donation is not very large, except in (PH$_3$)$_2$Cl(CO)Os−BH$_2$. There is also very little intraligand charge rearrangement in the boryl ligands when they bind to the osmium fragment, except for B → H$_2$ σ-donation in (PH$_3$)$_2$Cl(CO)Os−BH$_2$.

The theoretical results for the 18 VE complexes (PH$_3$)$_2$Cl(CO)$_2$Os−BR$_2$ and a comparison with the 16

VE monocarbonyl species is interesting because both classes of osmium boryl complexes are stable enough to become isolated. For example, X-ray structure analyses of (PPh$_3$)$_2$Cl(CO)Os−BR$_2$ and (PH$_3$)$_2$Cl-(CO)$_2$Os−BR$_2$ with BR$_2$ = B(OH)$_2$ and Bcat have been reported.[307,342] Table 19 shows that the Os−B bond energies of the 18 VE complexes are lower than those of the respective 16 VE complex but not very much. The bond energies of the *trans*-CO ligand in the 18 VE complexes are not very high ($D_0 < 30$ kcal/mol), which makes it plausible that the loss of one carbonyl yields a stable compound.

The differences in the NBO analysis of the Os−B bond between the two sets of boryl complexes are interesting. Although the Os−B BDE of the 18 VE complexes is not much lower than in the 16 VE species, the bond order for the Os−B bonds of the former are significantly lower than those of the latter. There is only one-half of a single Os−B bond in the 18 VE complexes (Table 19). The other osmium bonds also have a lower bond order, and the *trans*-CO has a clearly lower bond order with Os than the *cis*-CO. The Os−B σ bond in the 18 VE complexes is more polarized toward the osmium end, although the charge transfer is now always from the osmium fragment to the boryl ligand. The Os → BR$_2$ π-donation in the 18 VE complexes is clearly less than in the 16 VE complexes, which is reasonable because the boryl ligand competes in the former molecules with the *trans*-CO group for the π-donation from osmium.

The theoretical study shows that the Os−B bonds in the complexes have a high BDE. They are held together by a covalent σ bond which is slightly polarized toward osmium and by strong charge attraction between the positively charged boron atom and negatively charged Os. The NBO results indicate that the π component of the Os−BR$_2$ bond is very small when R has occupied p(π) orbitals. Os−B π-bonding becomes significant in BH$_2$ complexes. The enhanced π contribution compensates for the weaker charge attraction of the Os−BH$_2$ bond, which explains why the BDE is even slightly higher than the BDEs of the other Os−BR$_2$ bonds where R carries a π-type electron lone pair.

Table 19. Bond Dissociation Energy D_e (kcal/mol), Wiberg Bond Indices (WBI), and Results of the NBO Analysis in (PH$_3$)$_2$(CO)$_n$ClOs−BR$_2$ Complexes at the B3LYP/II Level^a

| | | | | | | | | | | OS−B | | | | | |
| | | | WBI | | | | | OS | | | | B | | |
BR$_2$	N	D_e (Os−B)	Os−B	Os−P	Os−Cl	Os−C	Os−C$_t$	%	%s	%p	%d	%s	%p	%d
BH$_2$	1	90.0	1.074	0.519	0.391	1.200		60.9	27.2	0.2	72.6	28.6	71.2	0.2
BF$_2$	1	90.8	0.910	0.519	0.428	1.169		57.9	28.1	0.5	71.4	55.5	44.4	0.1
B(OH)$_2$	1	84.7	0.856	0.520	0.415	1.199		60.2	30.8	0.3	68.9	38.4	61.5	0.1
B(OHC=CHO)$_{cyc}$	1	88.1	0.889	0.517	0.425	1.184		57.6	31.1	0.1	68.8	39.4	60.5	0.1
Bcat	1	87.1	0.901	0.515	0.428	1.174		55.6	28.3	0.1	71.6	47.1	52.8	0.1
BH$_2$	2	78.1	0.461	0.489	0.289	1.065	0.763	69.4	7.4	0.3	92.3	28.4	71.4	0.2
BF$_2$	2	80.5	0.537	0.490	0.365	1.037	0.662	69.9	16.9	1.1	82.0	45.5	54.4	0.1
B(OH)$_2$	2	75.2	0.494	0.487	0.357	1.049	0.696	54.9	31.3	0.6	68.2	49.8	50.2	0.0
B(OHC=CHO)$_{cyc}$	2	79.3	0.510	0.484	0.359	1.038	0.696	51.9	32.1	0.4	67.5	49.9	50.1	0.0
Bcat	2	77.8	0.517	0.483	0.360	1.034	0.690	81.0	14.9	0.1	85.0	35.8	62.7	1.5

^{a} Taken from ref 346.

Table 20. NBO Atomic Partial Charges, q, and Charge Donation, π and σ, between the Boryl Ligand [B] and the Osmium Fragment [Os] in $(PH_3)_2(CO)_nClOs-BR_2$ Complexes at the B3LYP/II Level; ΔQ, $\Delta \pi$, and $\Delta \sigma$ Give the Difference in the Intraligand Charge Transfer between the Complexes and the Free Ligands[a,b]

| BR$_2$	n	q Os	B	[Os] ← [B] q	[Os] → [B] (π)	[Os] ← [B] (σ)	B → R$_2$ (Δq)	B ← R$_2$ ($\Delta \pi$)	B → R$_2$ ($\Delta \sigma$)
BH$_2$	1	−0.24	0.13	−0.03	0.22	0.19	−0.16	0.00	−0.16
BF$_2$	1	−0.32	1.05	0.04	0.12	0.16	0.00	−0.01	−0.01
B(OH)$_2$	1	−0.28	0.96	0.04	0.08	0.12	−0.04	0.01	−0.03
B(OHC=CHO)$_{cyc}$	1	−0.26	0.89	−0.03	0.04	0.01	0.00	0.03	+0.03
Bcat	1	−0.26	0.91	−0.05	0.10	0.05	0.01	−0.03	−0.02
BF$_2$	2	−0.39	0.94	−0.09	0.11	0.02	0.02	−0.01	0.01
B(OH)$_2$	2	−0.33	0.83	−0.11	0.01	−0.10	−0.02	0.08	0.06
B(OHC=CHO)$_{cyc}$	2	−0.33	0.76	−0.17	0.02	−0.15	0.01	0.01	0.02
Bcat	2	−0.33	0.77	−0.18	0.04	−0.14	0.00	−0.01	−0.01

[a] Positive numbers indicate a charge transfer in the direction of the arrow, negative numbers indicate a reverse charge transfer. [b] Taken from ref 346.

Table 21. ETS Decomposition of the L_nM-(H_2) Bond Energy[a]

	ΔE^0	$\Delta E(a_1)$	$\Delta E(a_2)$	$\Delta E(b_1)$	$\Delta E(b_2)$	ΔE_{orb}	ΔE_{prep}	D_e
$(CO)_3(PH_3)_2Cr-(H_2)$	12.0	−16.9	−0.1	−1.2	−17.9	−36.1	2.8	21.3
$(CO)_3(PH_3)_2Mo-(H_2)$	13.0	−17.6	±0.0	−1.0	−18.9	−37.5	5.3	19.2
$(CO)_3(PH_3)_2W-(H_2)$	11.7	−18.2	−0.6	−0.2	−19.5	−38.5	5.9	20.9
$(CO)(PH_3)_4Mo-(H_2)$	12.5	−13.2	−0.2	−0.8	−21.2	−35.4	4.0	18.9
$(CO)_3(PH_3)_2Mo-(H_2)$	13.0	−17.6	±0.0	−1.0	−18.9	−37.5	5.3	19.2
$(CO)_5Mo-(H_2)$	13.5	−23.9	−0.4	−1.6	−11.9	−37.8	5.7	19.6

[a] Taken from ref 357. Values are given in kcal/mol.

V.7. Hydrogen Complexes

The nature of the chemical bonding in transition-metal complexes with dihydrogen as a ligand has been extensively studied by theoreticians after Kubas et al.[347] reported in 1984 the synthesis and X-ray structure analysis of the first TM complexes with an η^2-bonded dihydrogen ligand $(CO)_3(PR_3)_2W(H_2)$ (R = Cy, iPr). Transition-metal polyhydrides are the topic of another review in this issue by Maseras, Lledós, Clot, and Eisenstein[348] and, thus, shall not be covered in all details in this paper. The dichotomy of the bonding models π complex versus covalently bound compound, which is very helpful for the understanding of the TM complexes with carbene and carbyne ligands (Fischer vs Schrock) and in alkene and alkyne complexes (donor−acceptor complex vs metallacyclic compound), is also found in the description of hydrogen complexes (Figure 45). Therefore, we want to
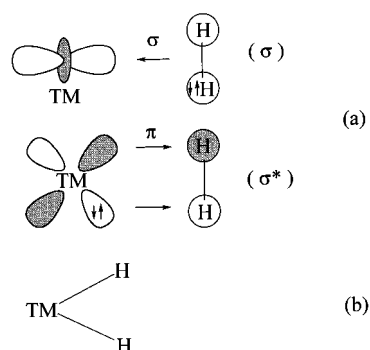
Figure 45. Schematic representation of the bonding models for TM−hydrogen complexes: (a) Donor−acceptor interactions in η^2-(H_2) complexes; (b) metalladihydrides.

include a short discussion of the nature of the chemical bond in dihydrogen complexes $L_nTM(H_2)$ as given by recent quantum chemical investigations.

The bonding model for the nonclassical dihydrogen complexes $L_nTM(H_2)$ involves electron donation from the H−H σ bond into an empty metal orbital (TM ← H_2 donation) and back-donation from an occupied d(π) orbital of the metal into the H−H antibonding σ^* orbital (Figure 45). The bonding model for the covalent electron-sharing interactions in L_nTMH_2 hydride complexes has two TM−H σ bonds, which means that there is no intraligand bond left as in the case of the metallacyclic compounds (Figures 29 and 32).

Numerous theoretical studies addressed the question of the relative strength of the two components of the orbital interactions in (η^2-H_2) complexes. They all agreed that the amount of TM ← H_2 σ-donation is larger than the TM → H_2 π-back-donation.[349−355] This does not mean that the energy contributions of the TM → H_2 π back-donation to the metal−H_2 bond is negligible. An energy decomposition analysis of group-6 dihydrogen complexes by Li and Ziegler (LZ)[356] showed that the stabilization gained by TM → H_2 π-back-donation can be as important or even higher than the energy contribution of the TM ← H_2 σ-donation and that the ratio of the two factors depends on the strength and the number of π acceptor ligands L in $L_nTM(H_2)$. Table 21 exhibits the NL-DFT results for complexes with the formula $(PH_3)_n(CO)_{5-n}TM(H_2)$ (TM = Cr, Mo, W; n = 0, 2, 4). The energy contribution of the $(CO)_5Mo$ ← H_2 donation, which has a_1 symmetry, is twice as high as the (b_2) back-donation. Successive substitution of the strong π acceptor CO by PH$_3$, which is a poor π acceptor, increases the back-donation. Already in $(PH_3)_2(CO)_3Mo(H_2)$ the back-donation is more important for the bond energy than the donation, an effect which is even more pronounced in $(PH_3)_4(CO)Mo(H_2)$. The increase in the strength of the Mo → H_2 π-back-

donation also manifests in the H−H bond length in $(PH_3)_n(CO)_{5-n}Mo(H_2)$, which increases from $n = 0$ (0.824 Å) to 4 (0.855 Å).[356] Donation and back-donation both slightly increase in $(PH_3)_2(CO)_3TM(H_2)$ with TM = Cr < Mo < W. A comparable or even larger energy contribution of the back-donation than donation has also been reported in the energy decomposition analysis of $(PH_3)_3H_2TM(H_2)$ (TM = Fe, Ru, Os) by Li, Dickson, and Ziegler (LDZ).[357] The strength of the two contributions to the TM−(H_2) interactions was found to be strongly influenced by the ligand (H or PH_3) which is trans to the TM−(H_2) bond.

The results of LZ[356] and LDZ[357] suggest that nonclassical isomers of polyhydrogen complexes are preferred for complexes with strong π-accepting ligands. The same conclusion had been reached in previous investigations by other groups.[353,358,359] Much insight into the nature of the metal−hydrogen bonding has been gained from the analysis of the electron density distribution.[353,355,360−363] Three different bonding situations for the TM−H_2 interactions are possible which can be distinguished by the topology of the electron density. Dihydrogen complexes may exhibit a T-shaped structure, which has bond paths for the H−H bond and from the metal to the center of the H−H bond. Alternatively, they may have a cyclic structure which has H−H bond paths and two TM−H bond paths for each metal−hydrogen bond. The third bonding situation which describes a dihydride has two TM−H bond paths but no longer a bond path for the H−H bond. Examples for the three situations have been reported by Maseras, Lledós, Costas, and Poblet (MLCP).[363] A T-shaped structure was found at the B3LYP level for $(PH_3)_2(CO)_3W(H_2)$, a cyclic structure was calculated for $(PH_3)_2Cl_2HIr$-(H_2), while a hydride form was found for $(PH_3)_3OsH_4$.

The nature of the chemical bond in TM hydrides has become the focus of numerous studies in the recent past, because calculations showed that the potential energy surfaces of apparently simple compounds such as CrH_6 and WH_6 are very complicated and that the octahedral form of the hexahydrides are energetically high-lying higher-order saddle points.[71−73,77,84,85] This led to an examination of the TM valence orbitals and the symmetry rules which are associated with the hybridization of sd and sdp orbitals. The ongoing discussion about this topic and the bonding models which have been suggested for covalent TM compounds have been reviewed in the first section of the paper.

VI. Concluding Remarks

The research reviewed in this paper shows the remarkable progress which has been made in the past decade toward gaining insight into the chemical bonding of transition metals. Several partitioning schemes have been developed and were successfully applied for analyzing the bonding situation in TM compounds after they were first calculated with accurate quantum chemical methods. Unlike earlier work, which was based on approximate methods and ad hoc assumptions of the binding interactions in molecules, these methods can be used to suggest qualitative bonding models which are in agreement with the physical mechanism that leads to a chemical bond. This is after all one of the most important goals of fundamental chemical research: To build a bridge between the basic laws of physics and the manifold of chemical bonding phenomena that are realized in millions of compounds. The models are not only useful for an understanding of the chemical bonds, but also as ordering schemes for the different classes of molecules.

The review shows that the bonding in many TM−ligand compounds can be described with a dichotomy of qualitative models which consider the DCD picture of TM ← ligand donation and TM → ligand back-donation as one extreme and covalent 2c-2e bonds between the metal and the ligand as the other extreme. These concepts are very helpful for understanding the chemical behavior of TM complexes with carbenes, carbynes, alkenes, alkynes, hydrogen, and other ligands which have not been discussed here. The real situation is always between the two extremes, and the electronic structure and the chemical behavior of the molecules can be rationalized with the contribution of each component. There are some ligands for which only one bonding situation is known so far. For example, all known TM carbonyl complexes are discussed in terms of donation and back-donation, and there is no compound with a $L_nTM=$C=O moiety which could be considered as metallaketene. Theory could make predictions about the possibility to make such molecules.

Although significant progress has been made in understanding the chemical bond of TM compounds, much work still has to be done. There are still many aspects of TM bonding which are not yet fully understood. The work by Davidson et al.[129] about the bonding in $Cr(CO)_6$ shows that the physical mechanism of the metal−CO interactions is more complicated than might be thought because of the success of the DCD model as an ordering scheme for many TM complexes. An important goal of quantum chemical research is to shed light on the connection between the bonding model and physical mechanism of the bond formation. Research in this area in the field of TM compounds has just started. However, powerful methods such as the EDA and ETS energy partitioning schemes developed by Morokuma and Ziegler, respectively, and the topological analysis of the electron density distribution of Bader are available. It is not difficult to predict that in the next decade quantum chemistry will bring a much deeper insight into the nature of the TM−ligand interactions and more refined models for TM compounds will be developed. Chemical bonding of TM compounds will be an exciting field for quantum chemical research in the decade to come.

VII. Glossary of Abbreviations

AIM	atoms in molecules
AOM	angular overlap model
BDE	bond dissociation energy
CCSD(T)	coupled-cluster theory with singles, doubles, and noniterative approximation of triples
CDA	charge decomposition analysis

CFT	crystal field theory
CI	configuration interaction
CIPSI	configuration interaction by perturbation with multiconfigurational zeroth-order wave function selected by iterative process
CSOV	constrained space orbital variation
DCD	Dewar−Chatt−Duncanson
DFT	density functional theory
ECP	effective core potential
EDA	energy decomposition analysis
ETS	extended transition state
FBDE	first bond dissociation energy
FORS	full optimized reaction space
GVB	generalized valence bond
HF	Hartree−Fock
HFS	Hartree−Fock−Slater
HOMO	highest occupied molecular orbital
LFT	ligand field theory
LUMO	lowest unoccupied molecular orbital
MCPF	modified coupled pair functional
MP2	Møller−Plesset perturbation theory terminated at second order
MSX$_\alpha$	multiple scattering X$_\alpha$
NL-DFT	nonlocal density functional theory
NAO	natural atomic orbital
NBO	natural bond orbital
NHO	natural hybrid orbital
ORSAM	orbital ranked symmetry analysis method
OWSO	occupancy-weighted symmetric orthogonalization
SAC	symmetry adapted cluster
SCF	self-consistent field
TM	transition metal

VIII. Acknowledgments

IX. References

(1) Hückel, E. *Z. Phys.* **1931**, *70*, 204.
(2) Berson, J. A. *Angew. Chem.* **1996**, *108*, 2750; *Angew. Chem., Int. Ed. Engl.* **1996**, *35*, 2922.
(3) Frenking, G. *Chem. Zeit* **1997**, *31*, 27.
(4) Pauling, L. *The Nature of the Chemical Bond*, 3rd ed.; Cornell University Press: Ithaca, NY, 1960; p 286.
(5) Kutzelnigg, W. *Angew. Chem.* **1984**, *96*, 262; *Angew. Chem., Int. Ed. Engl.* **1984**, *23*, 272.
(6) (a) Fukui, K. *Acc. Chem. Res.* **1971**, *4*, 57. (b) Fukui, K. *Theory of Orientation and Stereoselection*; Springer-Verlag: Berlin, 1975.
(7) Woodward, R. B.; Hoffmann, R. *The Conservation of Orbital Symmetry*; Verlag Chemie: Weinheim, 1970.
(8) Fleming, I. *Frontier Orbitals and Organic Chemical Reactions*; Wiley: New York, 1976.
(9) Gilchrist, T. L.; Storr, R. C. *Organic reactions and orbital symmetry*, 2nd ed.; Cambridge University Press: Cambridge, 1971.
(10) Houk, K. N. *Acc. Chem. Res.* **1975**, *8*, 361.
(11) Sustmann, R. *Pure Appl. Chem.* **1975**, *40*, 569.
(12) Streitwieser, A. *Molecular Orbital Theory for Organic Chemists*; Wiley: New York, 1961.
(13) Dewar, M. J. S. *Molecular Orbital Theory for Organic Chemists*; Prentice-Hall: Englewood Cliffs, NJ, 1975.
(14) Borden, W. T. *Modern Molecular Orbital Theory for Organic Chemists*; Prentice-Hall: Englewood Cliffs, NJ, 1975.
(15) Carey, F. A.; Sundberg, R. J. *Advanced Organic Chemistry*, 3rd ed.; Plenum Press: New York, 1993.
(16) Streitwieser, A.; Heathcock, C. H.; Kosower, E. M. *Introduction to Organic Chemistry*; Macmillan Publishing Co.: New York, 1992.
(17) Vollhardt, K. P. C.; Schore, N. E. *Organic Chemistry*, 2nd ed.; W. H. Freeman and Co.: New York, 1994.
(18) Cotton, F. A.; Wilkinson, G.; Gaus, P. L. *Basic Inorganic Chemistry*, 3rd ed.; John Wiley: New York, 1995.
(19) Cotton, F. A.; Wilkinson, G. *Advanced Inorganic Chemistry*, 5th ed.; John Wiley: New York, 1988.
(20) Shriver, D. F.; Atkins, P. W.; Langford, C. H. *Inorganic Chemistry*, 2nd ed.; Oxford University Press: Oxford, 1994.
(21) Huheey, J. E.; Keiter, E. A.; Keiter, R. L. *Inorganic Chemistry: Principles of Structure and Reactivity*, 4th ed.; Benjamin/Cummings: New York, 1993.
(22) Davidson, E. R. *Chem. Rev.* **1991**, *91*, 649.
(23) *Topics in Current Chemistry*; Nalewajski, R. F., Ed.; Springer-Verlag, Berlin, 1996; Vols. 180−183.
(24) *Density Functional Methods in Chemistry*; Labanowski, J., Andzelm, J., Eds.; Springer-Verlag: Heidelberg, 1991.
(25) Ziegler, T. *Chem. Rev.* **1991**, *91*, 651.
(26) *Density Functional Theory of Atoms and Molecules*; Parr, R. G., Yang, W., Eds.; Oxford University Press: New York, 1988.
(27) (a) Szasz, L. *Pseudopotential Theory of Atoms and Molecules*; J. Wiley & Sons: New York, 1986. (b) Krauss, M.; Stevens, W. J. *Ann Rev. Phys. Chem.* **1984**, *35*, 357. (c) Durand, P.; Malrieu, J. P. *Adv. Chem. Phys.* **1987**, *67*, 321.
(28) Frenking, G.; Antes, I.; Boehme, M.; Dapprich, S.; Ehlers, A. W.; Jonas, V.; Neuhaus, A.; Otto, M.; Stegmann, R.; Veldkamp, A.; Vyboishchikov, S. F. *Reviews in Computational Chemistry*; Lipkowitz, K. B., Boyd, D. B., Eds.; VCH: New York, Vol. 8, 1996; pp 63−144.
(29) Cundari, T. R.; Benson, M. T.; Lutz, M. L.; Sommerer, S. O. *Reviews in Computational Chemistry*; Lipkowitz, K. B., Boyd, D. B., Eds.; VCH: New York, Vol. 8, 1996; pp 145−202.
(30) Reed, A.; Schleyer, P. v. R. *J. Am. Chem. Soc.* **1990**, *112*, 1434.
(31) Magnusson, E. *J. Am. Chem. Soc.* **1990**, *112*, 7940.
(32) Cioslowski, J.; Mixon, S. T. *Inorg. Chem.* **1993**, *32*, 3209.
(33) Cooper, D. L.; Cunningham, T. P.; Gerratt, J.; Karadakov, P. B.; Raimondi, M. *J. Am. Chem. Soc.* **1994**, *116*, 4414.
(34) Häser, M. *J. Am. Chem. Soc.* **1996**, *118*, 7311.
(35) Dobado, J. A.; Martinez-Garcia, H.; Molina, J. M.; Sundberg, M. R. *J. Am. Chem. Soc.* **1998**, *120*, 8461.
(36) Reference 18, p 84.
(37) Ruedenberg, K. *Rev. Mod. Phys.* **1962**, *34*, 326.
(38) Feinberg, M. J.; Ruedenberg, K.; Mehler, E. L. *Adv. Quantum Chem.* **1970**, *5*, 27.
(39) Feinberg, M. J.; Ruedenberg, K. *J. Chem. Phys.* **1971**, *54*, 1495.
(40) Kutzelnigg, W. *Angew. Chem.* **1973**, *85*, 551; *Angew. Chem., Int. Ed. Engl.* **1973**, *12*, 546.
(41) Driessler, F.; Kutzelnigg, W. *Theor. Chim. Acta* **1976**, *43*, 1.
(42) For example, the role of the kinetic and potential energy for the chemical bonding is quite paradox. The virial theorem ($E = 0.5$ $V = −T$) predicts that the energy gain due to the formation of a covalent bond leads to an increase of the kinetic energy and a lowering of the potential energy. Ruedenberg has shown, however, that the driving force for the formation of a covalent bond is the *decrease* of the kinetic energy of the electrons. This is because the intraatomic promotion of the atomic orbitals which

brings them into the bonding state increases the kinetic energy of the electron, which then decreases upon bond formation. For further details, see ref 37−41.

(43) Gerloch, M.; Constable, E. C. *Transition-Metal Chemistry*; VCH: Weinheim, 1994.
(44) Constable, E. C. *Metals and Ligand Reactivity*; VCH: Weinheim, 1996.
(45) Elschenbroich, Ch.; Salzer, A. *Organometallics*, 2nd ed.; VCH: Weinheim, 1992.
(46) Albright, T. A.; Burdett, J. K.; Whangbo, M. H. *Orbital Interactions in Chemistry*; Wiley: New York, 1985.
(47) Burdett, J. K. *Chemical Bonds: A Dialogue*; Wiley: New York, 1997.
(48) Ballhausen, C. L. *Introduction to Ligand Field Theory*; McGraw-Hill: New York, 1962.
(49) Jørgensen, C. K. *Modern Aspects of Ligand Field Theory*; Elsevier: New York, 1971.
(50) Schläfer, H. L.; Glieman, G. *Basic Principles of Ligand Field Theory*; Wiley: New York, 1969.
(51) Burdett, J. K. *Adv. Inorg. Chem. Radiochem.* **1978**, *21*, 113.
(52) Schönherr, T. *Top. Curr. Chem.* **1997**, *191*, 87.
(53) Dewar, M. J. S. *Bull. Soc. Chim. Fr.* **1951**, *18*, C79.
(54) Chatt, J.; Duncanson, L. A. *J. Chem. Soc.* **1953**, 2929.
(55) Reference 18, p 165.
(56) Landis, C. R.; Cleveland, T.; Firman, T. K. *J. Am. Chem. Soc.* **1995**, *117*, 1859.
(57) Landis, C. R.; Firman, T. K.; Root, D. M.; Cleveland, T. *J. Am. Chem. Soc.* **1998**, *120*, 1842.
(58) Landis, C. R.; Cleveland, T.; Firman, T. K. *J. Am. Chem. Soc.* **1998**, *120*, 2641.
(59) Firman, T. K.; Landis, C. R. *J. Am. Chem. Soc.* **1998**, *120*, 12650.
(60) Other frequently used names are dative bond, semipolar bond, and coordinative bond.
(61) Moore, C. E. *Atomic Energy Levels*; NSDRS-NBS 35; U.S. National Bureau of Standards: Washington, DC, 1971.
(62) Vanquickenborne, L. G.; Pierloot, K.; Devoghel, D. *J. Chem. Educ.* **1994**, *71*, 469.
(63) Melrose, M. P.; Scerri, E. R. *J. Chem. Educ.* **1996**, *73*, 498.
(64) Pilar, F. L. *J. Chem. Educ.* **1978**, *55*, 3.
(65) Pilar, F. L. *J. Chem. Educ.* **1979**, *56*, 767.
(66) Scerri, E. R. *J. Chem. Educ.* **1992**, *69*, 602.
(67) Desclaux, J. P. *At. Data Nucl. Data Tables* **1973**, *12*, 311.
(68) Gerloch, M. *Coord. Chem. Rev.* **1990**, *99*, 199.
(69) Berger, S.; Bock, W.; Frenking, G.; Jonas, V.; Müller, F. *J. Am. Chem. Soc.* **1995**, *117*, 3820.
(70) Jonas, V.; Boehme, C.; Frenking, G. *Inorg. Chem.* **1996**, 2097.
(71) Shen, M.; Schaefer, H. F.; Partridge, H. *J. Chem. Phys.* **1992**, *98*, 508.
(72) Kang, S. K.; Tang, H.; Albright, T. A. *J. Am. Chem. Soc.* **1993**, *115*, 1971.
(73) Tanpipat, N.; Baker, I. *J. Phys. Chem.* **1996**, *100*, 19818.
(74) Shortland, A. J.; Wilkinson, G. *J. Chem. Soc., Dalton Trans.* **1973**, 872.
(75) Haaland, A.; Hammel, A.; Rypdal, K.; Volden, H. V. *J. Am. Chem. Soc.* **1990**, *112*, 4547.
(76) Pfennig, V.; Seppelt, K. *Science* **1996**, *271*, 626.
(77) Kaupp, M. *J. Am. Chem. Soc.* **1996**, *118*, 3018.
(78) Theoretical analyses of the chemical bonding in TM compounds which have equilibrium geometries that deviate from maximum symmetry have also been reported in (a) Kaupp, M. *Chem. Eur. J.* **1998**, *4*, 1678. (b) Kaupp, M. *Chem. Eur. J.* **1998**, *4*, 2059. (c) Kaupp, M. *Angew. Chem.* **1999**, *111*, 3219; *Angew. Chem., Int. Ed. Engl.* **1999**, *38*, 3034.
(79) Gillespie, R. J. *Molecular Geometry*; Van Nostrand Reinhold: London, 1972.
(80) Gillespie, R. J.; Hargittai, I. *The VSEPR Model of Molecular Geometry*; Prentice-Hall: New Jersey, 1991.
(81) Gillespie, R. J. *Chem. Soc. Rev.* **1991**, *21*, 59.
(82) Root, D. M.; Landis, C. R.; Cleveland, T. *J. Am. Chem. Soc.* **1993**, *115*, 4201.
(83) (a) Pauling, L. *Proc. Natl. Acad. Sci. U.S.A.* **1975**, *72*, 4200. (b) Pauling, L. *Proc. Natl. Acad. Sci. U.S.A.* **1976**, *73*, 274.
(84) Kang, S. F.; Albright, T. A.; Eisenstein, O. *Inorg. Chem.* **1989**, *28*, 1612.
(85) Zyubin, A. S.; Musaev, D. G.; Charkin, O. P. *Russ. J. Inorg. Chem.* **1992**, *37*, 1214.
(86) Bent, H. A. *Chem. Rev.* **1961**, *61*, 275.
(87) Kaupp, M. *Chem. Eur. J.* **1999**, *5*, 3631.
(88) Griffith, W. P.; Wickins, T. D. *J. Chem. Soc. A* **1968**, 400.
(89) Tatsumi, R.; Hoffmann, R. *Inorg. Chem.* **1980**, *19*, 2656.
(90) Mingos, D. M. P. *J. Organomet. Chem.* **1979**, *179*, C29.
(91) (a) Brower, D. C.; Templeton, J. L.; Mingos, D. M. P. *J. Am. Chem. Soc.* **1987**, *109*, 5203. (b) Pyykkö, P. *J. Phys. Chem. A* **1997**, *101*, 8017.
(92) Reed, A. E.; Curtiss, L. A.; Weinhold, F. *Chem. Rev.* **1988**, *88*, 899.
(93) Weinhold, F. in *Encyclopedia of Computational Chemistry*, Vol. 3, p 1792, Schleyer, P.v. R.; Allinger, N. L.; Kollmann, P. A.; Clark, T.; Schaefer, H. F. S.; Gasteiger, J.; Schreiner, P. R. (Eds), Wiley-VCH: Chichester, 1998.
(94) Maseras, F.; Morokuma, K. *Chem. Phys. Lett.* **1992**, *195*, 500.
(95) Mulliken, R. S. *J. Chem. Phys.* **1955**, *23*, 1833.
(96) Bayse, C. A.; Hall, M. B. *J. Am. Chem. Soc.* **1999**, *121*, 1348.
(97) Foster, J.; Boys, S. F. *Rev. Mod. Phys.* **1960**, *32*, 300.
(98) Pipek, J.; Mezey, P. G. *J. Chem. Phys.* **1989**, *90*, 4916.
(99) Couty, M.; Hall, M. B. *J. Comput. Chem.* **1996**, *17*, 1359.
(100) King, R. B. *Inorg. Chem.* **1998**, *37*, 3057.
(101) Diefenbach, A.; Bickelhaupt, F. M.; Frenking, G. *J. Am. Chem. Soc.*, submitted for publication.
(102) Demolliens, A.; Jean, Y.; Eisenstein, O. *Organometallics* **1986**, *5*, 1457.
(103) Gillespie, R. J.; Bytheway, I.; Tang, T.-H.; Bader, R. F. W. *Inorg. Chem.* **1996**, *35*, 3954.
(104) Gillespie, R. J.; Robinson, E. A. *Angew. Chem.* **1996**, *108*, 539; *Angew. Chem., Int. Ed. Engl.* **1996**, *35*, 495.
(105) Marsden, C. J.; Wolynec, P. P. *Inorg. Chem.* **1991**, *30*, 1681.
(106) *Encyclopedia of Computational Chemistry*; Schleyer, P.v. R., Allinger, N. L., Kollmann, P. A., Clark, T., Schaefer, H. F. S., Gasteiger, J., Schreiner, P. R., Eds.; Wiley-VCH: Chichester, 1998.
(107) Dapprich, S.; Frenking, G. *J. Phys. Chem.* **1995**, *99*, 9352.
(108) (a) Bader, R. F. W. *Atoms in Molecules. A Quantum Theory*; Oxford University Press: Oxford, 1990. (b) Bader, R. F. W. In *Encyclopedia of Computational Chemistry*; Schleyer, P. v. R., Allinger, N. L., Kollmann, P. A., Clark, T., Schaefer, H. F. S., Gasteiger, J., Schreiner, P. R., Eds.; Wiley-VCH: Chichester, 1998. Vol. 1, p 64.
(109) (a) Morokuma, K. *J. Chem. Phys.* **1971**, *55*, 1236. (b) Morokuma, K. *Acc. Chem. Res.* **1977**, *10*, 294.
(110) Ziegler, T.; Rauk, A. *Theor. Chim. Acta* **1977**, *46*, 1.
(111) Bagus, P. S.; Hermann, K.; Bauschlicher, C. W. *J. Chem. Phys.* **1984**, *80*, 4378.
(112) Cioslowski, J. in *Encyclopedia of Computational Chemistry*; Schleyer, P. v. R., Allinger, N. L., Kollmann, P. A., Clark, T., Schaefer, H. F. S., Gasteiger, J., Schreiner, P. R., Eds.; Wiley-VCH: Chichester, 1998; Vol. 2, p 892.
(113) Reed, A. E.; Weinstock, R. B.; Weinhold, F. *J. Chem. Phys.* **1985**, *83*, 735.
(114) (a) Glendening, E. D.; Weinhold, F. *J. Comput. Chem.* **1998**, *19*, 593. (b) Glendening, E. D.; Weinhold, F. *J. Comput. Chem.* **1998**, *19*, 610. (c) Glendening, E. D.; Badenhoop, J. K.; Weinhold, F. *J. Comput. Chem.* **1998**, *19*, 628.
(115) Pidun, U.; Frenking, G. *J. Organomet. Chem.* **1996**, *525*, 269.
(116) Pidun, U.; Frenking, G. *J. Chem. Soc., Dalton Trans.* **1997**, 1653.
(117) Janssen, M. D.; Köhler, K.; Herres, M.; Dedieu, A.; Smeets, W. J. J.; Spek, A. L.; Grove, D. M.; Lang, H.; van Koten, G. *J. Am. Chem. Soc.* **1996**, *118*, 4817.
(118) Janssen, M. D.; Herres, M.; Zsolnai, L.; Spek, A. L.; Grove, D. M.; Lang, H.; van Koten, G. *Inorg. Chem.* **1996**, *35*, 2476.
(119) Janssen, M. D.; Herres, M.; Zsolnai, L.; Grove, D. M.; Spek, A. L.; Lang, H.; van Koten, G. *Organometallics* **1995**, *14*, 1098.
(120) Janssen, M. D.; Herres, M.; Spek, A. L.; Grove, D. M.; Lang, H.; van Koten, G. *J. Chem. Soc., Chem. Commun.* **1995**, 925.
(121) Lang, H.; Herres, M.; Zsolnai, L. *Organometallics* **1993**, *12*, 5008.
(122) Bader, R. F. W.; MacDougall, P. J. *J. Am. Chem. Soc.* **1985**, *107*, 6788.
(123) Gillespie, R. J. *J. Chem. Educ.* **1998**, *75*, 923.
(124) Slee, T. S. *J. Am. Chem. Soc.* **1986**, *108*, 7541.
(125) Cioslowski, J.; Mixon, S. T. *J. Am. Chem. Soc.* **1991**, *113*, 4142.
(126) Wiberg, K. *Tetrahedron* **1968**, *24*, 1083.
(127) Wichmann, K.; Frenking, G. Unpublished result.
(128) Cremer, D.; Kraka, E. *Angew. Chem.* **1984**, *96*, 612; *Angew. Chem., Int. Ed. Engl.* **1984**, *23*, 62.
(129) Davidson, E. R.; Kunze, K. L.; Machado, F. B. C.; Chakravorty, S. J. *Acc. Chem. Res.* **1993**, *26*, 628.
(130) Kunze, K. L.; Davidson, E. R. *J. Phys. Chem.* **1992**, *96*, 2129.
(131) Machado, F. B. C.; Davidson, E. R. *J. Phys. Chem.* **1993**, *97*, 4397.
(132) Bauschlicher, C. W.; Bagus, P. S. *J. Chem. Phys.* **1984**, *81*, 5889.
(133) Bauschlicher, C. W.; Petterson, L. G. M.; Siegbahn, P. E. M. *J. Chem. Phys.* **1987**, *87*, 2129.
(134) Bauschlicher, C. W.; Langhoff, S. R.; Barnes, L. A. *Chem. Phys.* **1989**, *129*, 431.
(135) Bauschlicher, C. W. *J. Chem. Phys.* **1986**, *84*, 260.
(136) Bauschlicher, C. W.; Bagus, P. S.; Nelin, C. J.; Roos, B. O. *Chem. Phys.* **1986**, *85*, 354.
(137) Barnes, L. A.; Rosi, M.; Bauschlicher, C. W. *J. Chem. Phys.* **1991**, *94*, 2031.
(138) Barnes, L. A.; Rosi, M.; Bauschlicher, C. W. *J. Chem. Phys.* **1990**, *93*, 609.
(139) Barnes, L. A.; Bauschlicher, C. W. *J. Chem. Phys.* **1989**, *91*, 314.
(140) Blomberg, M. R. A.; Brandemark, U. B.; Siegbahn, P. E. M.; Wennerberg, J.; Bauschlicher, C. W. *J. Am. Chem. Soc.* **1988**, *110*, 6650.
(141) Hall, M. B.; Fenske, R. F. *Inorg. Chem.* **1972**, *11*, 1620.
(142) Sherwood, P. E.; Hall, M. B. *Inorg. Chem.* **1979**, *18*, 2325.
(143) Sherwood, P. E.; Hall, M. B. *Inorg. Chem.* **1980**, *19*, 1805.

(144) Williamson, R. L.; Hall, M. B. *Int. J. Quantum Chem.* **1987**, *21S*, 503.
(145) Hillier, I. H.; Saunders: V. R. *Mol. Phys.* **1971**, *23*, 1025.
(146) Hillier; I. H.; Saunders: V. R. *J. Chem. Soc., Chem. Commun.* **1971**, 642.
(147) Ford, P. C.; Hillier, I. H. *J. Chem. Phys.* **1984**, *80*, 5664.
(148) Ford, P. C.; Hillier, I. H.; Pope, S. A.; Guest, M. F. *Chem. Phys. Lett.* **1983**, *102*, 555.
(149) Cooper, G.; Green, J. C.; Payne, M. P.; Dobson, B. R.; Hillier, I. H. *Chem. Phys. Lett.* **1986**, *125*, 97.
(150) Cooper, G.; Green, J. C.; Payne, M. P.; Dobson, B. R.; Hillier, I. H.; Vincent, M.; Rosi, M. *J. Chem. Soc., Chem. Commun.* **1986**, 438.
(151) Moncrieff, D.; Ford, P. C.; Hillier, I. H.; Saunders: V. R. *J. Chem. Soc., Chem. Commun.* **1983**, 1108.
(152) Smith, S.; Hillier, I. H.; von Niessen, W.; Guest, M. C. *Chem. Phys.* **1989**, *135*, 357.
(153) Vanquickenborne, L. G.; Verhulst, J. *J. Am. Chem. Soc.* **1987**, *109*, 4825.
(154) Pierfoot, K.; Verhulst, J.; Verbeke, P.; Vanquickenborne, L. G. *Inorg. Chem.* **1989**, *28*, 3059.
(155) Yamamoto, S.; Kashiwagi, H. *Chem. Phys. Lett.* **1993**, *205*, 306.
(156) Blomberg, M. R. A.; Siegbahn, P. E. M.; Lee, T. L.; Rendell, A. P.; Rice, J. E. *J. Chem. Phys.* **191**, *95*, 5898.
(157) Johnson, J. B.; Klemperer, W. G. *J. Am. Chem. Soc.* **1977**, *99*, 7132.
(158) Szilagyi, R.; Frenking, G. *Organometallics* **1997**, *16*, 4807.
(159) Weiss, J.; Stetzkamp, D.; Nuber, B.; Fischer, R. A.; Boehme, C.; Frenking, G. *Angew. Chem.* **1997**, *109*, 95; *Angew. Chem., Int. Ed. Engl.* **1997**, *36*, 70.
(160) Ehlers, A. W.; Ruiz-Molares, Y.; Baerends, E. J.; Ziegler, T. *Inorg. Chem.* **1997**, *36*, 5031.
(161) Ziegler, T.; Tschinke, V.; Ursenbach, C. *J. Am. Chem. Soc.* **1987**, *109*, 4825.
(162) Li, J.; Schreckenbach, G.; Ziegler, T. *J. Am. Chem. Soc.* **1995**, *117*, 486.
(163) Mavridis, A.; Harrison, J. F.; Allison, J. *J. Am. Chem. Soc.* **1989**, *111*, 2482.
(164) Allison, J.; Mavridis, A.; Harrison, J. F. *Polyhedron* **1988**, *7*, 1559.
(165) Barnes, L. A.; Rosi, M.; Bauschlicher, C. W. *J. Chem. Phys.* **1990**, *93*, 609.
(166) Bauschlicher, C. W.; Barnes, L. A. *Chem. Phys.* **1988**, *124*, 383.
(167) Büker, H. J.; Maitre, P.; Ohanessian, G. *J. Phys. Chem. A* **1997**, *101*, 3966.
(168) Lupinetti, A. J.; Jonas, V.; Thiel, W.; Strauss, S. H.; Frenking, G. *Chem. Eur. J.* **1999**, *5*, 2573.
(169) Veldkamp, A.; Frenking, G. *Organometallics* **1993**, *12*, 4613.
(170) Lupinetti, A. J.; Fau, S.; Frenking, G.; Strauss, S. H. *J. Phys. Chem. A* **1997**, *101*, 9551.
(171) Meyer, F.; Chen, Y. M.; Armentrout, P. *J. Am. Chem. Soc.* **1995**, *117*, 4071.
(172) Barnes, L. A.; Bauschlicher, C. W. *J. Chem. Phys.* **1989**, *91*, 314.
(173) Moore, C. E. *Atomic Energy Levels*; Natl. Bur. Stand., U.S. GPO: Washington, D. C., 1949; Circ. No. 467.
(174) Barnes, L. A.; Rosi, M.; Bauschlicher, C. W. *J. Chem. Phys.* **1991**, *94*, 2031.
(175) Persson, B.; Roos, B. O.; Pierlot, K. *J. Chem. Phys.* **1994**, *101*, 6810.
(176) Barthelat, J. C.; Durand, P.; Pelissier, M. *Phys. Rev. A* **1980**, *21*, 1773.
(177) Balasubramanian, K.; Pitzer, K. S. *Adv. Chem. Phys.* **1987**, *67*, 287.
(178) Pyykkö, P. *Chem. Rev.* **1988**, *88*, 563.
(179) Pisani, L.; André, J.-M.; André, M.-C.; Clementi, E. *J. Chem. Educ.* **1993**, *70*, 894.
(180) Goldman, A. S.; Krogh-Jespersen, K. *J. Am. Chem. Soc.* **1996**, *118*, 12159.
(181) Strauss, S. H. *Chemtracts: Inorg. Chem.* **1997**, *10*, 77.
(182) Lupinetti, A. J.; Frenking, G.; Strauss, S. H. *Angew. Chem.* **1998**, *110*, 2229; *Angew. Chem., Int. Ed. Engl.* **1998**, *37*, 2113.
(183) Lupinetti, A. J.; Frenking, G.; Strauss, S. H. *Rev. Inorg. Chem.*, in print.
(184) Graham, W. A. G. *Inorg. Chem.* **1968**, *7*, 315.
(185) Hall, M. B.; Fenske, R. F. *Inorg. Chem.* **1972**, *11*, 768.
(186) DeKock, R. L.; Sarapu, A. C.; Fenske, R. F. *Inorg. Chem.* **1971**, *10*, 38.
(187) Ehlers, A. W.; Baerends, E. J.; Bickelhaupt, F. M.; Radius, U. *Chem. Eur. J.* **1998**, *4*, 210.
(188) Radius, U.; Bickelhaupt, F. M.; Ehlers, A. W.; Goldberg, N.; Hoffmann, R. *Inorg. Chem.* **1998**, *37*, 1080.
(189) Hirota, E.; Endo, J. *J. Mol. Spectrosc.* **1988**, *127*, 524.
(190) Botschwina, P.; Oswald, M.; Flugge, J.; Heyl, A.; Oswald, R. *Chem. Phys. Lett.* **1993**, *209*, 117.
(191) Jaffé, H. H.; Orchin, M. *Tetrahedron* **1960**, *10*, 212.
(192) Aubke, F.; Wang, C. *Coord. Chem. Rev.* **1994**, *137*, 483.
(193) Poulton, J. T.; Sigalas, M. P.; Folting, K.; Streib, W. E.; Eisenstein, O.; Caulton, K. G. *Inorg. Chem.* **1994**, *33*, 1476.

(194) Ehlers, A. W.; Dapprich, S.; Vyboishchikov, S. F.; Frenking, G. *Organometallics* **1996**, *15*, 105.
(195) Barckholtz, T. A.; Bursten, B. E. *J. Am. Chem. Soc.* **1998**, *120*, 1926.
(196) Furet, E.; Weber, J. *Theor. Chim. Acta* **1995**, *91*, 157.
(197) Delley, B.; Wrinn, M.; Lüthi, H. P. *J. Chem. Phys.* **1994**, *100*, 5785.
(198) Fan, L.; Ziegler, T. *J. Phys. Chem.* **1992**, *17*, 6937.
(199) Barnes, L. A.; Liu, B.; Lindh, R. *J. Chem. Phys.* **1993**, 98, 3978.
(200) Marquez, A.; Daniel, C.; Sanz, J. F. *J. Phys. Chem.* **1992**, *96*, 121.
(201) Sosa, R. M.; Gardiol, P. *Int. J. Quantum Chem. S.* **1996**, *30*, 1429.
(202) Jackson, S. A.; Eisenstein, O.; Martin, J. D.; Albeniz, A. C.; Crabtree, R. H. *Organometallics* **1991**, *10*, 3062.
(203) v. C. Wüllen, *J. Comput. Chem.* **1997**, *18*, 1985.
(204) Ruiz-Morales, Y.; Schreckenbach, G.; Ziegler, T. *J. Phys. Chem.* **1996**, *100*, 3359.
(205) Smith, G. W.; Carter, E. A. *J. Phys. Chem.* **1991**, *95*, 2327.
(206) Maasböl, A.; Fischer, E. O. *Angew. Chem.* **1964**, *76*, 645; *Angew. Chem., Int. Ed. Engl.* **1964**, *3*, 580.
(207) Hofmann, P. in ref 208, p 113.
(208) Dötz, K. H.; Fischer, H.; Hofmann, P.; Kreissl, F. R.; Schubert, U.; Weiss, K. *Transition Metal Carbene Complexes*; Verlag Chemie: Weinheim, 1983.
(209) Schrock, R. R. *Acc. Chem. Res.* **1979**, *12*, 98.
(210) Nugent, W. A.; Mayer, J. M. *Metal-Ligand Multiple Bonds*; Wiley: New York, 1988.
(211) Brothers, P. J.; Roper, W. R. *Chem. Rev.* **1988**, *88*, 1293.
(212) Nakatsuji, H.; Ushio, J.; Han, S.; Yonezawa, T. *J. Am. Chem. Soc.* **1983**, *105*, 426.
(213) Ushio, J.; Nakatsuji, H.; Yonezawa, T. *J. Am. Chem. Soc.* **1984**, *106*, 5892.
(214) Taylor, T. E.; Hall, M. B. *J. Am. Chem. Soc.* **1984**, *106*, 1576.
(215) Rappé, A. K.; Goddard, W. A., III *J. Am. Chem. Soc.* **1977**, *99*, 3966.
(216) Rappé, A. K.; Goddard, W. A., III *J. Am. Chem. Soc.* **1982**, *104*, 448.
(217) Carter, E. A.; Goddard, W. A., III *J. Phys. Chem.* **1984**, *88*, 1485.
(218) Carter, E. A.; Goddard, W. A., III *J. Am. Chem. Soc.* **1986**, *108*, 2180.
(219) Carter, E. A.; Goddard, W. A., III *J. Am. Chem. Soc.* **1986**, *108*, 4746.
(220) Herrmann, W. A.; Köcher, C. *Angew. Chem.* **1997**, *109*, 2257; *Angew. Chem., Int. Ed. Engl.* **1997**, *36*, 2162.
(221) Boehme, C.; Frenking, G. *Organometallics* **1998**, *17*, 5801.
(222) Gobbi, A.; Frenking, G. *Bull. Chem. Soc. Jpn.* **1993**, *66*, 3153.
(223) Gutsev, G. L.; Ziegler, T. *J. Phys. Chem.* **1991**, *95*, 7220.
(224) Haaland, A. *Angew. Chem.* **1989**, *101*, 1017; *Angew. Chem., Int. Ed. Engl.* **1989**, *28*, 992.
(225) Cundari, T. R.; Gordon, M. S. *J. Am. Chem. Soc.* **1991**, *113*, 5231.
(226) Cundari, T. R.; Gordon, M. S. *J. Am. Chem. Soc.* **1992**, *114*, 539.
(227) Matsunaga, N.; Koseki, S.; Gordon, M. S. *J. Chem. Phys.* **1996**, *104*, 7988.
(228) (a) Ruedenberg, K.; Schmidt, M. W.; Dombek, M. M.; Elbert, S. T. *Chem. Phys.* **1982**, *71*, 41. (b) Ruedenberg, K.; Schmidt, M. W.; Dombek, M. M.; Elbert, S. T. *Chem. Phys.* **1982**, *71*, 51. (c) Ruedenberg, K.; Schmidt, M. W.; Dombek, M. M.; Elbert, S. T. *Chem. Phys.* **1982**, *71*, 65.
(229) Cundari, T. R.; Gordon, M. S. *J. Phys. Chem.* **1992**, *96*, 631.
(230) Cundari, T. R.; Gordon, M. S. *Organometallics* **1992**, *11*, 3122.
(231) McKellar, A. R. W.; Bunker, P. R.; Sears, T. J.; Evenson, K. M.; Saykally, R. J.; Langhoff, S. R. *J. Chem. Phys.* **1983**, *79*, 5251.
(232) Leopold, D. G.; Murray K. K.; Lineberger, W. C. *J. Chem. Phys.* **1984**, *81*, 1048.
(233) Leopold, D. G.; Murray, K. K.; Miller, A. E. S.; Lineberger, W. C. *J. Chem. Phys.* **1985**, *83*, 4849.
(234) Buenker, P. R.; Sears, T. J. *J. Chem. Phys.* **1985**, *83*, 4866.
(235) Nakatsuji, H.; Hada, M.; Kondo, K. *Chem. Phys. Lett.* **1992**, *196*, 404.
(236) Nakatsuji, H.; Hirao, K. *J. Chem. Phys.* **1978**, *68*, 2035.
(237) Márquez, A.; Sanz, J. F. *J. Am. Chem. Soc.* **1992**, *114*, 2903.
(238) Márquez, A.; Sanz, J. F. *J. Am. Chem. Soc.* **1992**, *114*, 10019.
(239) Jacobsen, H.; Schreckenbach, G.; Ziegler, T. *J. Phys. Chem.* **1994**, 98, 11406.
(240) Jacobsen, H.; Ziegler, T. *Organometallics* **1995**, *14*, 224.
(241) Jacobsen, H.; Ziegler, T. *Inorg. Chem.* **1996**, *35*, 775.
(242) Zybill, C.; Müller, G. *Angew. Chem.* **1987**, *99*, 683; *Angew. Chem., Int. Ed. Engl.* **1987**, *26*, 669.
(243) Straus, D. A.; Tilley, T. D.; Rheingold, A. L.; Geib, S. J. *J. Am. Chem. Soc.* **1987**, *109*, 5872.
(244) Vyboishchikov, S. F.; Frenking, G. *Chem. Eur. J.* **1998**, *4*, 1428.
(245) (a) Koda, S. *Chem. Phys. Lett.* **1978**, *55*, 353. (b) Koda, S. *Chem. Phys. Lett.* **1986**, *66*, 383.
(246) Öfele, K. *J. Organomet. Chem.* **1968**, *12*, P42.
(247) Wanzlick, H.-W.; Schönherr, H.-J. *Angew. Chem.* **1968**, *80*, 154; *Angew. Chem., Int. Ed. Engl.* **1968**, *7*, 141.
(248) (a) Öfele, K.; Kreiter, C. G. *Chem. Ber.* **1972**, *105*, 529. (b) Öfele, K.; Herberhold, M. *Chem. Ber.* **1973**, *28*, 8b, 306.

(249) Arduengo, A. J., III.; Harlow, R. L.; Kline, M. *J. Am. Chem. Soc.* **1991**, *113*, 361.
(250) Heinemann, C.; Müller, T.; Apeloig, Y.; Schwarz, H. *J. Am. Chem. Soc.* **1996**, *118*, 2023.
(251) Boehme, C.; Frenking, G. *J. Am. Chem. Soc.* **1996**, *118*, 2039.
(252) Alder, R. W.; Allen, P. R.; Murray, M.; Orpen, A. G. *Angew. Chem.* **1996**, *108*, 1211; *Angew. Chem., Int. Ed. Engl.* **1996**, *35*, 1121.
(253) Beste, A.; Krämer, O.; Gerhard, A.; Frenking, G. *Eur. J. Inorg. Chem.* **1999**, 2037.
(254) Fischer, E. O.; Kreis, G.; Kreiter, C. G.; Müller, J.; Huttner, G.; Lorenz, H. *Angew. Chem.* **1973**, *85*, 618; *Angew. Chem., Int. Ed. Engl.* **1973**, *12*, 564.
(255) McLain, S. J.; Wood, C. D.; Messerle, L. W.; Schrock, R. R.; Hollander, F. J.; Youngs, W. J.; Churchill, M. R. *J. Am. Chem. Soc.* **1978**, *100*, 5962.
(256) Fischer, H.; Hofmann, P.; Kreissl, F. R.; Schrock, R. R.; Schubert, U.; Weiss, K. *Carbyne Complexes*; VCH: New York, 1988.
(257) *Transition Metal Carbyne Complexes*; Kreissl, F. R., Ed.; Kluwer Academic Publishers: Dordrecht, The Netherlands, 1993.
(258) Mayr, A.; Hoffmeister, H. *Adv. Organomet. Chem.* **1991**, *32*, 227.
(259) Kim, H. P.; Angelici, R. J. *Adv. Organomet. Chem.* **1987**, *27*, 51.
(260) Hall, M. B.; Fenske, R. F. *Inorg. Chem.* **1976**, *21*, 179.
(261) (a) Kostic, N. M.; Fenske, R. F. *J. Am. Chem. Soc.* **1981**, *103*, 4677. (b) Kostic, N. M.; Fenske, R. F. *Organometallics* **1982**, *1*, 489. (c) Kostic, N. M.; Fenske, R. F. *J. Am. Chem. Soc.* **1982**, *104*, 3879.
(262) Schubert, U.; Neugenauer, D.; Hofmann, P.; Schilling, B. E. R.; Fischer, H.; Motsch, A. *Chem. Ber.* **1981**, *114*, 3365.
(263) Poblet, J. M.; Strich, A.; West, R.; Bénard, M. *Chem. Phys. Lett.* **1986**, *126*, 169.
(264) Aristov, N.; Armentrout, P. *J. Am. Chem. Soc.* **1984**, *106*, 4065.
(265) Hofmann, P. in ref 256, p 59f.
(266) Vyboishchikov, S. F.; Frenking, G. *Chem. Eur. J.* **1998**, *4*, 1439.
(267) Yates, J. H.; Pitzer, R. M. *J. Chem. Phys.* **1979**, *70*, 4049.
(268) Lie, G. C.; Hinze, J.; Liu, B. *J. Chem. Phys.* **1973**, *59*, 1872.
(269) Dunning, T. H., Jr.; White, W. P.; Pitzer, R. M.; Mathews, C. W. *J. Mol. Spectrosc.* **1979**, *75*, 297.
(270) Footnote 39 in ref 244.
(271) Dewar, M. J. S.; Ford, G. P. *J. Am. Chem. Soc.* **1979**, *101*, 783.
(272) Albright, T. A.; Hofmann, R.; Thibeault, J. C.; Thorn, D. L. *J. Am. Chem. Soc.* **1979**, *101*, 3801.
(273) Åkermark, B.; Almemarte, M.; Almlöf, J.; Bäckvall, J.-E.; Roos, B.; Stoga, Å. *J. Am. Chem. Soc.* **1977**, *99*, 4617.
(274) Steigerwald, M. L.; Goddard, W. A., III *J. Am. Chem. Soc.* **1985**, *107*, 5027.
(275) Sodupe, M.; Bauschlicher, C. W.; Langhoff, S. R.; Partridge, H. *J. Phys. Chem.* **1992**, *96*, 2118.
(276) Böhme, M.; Wagener, T.; Frenking, G. *J. Organomet. Chem.* **1996**, *520*, 31.
(277) Hertwig, R. H.; Koch, W.; Schröder, D.; Schwarz, H.; Hrusak, J.; Schwerdtfeger, P. *J. Phys. Chem.* **1996**, *100*, 12253.
(278) Kitaura, K.; Sakaki, S.; Morokuma, K. *Inorg. Chem.* **1981**, *20*, 2292.
(279) Ziegler, T. *Inorg. Chem.* **1985**, *24*, 1547.
(280) Li, J.; Schreckenbach, G.; Ziegler, T. *Inorg. Chem.* **1995**, *34*, 3245.
(281) Fagan, P. J.; Calabrese, J. C.; Malone, B. *Science* **1991**, *252*, 1160.
(282) Balch, A. L.; Catalono, V. J.; Lee, J. W. *Inorg. Chem.* **1991**, *30*, 3980.
(283) Koefod, R. S.; Hudgens, M. F.; Shapley, J. R. *J. Am. Chem. Soc.* **1991**, *113*, 8957.
(284) Fagan, P. J.; Calabrese, J. C.; Malone, B. *J. Am. Chem. Soc.* **1991**, *113*, 9408.
(285) Balch, A. L.; Catalono, V. J.; Lee, J. W.; Olmstead, M. M.; Parkin, S. R. *J. Am. Chem. Soc.* **1991**, *113*, 8953.
(286) Koga, N.; Morokuma, K. *Chem. Phys. Lett.* **1993**, *202*, 330.
(287) Bo, C.; Costas, M.; Poblet, J. M. *J. Phys. Chem.* **1995**, *99*, 5914.
(288) Morokuma, K.; Borden, W. T. *J. Am. Chem. Soc.* **1991**, *113*, 1912.
(289) Kumar, A.; Lichtenhan, J. D.; Critchlow, S. C.; Eichinger, B. E.; Borden, W. T. *J. Am. Chem. Soc.* **1990**, *112*, 5633.
(290) Uddin, J.; Dapprich, S.; Frenking, G.; Yates, B. *Organometallics* **1999**, *18*, 457.
(291) Pidun, U.; Frenking, G. *Organometallics* **1995**, *14*, 5325.
(292) Sakaki, S.; Ieki, M. *Inorg. Chem.* **1991**, *30*, 4218.
(293) Cundari, T. R.; Gordon, M. S. *J. Mol. Struct.* **1994**, *313*, 47.
(294) King, R. B. *Inorg. Chem.* **1968**, *7*, 1044.
(295) Tatsumi, K.; Hoffmann, R.; Templeton, J. L. *J. Am. Chem. Soc.* **1982**, *21*, 466.
(296) Sodupe, M.; Bauschlicher, C. W. *J. Phys. Chem.* **1991**, *95*, 8640.
(297) Miralles-Sabater, J.; Merchán, M.; Nebot-Gil, I.; Viruela-Martin, P. M. *J. Phys. Chem.* **1988**, *92*, 4853.
(298) (a) Böhme, M. Dissertation, Marburg, 1995. (b) Fröhlich, N.; Frenking, G. Unpublished results.
(299) Kovács, A.; Frenking, G. *Organometallics* **1999**, *18*, 887.
(300) Hyla-Kryspin, I.; Koch, J.; Gleiter, R.; Klettke, T.; Walther, D. *Organometallics* **1998**, *17*, 4724.
(301) Stegmann, R.; Neuhaus, A.; Frenking, G. *J. Am. Chem. Soc.* **1993**, *115*, 11930.

(302) Nielson, A. J.; Boyd, P. D. W.; Clark, G. R.; Hunt, T. A.; Metson, J. B.; Rickard, C. E. F.; Schwerdtfeger, P. *Polyhedron* **1992**, *11*, 1419.
(303) Decker, S. A.; Klobukowski, M. *J. Am. Chem. Soc.* **1998**, *120*, 9342.
(304) Lichtenberger, D. L.; Brown, T. L. *J. Am. Chem. Soc.* **1978**, *100*, 366.
(305) Davy, R. D.; Hall, M. B. *Inorg. Chem.* **1989**, *28*, 3524.
(306) Stegmann, R.; Frenking, G. *Organometallics* **1995**, *14*, 5310.
(307) Irvine, G. J.; Lesley, M. J. G.; Marder, T. B.; Norman, N. C.; Rice, C. R.; Robins, E. G.; Roper, W. R.; Whittell, G. R.; Wright, L. J. *Chem. Rev.* **1998**, *98*, 2685.
(308) Braunschweig, H. *Angew. Chem.* **1998**, *110*, 1882; *Angew. Chem., Int. Ed. Engl.* **1998**, *37*, 1786.
(309) Wrackmeyer, B. *Angew. Chem.* **1999**, *111*, 817; *Angew. Chem. Int. Ed.* **1999**, *38*, 771.
(310) Fischer, R. A.; Weiβ, J. *Angew. Chem.* **1999**, *111*, 3002; *Angew. Chem., Int. Ed. Engl.* **1999**, *38*, 2830.
(311) Carmalt, C. J.; Norman, N. C.; Clarkson, L. M. *Comprehensive Organometallic Chemistry II*; Abel, E. W., Stone, F. G. A., Wilkinson, G., Eds.; Pergamon: 1995; Vol. 1, pp 545−571.
(312) Su, J.; Li, X.-W.; Crittendon, R. C.; Campana, C. F.; Robinson, G. H. *Organometallics* **1997**, *16*, 4511.
(313) (a) Dagani, R. *Chem. Eng. News* **1998**, *76* (11), 31. (b) Dagani, R. *Chem. Eng. News* **1997**, *75* (24), 9.
(314) Cotton, F. A.; Feng, X. *Organometallics* **1998**, *17*, 128.
(315) Boehme, C.; Frenking, G. *Chem. Eur. J.* **1999**, *5*, 2184.
(316) Uddin, J.; Boehme, C.; Frenking, G. *Organometallics* **2000**, *19*, in press.
(317) Bickelhaupt, F. M.; Radius, U.; Ehlers, A. W.; Hoffmann, R.; Baerends, E. J. *New J. Chem.* **1998**, 1.
(318) Braunschweig, H.; Kollann, C.; Englert, U. *Angew. Chem.* **1998**, *110*, 3355; *Angew. Chem., Int. Ed. Engl.* **1998**, *37*, 3179.
(319) Fischer, R. A.; Schulte, M. M.; Weiss, J.; Zsolnai, L.; Jacobi, A.; Huttner, G.; Frenking, G.; Boehme, C.; Vyboishchikov, S. F. *J. Am. Chem. Soc.* **1998**, *120*, 1237.
(320) Jug, K.; Maksic, Z. B. *Theoretical Models of Chemical Bonding*; Maksic, Z. B., Ed.; Springer-Verlag, Berlin, 1991; Vol. 3, p 235.
(321) Reference 45, p 227.
(322) Ehlers, A. W.; Frenking, G. *J. Am. Chem. Soc.* **1995**, *14*, 423.
(323) Lewis, K. E.; Golden, D. M.; Smith, G. P. *J. Am. Chem. Soc.* **1984**, *106*, 3905.
(324) Jutzi, P.; Neumann, B.; Reumann, G.; Stammler, H.-G. *Organometallics* **1998**, *17*, 1305.
(325) Cowley, A. H.; Lomeli, V.; Voigt, A. *J. Am. Chem. Soc.* **1998**, *120*, 6401.
(326) Uhl, W.; Pohlmann, M.; Wartchow, R. *Angew. Chem.* **1998**, *110*, 1007; *Angew. Chem., Int. Ed. Engl.* **1998**, *37*, 961.
(327) Frenking, G.; Uddin, J.; Uhl, W.; Benter, M.; Melle, S.; Saak, W. *Organometallics* **1999**, *18*, 3778.
(328) Musaev, D. G.; Mebel, A. M.; Morokuma, K. *J. Am. Chem. Soc.* **1994**, *116*, 10693.
(329) Cui, Q.; Musaev, D. G.; Morokuma, K. *Organometallics* **1997**, *16*, 1355.
(330) Cui, Q.; Musaev, D. G.; Morokuma, K. *Organometallics* **1998**, *17*, 742.
(331) Cui, Q.; Musaev, D. G.; Morokuma, K. *Organometallics* **1998**, *17*, 1383.
(332) Dorigo, A. E.; Schleyer, P. v. R. *Angew. Chem.* **1995**, *107*, 108; *Angew. Chem., Int. Ed. Engl.* **1995**, *34*, 115.
(333) Sakaki, S.; Kikuno, T. *Inorg. Chem.* **1997**, *2*, 2226.
(334) Nöth, H.; Schmid, G. *Angew. Chem.* **1963**, *75*, 861; *Angew. Chem., Int. Ed. Engl.* **1963**, *2*, 623.
(335) Schmid, G.; Petz, W.; Arloth, W.; Nöth, H.; *Angew. Chem.* **1967**, *79*, 683; *Angew. Chem., Int. Ed. Engl.* **1967**, *6*, 696.
(336) Nöth, H.; Schäfer, H.; Schmid, G. *Angew. Chem.* **1969**, *81*, 530; *Angew. Chem., Int. Ed. Engl.* **1969**, *8*, 515.
(337) Männig, D.; Nöth, H.; *Angew. Chem.* **1985**, *97*, 854; *Angew. Chem., Int. Ed. Engl.* **1985**, *24*, 878.
(338) Schmid, G. *Angew. Chem.* **1970**, *82*, 920; *Angew. Chem., Int. Ed. Engl.* **1970**, *9*, 819.
(339) Braunschweig, H.; Kollann, C.; Müller, M. *Eur. J. Inorg. Chem.* **1998**, 291.
(340) Hartwig, J. F.; Huber, S. *J. Am. Chem. Soc.* **1993**, *115*, 4908.
(341) Hartwig, J. F.; De Gala, S. R. *J. Am. Chem. Soc.* **1994**, *116*, 3661.
(342) Rickard, C. E. F.; Roper, W. R.; Williamson, A.; Wright, L. J. *Organometallics* **1998**, *17*, 4869.
(343) Reference 307, page 2707.
(344) Rablen, P. R.; Hartwig, J. F.; Nolan, S. P. *J. Am. Chem. Soc.* **1994**, *116*, 4121.
(345) Musaev, D. G.; Morokuma, K. *J. Phys. Chem.* **1996**, *100*, 6509.
(346) Giju, K. T.; Bickelhaupt, F. M.; Frenking, G. *Inorg. Chem.*, submitted for publication.
(347) Kubas, G. J.; Ryan, R. R.; Swanson, B. I.; Vergamini, P. J.; Wasserman, H. J. *J. Am. Chem. Soc.* **1984**, *106*, 451.
(348) Maseras, F.; Lledós, A.; Clot, E.; Eisenstein, O. *Chem. Rev.* **2000**, *100*, 601.
(349) Hay, P. J. *J. Am. Chem. Soc.* **1987**, *109*, 705.

(350) Eckart, J.; Kubas, G. J.; Hall, J. H.; Hay, P. J.; Boyle, C. M. *J. Am. Chem. Soc.* **1990**, *112*, 2324.
(351) Haynes, G. R.; Martin, R. L.; Hay, P. J. *J. Am. Chem. Soc.* **1992**, *114*, 28.
(352) Noell, J. O.; Hay, P. J. *J. Am. Chem. Soc.* **1982**, *104*, 4578.
(353) Lin, Z.; Hall, M. B. *J. Am. Chem. Soc.* **1992**, *114*, 2928.
(354) Lin, Z.; Hall, M. B. *Coord. Chem. Rev.* **1994**, *135/136*, 845.
(355) Dapprich, S.; Frenking, G. *Angew. Chem.* **1995**, *107*, 383; *Angew. Chem., Int. Ed. Engl.* **1995**, *34*, 354.
(356) Li, J.; Ziegler, T. *Organometallics* **1996**, *15*, 3844.
(357) Li, J.; Dickson, R. M.; Ziegler, T. *J. Am. Chem. Soc.* **1995**, *117*, 11482.
(358) Bayse, C. A.; Hall, M. B. *Organometallics* **1998**, *17*, 4861.
(359) Dapprich, S.; Frenking, G. *Organometallics* **1996**, *15*, 4547.
(360) Maseras, F.; Duran, M.; Lledós, A.; Bertrán, J. *J. Am. Chem. Soc.* **1991**, *113*, 2879.
(361) Lin, Z.; Hall, M. B. *Inorg. Chem.* **1992**, *31*, 4246.
(362) Lin, Z.; Hall, M. B. *Organometallics* **1993**, *12*, 4046.
(363) Maseras, F.; Lledós, A.; Costas, M.; Poblet, J. M. *Organometallics* **1996**, *15*, 2947.
(364) (a) Pierloot, K.; Roos, B. O. *Inorg. Chem.* **1992**, *31*, 5353. (b) Neuhaus, A.; Frenking, G.; Huber, C.; Gauss, J. *Inorg. Chem.* **1992**, *31*, 5355. (c) Vovna, V. I.; Prigornev, A. I. *Russ. J. Phys. Chem.* **1991**, *65*, 1121. (d) Kang, S. K.; Tang, H.; Albright, T. A. *J. Am. Chem. Soc.* **1993**, *115*, 1971. (e) Marsden, C. J.; Moncrieff, D.; Quelch, G. E. *J. Phys. Chem.* **1994**, *98*, 2038. (f) Russo, T. V.; Martin, R. L.; Hay, P. J. *J. Chem. Phys.* **1995**, *102*, 8023. (g) Vanquickenborne, L. G.; Vinckier, A. E.; Pierloot, K. *Inorg. Chem.* **1996**, *35*, 1305. (h) Gillespie, R. J.; Bytheway, I.; Tang, T.-H.; Bader, R. F. W. *Inorg. Chem.* **1996**, *35*, 3954.